

IS-T--1405

DE90 011744

Fundamental Studies of Hydrocarbon Conversions over Supported Bimetallic
Catalysts

by

Mark Wilton Smale

PHD Thesis submitted to Iowa State University

Ames Laboratory, U.S. DOE

Iowa State University

Ames, Iowa 50011

Date Transmitted: January 1990

PREPARED FOR THE U. S. DEPARTMENT OF ENERGY

UNDER CONTRACT NO. W-7405-Eng-82.

MASTER

DISTRIBUTION OF THIS DOCUMENT IS UNLIMITED

DISCLAIMER

This report was prepared as an account of work sponsored by an agency of the United States Government. Neither the United States Government nor any agency thereof, nor any of their employees, makes any warranty, express or implied, or assumes any legal liability or responsibility for the accuracy, completeness, or usefulness of any information, apparatus, product, or process disclosed, or represents that its use would not infringe privately owned rights. Reference herein to any specific commercial product, process, or service by trade name, trademark, manufacturer, or otherwise does not necessarily constitute or imply its endorsement, recommendation, or favoring by the United States Government or any agency thereof. The views and opinions of authors expressed herein do not necessarily state or reflect those of the United States Government or any agency thereof.

DISCLAIMER

Portions of this document may be illegible in electronic image products. Images are produced from the best available original document.

DISCLAIMER

This report was prepared as an account of work sponsored by an agency of the United States Government. Neither the United States Government nor any agency thereof, nor any of their employees, makes any warranty, express or implied, or assumes any legal liability or responsibility for the accuracy, completeness or usefulness of any information, apparatus, product, or process disclosed, or represents that its use would not infringe privately owned rights. Reference herein to any specific commercial product, process, or service by trade name, trademark, manufacturer, or otherwise, does not necessarily constitute or imply its endorsement, recommendation, or favoring by the United States Government or any agency thereof. The views and opinions of authors expressed herein do not necessarily state or reflect those of the United States Government or any agency thereof.

1405

Fundamental studies of hydrocarbon conversions
over supported bimetallic catalysts

Mark Wilton Smale

Under the supervision of Terry S. King
From the Department of Chemical Engineering
Iowa State University

The reactions of ethane and ethylene over selected silica-supported group VIII metal catalysts have been investigated using reaction studies and nuclear magnetic resonance (NMR) spectroscopy. The activity of the ruthenium-group IB bimetallic system for the ethane hydrogenolysis reaction was investigated as a function of group IB metal content and ethane and hydrogen partial pressures, while the reactions of ethylene over silica-supported platinum catalysts were studied using NMR.

The turnover frequency of the silica-supported ruthenium catalysts for ethane hydrogenolysis as either copper or silver was added tended to change as the group IB metal was first added until a critical point was reached. After this point, increasing the proportion of group IB metal had no significant effect on the specific activity of the catalyst. As was expected, copper, the more strongly segregating element, reached this critical point before silver. The critical point is believed to correspond to the point at

which all the edge and corner sites in the supported bimetallic crystallite are occupied by the group IB metal.

The apparent orders of reaction for ethane hydrogenolysis over the ruthenium-group IB catalysts was measured as a function of temperature. It appears from these measurements that the principal role of the edge and corner sites of a ruthenium catalyst for this reaction is the desorption and adsorption of hydrogen. At the higher temperatures studied, it appears that copper occupying the low coordination sites of a bimetallic crystallites is also active for the desorption/adsorption of hydrogen.

The reactions of ethylene over silica-supported platinum catalysts has been investigated using NMR. The ethylene to surface platinum atom ratio used in this work was in the 10 to 20 range, far higher than that used for typical single crystal studies. No significant activity was observed at room temperature. At temperatures in the 400 K to 550 K region a number of products were identified, including ethane, methane, and cis- and trans-but-2-ene. At still higher temperatures coke was formed on the surface of the catalyst. This coke was characterized as being predominantly aromatic in nature.

Fundamental studies of hydrocarbon conversions
over supported bimetallic catalysts

by

Mark Wilton Smale

A Dissertation Submitted to the
Graduate Faculty in Partial Fulfillment of the
Requirements for the Degree of
DOCTOR OF PHILOSOPHY

Major: Chemical Engineering

Approved:

In Charge of Major Work

For the Major Department

For the Graduate College

Iowa State University
Ames, Iowa

1989

TABLE OF CONTENTS

DEDICATION	vi
GENERAL INTRODUCTION	1
Explanation of Dissertation Format	4
SECTION I	
ETHANE HYDROGENOLYSIS OVER WELL-DEFINED Ru-Cu/SiO ₂ CATALYSTS	6
ABSTRACT	8
INTRODUCTION	9
METHODS	14
RESULTS	17
DISCUSSION	28
CONCLUSION	34
ACKNOWLEDGMENT	36
REFERENCES	37
SECTION II	
KINETICS OF ETHANE HYDROGENOLYSIS OVER SILICA-SUPPORTED RUTHENIUM-GROUP IB METAL CATALYSTS	41
ABSTRACT	43
INTRODUCTION	45
METHODS	57
RESULTS	60
DISCUSSION	75
CONCLUSION	90
ACKNOWLEDGMENT	91
REFERENCES	92

SECTION III

NMR STUDIES OF HIGH COVERAGES OF ETHYLENE ADSORBED ON SILICA-SUPPORTED PLATINUM CATALYSTS	97
ABSTRACT	99
INTRODUCTION	100
EXPERIMENTAL	110
RESULTS	116
Background	116
C ₂ H ₄ on SiO ₂	119
C ₂ H ₄ on Pt/SiO ₂	123
DISCUSSION	144
CONCLUSION	151
ACKNOWLEDGMENT	153
REFERENCES	154
SUMMARY AND RECOMMENDATIONS	160
Recommendations for Future Work	162
ADDITIONAL LITERATURE CITED	168
ACKNOWLEDGMENTS	169

DEDICATION

To the memory of my father

Mr. Roger James Smale, B.Sc. (Hons.)

GENERAL INTRODUCTION

The combination of two metals on an oxide support can lead to a catalyst with different properties than either of the corresponding monometallic catalysts. This is the case even when one of the metals is relatively catalytically active and the other comparatively inert, for example an active group VIII metal together with an inactive group IB metal. A particularly interesting case is when the two metals do not form a bulk alloy, as is the case with the Ru-Cu system [1], and yet the presence of the inactive group IB metal is obviously affecting the catalytic activity of the ruthenium, as has been shown by Sinfelt [2]. In this case the two metals are obviously interacting on the surface even though a bulk alloy is not formed, and Sinfelt [2] has coined the term "bimetallic cluster" to describe the metal crystallites present on the support of a supported bimetallic catalyst.

There are two general approaches to studying these catalyst systems. The first is to investigate the properties of the catalyst by doing reaction studies under conditions more or less closely approximating the conditions which might be expected to occur in a typical industrial reactor. The catalyst is then characterized by its reactivity under different conditions such as temperature, pressure, or concentrations of reactants. The alternative approach is to

investigate the catalyst surface and the species present on it using one of the spectroscopic techniques available, such as low energy electron diffraction spectroscopy (LEED), X-ray diffraction (XRD), and infrared spectroscopy (IR) to name but a few. Each of these approaches gives different, complementary information about the catalyst system. The work reported in this dissertation has used both reactor studies and spectroscopic techniques to study the reactions of C_2 hydrocarbons over supported group VIII metal catalysts.

The reactions that are reported in this dissertation are limited to those where the initial feed is a C_2 hydrocarbon. These reactions are useful models of some of the more complicated reactions that occur in a typical industrial reactor. Even such apparently simple reactions as the hydrogenolysis of ethane to form methane are not fully understood. Indeed, as will be seen in Section III of this dissertation, C_2 hydrocarbon reactions are potentially considerably more complex than might at first be apparent.

An important piece of information in the understanding of reaction study results is the proportion of the surface of a bimetallic crystallites which is made up of the active metal. The most common method of elucidating this is by selective titration of the surface by a chemisorbing species, such as hydrogen. It has recently been discovered that the titration of surface ruthenium atoms in a Ru-Cu bimetallic

catalyst using hydrogen is not a reliable method for obtaining the fraction of ruthenium atoms at the surface since hydrogen can spill over onto surface copper atoms. However, nuclear magnetic resonance spectroscopy (NMR) of adsorbed hydrogen is able to measure the ruthenium dispersion of these catalysts [3]. This ability, together with the ability to model the surface structure of these catalysts [4], led to the decision to re-evaluate the ethane hydrogenolysis reaction over Ru-Cu/SiO₂ catalyst system, as reported in Section I. This work was extended to a comparison of the effects of the two group IB metals copper and silver on silica-supported ruthenium catalysts, as reported in Section II.

In order to carry out reactor studies it is, of course, necessary to have a reactor system. The first part of my work, which is briefly mentioned in Section I, was the design and construction of the reactor system used in the reactor studies detailed in Sections I and II. The reactor system was designed to operate at temperatures between 400 K and 1000 K and pressures from 1 atm. to 50 atm., though these extremes were not required for the work described here. Analysis of the products is achieved by means of an on-line gas chromatograph. A full description of the reactor system and operating instructions is available. This includes manufacturers' instructions for the various individual pieces

of equipment and is therefore not included in this dissertation due to copyright considerations.

The third section of this dissertation details work done using nuclear magnetic resonance spectroscopy to characterize the species present after dosing a Pt/SiO₂ catalyst with ¹³C-labelled ethylene. The use of NMR in the investigation of species adsorbed on metal surfaces has recently been reviewed [5-7]. NMR is a low-powered, non-invasive spectroscopic technique that is unlikely to perturb the system being studied. One of the problems with many of the spectroscopic techniques commonly used to study adsorbed species on catalyst surfaces is that they require ultra-high vacuum conditions. NMR has the advantage that the catalysts may be studied with high coverages of the adsorbate present, thus more closely approximating the conditions that might be expected under normal reaction conditions. This feature has been taken advantage of in the work detailed in Section III of this dissertation.

Explanation of Dissertation Format

This thesis contains three sections, each presented in a form suitable for submission for publication in a technical journal. The first two sections detail original work carried out by the author. The work reported in the third section was carried out in collaboration with members of the chemistry department at Iowa State University and will be

submitted for publication with the author of this
dissertation as the primary author.

SECTION I

ETHANE HYDROGENOLYSIS OVER WELL-DEFINED
Ru-Cu/SiO₂ CATALYSTS

ETHANE HYDROGENOLYSIS OVER WELL-DEFINED
Ru-Cu/SiO₂ CATALYSTS

Mark W. Smale

Terry S. King

Department of Chemical Engineering and Ames Laboratory
Iowa State University
231 Sweeney Hall
Ames, Iowa 50011

ABSTRACT

This work was undertaken to investigate the behavior of the ethane hydrogenolysis reaction over well-characterized, chlorine-free, silica-supported, ruthenium-copper catalysts. The total dispersion of all catalysts was about 29%. The reaction studies were carried out in a laboratory-scale reactor, and catalyst activity was correlated with ruthenium surface composition, as measured previously by using nuclear magnetic resonance spectroscopy of chemisorbed hydrogen. Monte Carlo simulations of the catalyst were used to assist in the interpretation of the results.

The reaction studies indicate that the catalysts with a Cu:Ru atom ratio greater than 1:9 have a constant specific activity (rate per surface ruthenium atom), analogous to the behavior of single crystal surfaces. Below this Cu:Ru ratio, the specific activity drops rapidly as copper is added to the system at the lower temperatures studied (around 500 K). At a Cu:Ru ratio of 1:9 the modeling suggests all edge and corner sites of the catalyst crystallite are occupied by copper. We conclude that the ethane hydrogenolysis reaction over silica-supported ruthenium-copper catalysts is sensitive to the crystallite structure but no geometric effects are observed.

INTRODUCTION

Supported bimetallic catalysts have received much attention from both industrial and academic sectors. The ruthenium-copper catalyst is of particular interest as a model system in that the two metals are virtually immiscible in the bulk (1). However, for the supported catalyst, the relatively inactive copper has a large influence on the activity of ruthenium, indicating that the metals are together on the oxide support (2).

The use of model reactions can greatly enhance the understanding of these catalysts. One commonly studied reaction is the hydrogenolysis of ethane. This is a relatively simple, clean reaction and as such is a good candidate for use as a diagnostic tool. Ethane hydrogenolysis has been studied over a number of metal catalysts other than ruthenium. Goodman (3) has studied the reaction over the nickel (100) and (111) single crystal surfaces and found that the apparent activation energy is lower for the more open (100) surface. His findings indicate that the reaction is structure-sensitive over this metal. Ethane hydrogenolysis has also been studied over silica-supported platinum catalysts by Guczi and Gudkov (4). They found that the edge and corner atoms of the supported metal crystallites had an enhanced activity as compared to the basal planes. Kane and Clarke (5) studied ethane

hydrogenolysis over platinum-gold polycrystalline foils and found that the apparent activation energy for the reaction increased with the addition of gold. They indicated this result was due to the segregation of gold to the defect sites that were most active for the reaction, and they speculated that ethane hydrogenolysis over platinum films is structure sensitive.

Sinfelt et al. (2,6,7) studied the ethane hydrogenolysis reaction over silica-supported ruthenium-copper catalysts. In order to calculate the specific activity of the catalyst (rate per surface ruthenium atom), they had to measure the proportion of the ruthenium in the catalyst that was at a crystallite surface. These measurements were made by titrating the catalyst surface with hydrogen; it was inferred that the hydrogen would only chemisorb on ruthenium. This assumption would appear to be valid because it is known that hydrogen will not appreciably chemisorb on a pure copper surface at room temperature. The activity of the ruthenium catalyst per hydrogen chemisorption site thus calculated was seen to decrease as the copper content was increased. This result led to the suggestion that the ethane hydrogenolysis reaction over supported ruthenium-copper catalysts exhibits geometric effects; that is, the active site for the reaction consists of a number of adjacent surface ruthenium atoms. Thus the placement of a single copper atom onto a predomi-

nantly ruthenium surface would deactivate an ensemble of ruthenium atoms.

Hong et al. (8) have studied ethane hydrogenolysis over silica-supported Ru-Cu catalysts and reported a dramatic decrease in the rate per total ruthenium atom as the copper content increased. The catalysts in their work used two different ruthenium salts as a catalyst precursor: RuCl_3 and $\text{Ru}(\text{NO})_3(\text{NO}_3)_3$. Because chlorine is a known contaminant, when the chloride salt was used they were able to compare contaminated and chlorine-free catalysts. Hong et al. (8) also have suggested ensemble effects to explain this decrease in activity.

In order to report the specific activities of these catalysts, one must measure the proportion of ruthenium atoms in the catalyst that are at a surface. Selective hydrogen chemisorption is often used for this type of measurement. Since hydrogen chemisorbs very little on a supported copper catalyst, the amount of hydrogen chemisorbed on a supported ruthenium-copper catalyst is assumed to be a measure of the ruthenium dispersion. More recently, studies of single crystal ruthenium-copper catalysts by Goodman and Peden (9) have shown that hydrogen will absorb dissociatively on ruthenium surfaces and then migrate to the copper. This result has been confirmed for the case of the silica-supported catalyst (10). Spillover of hydrogen from

ruthenium to copper indicates that the use of hydrogen chemisorption to measure the dispersion of the supported ruthenium-copper catalysts will lead to over-estimating the number of surface ruthenium atoms. Hong et al. (8) have also postulated hydrogen spillover for silica-supported ruthenium-copper catalysts.

Goodman and Peden (11-14) have investigated the effect of adding copper to single-crystal ruthenium catalysts, making allowance for the hydrogen spillover effect. In contrast to the earlier work by Sinfelt et al. (2,6,7), the authors observed no geometric effects for the ethane hydro-glycolysis reaction. Instead, the specific activity of the catalyst was unchanged as copper was added.

However, the morphology of a supported metal crystallite is very different from that of a single crystal surface. While the supported particles might be expected to contain surfaces which are analogous to a single crystal, a significant number of the metal atoms in highly dispersed catalysts will be in defect-like sites. Consideration of the thermodynamics of supported bimetallic catalysts allowed Strohl and King (15) to model catalysts similar to the ruthenium-copper system. They suggest that the segregating element will preferentially populate the edge and corner sites of the supported crystallites. Addition of the segregating element, copper, to ruthenium particles after

these low coordination sites have been filled leads to the formation of two-dimensional islands on the basal planes of the particle. These islands are characteristic of systems that do not mix well. Experimental evidence of the preferential population of ruthenium defect sites by copper has been recently presented by Kim et al. (16). Also, work with submonolayer amounts of copper deposited on ruthenium single crystals reveals that copper layers grow in a highly dispersed mode at 100 K, but subsequent annealing to 300 K produces two-dimensional islands pseudomorphic to the Ru (001) substrate (9,11,17-20). In this paper, we shall discuss the activity of supported ruthenium-copper catalysts adjusted to reflect the effect of the hydrogen spillover phenomenon.

METHODS

The details of the catalyst preparation and characterization are reported elsewhere (21). The catalysts used were all supported on Cab-O-Sil HS-5 amorphous fumed silica with a surface area of $300 \text{ m}^2/\text{g}$ as measured by the BET method, and all contained 4% ruthenium (by weight). We used the incipient wetness co-impregnation technique to prepare the bimetallic catalysts from an aqueous solution of $\text{Ru}(\text{NO}_3)_3$ and $\text{Cu}(\text{NO}_3)_2$. The catalysts were characterized by a number of methods including hydrogen chemisorption and nuclear magnetic resonance (NMR) of chemisorbed hydrogen. The total metal dispersion of the pure ruthenium catalyst was determined by strong hydrogen chemisorption to be 29% for all copper-containing catalysts. The total hydrogen chemisorption was about equal to that of the pure ruthenium catalyst, suggesting that the total metal dispersion for all catalysts was about the same.

After the catalysts were prepared, we carried out reaction studies using a continuous tubular reactor system. The hydrogen was first stripped of oxygen, after which we used molecular sieve traps to dry the feed gases. Flow rates of the purified gases were controlled with Brooks mass flow controllers. To preheat the feed gas, we used temperature-controlled heating tapes. The final preheat was achieved by flowing the feed gas mixture up through the

furnace used to heat the reactor tube. The feed then flowed down through the catalyst bed, which was contained in a 1/4-in. schedule 40 type 316 stainless steel pipe. A programmable temperature controller was used to control the temperature for the catalyst bed, and the temperature for the controller was measured by means of a type-K thermocouple contained in a 1/16-in. tube positioned axially in the reactor. In order to ensure a rapid response from the temperature controller, we placed the thermocouple so that the temperature measurement was made in the middle of the catalyst bed. The sample was diluted with 100-200 mesh crystalline silica to a volume of 3.0 cm³. The catalyst was supported in the reactor so that it remained in the 2-in. region of the furnace that was isothermal (± 1 K).

We used automatic sampling valves to introduce the reaction products into a 6-ft-long, 1/8-in.-o.d., stainless steel gas chromatograph column, packed with 80/100 mesh Haysep Q, and the separated products were fed to the thermal conductivity detector (TCD) of a Varian 3700 gas chromatograph. After the column oven was held at 308 K for 10 min, the temperature was ramped at 4 K/min. A commercial data acquisition package on an IBM personal computer digitized and manipulated the signal from the TCD, and the times at which samples of reaction products were taken were controlled by a custom-built, microprocessor-based timer.

The catalyst in the reactor was heated to the reduction temperature in 1 h, while it was exposed to a $500 \text{ cm}^3/\text{min}$ (STP) flow of hydrogen. After the catalyst was reduced for 2 h, normally at 723 K, the temperature was lowered to the desired reaction temperature over a period of 7 h. The flow rate of the hydrogen was unchanged throughout this period. The gas feed was then switched to the reactant mixture consisting of a 10:2:1 molar ratio mixture of hydrogen, ethane, and argon (the argon was used as an internal standard for the gas chromatographic analysis). All the reaction studies were carried out at atmospheric pressure. The volumetric space velocity (STP) inside the reactor was around $20,000 \text{ hr}^{-1}$ for all runs. We analyzed samples of the product after 20 min, 1.5 h, 3.5 h, and 7.5 h on line.

All rate data are presented as turnover frequencies in terms of disappearance of ethane. The units used are molecules of ethane per second per site. The rates show in different graphs for the same catalyst composition and reaction temperature differ only in the method used to calculate the number of sites for the reaction.

RESULTS

All activity data are presented in terms of the rate of ethane consumed. Figure 1(a) shows the activity of the catalyst as a function of time on line for a 1:9 Cu:Ru atomic ratio catalyst at a number of different temperatures, and Fig. 1(b) shows the activity of several catalysts as a function of time on line at a reaction temperature of 508 K. Note that no significant change in activity occurs between 20 min and 7.5 h. This indicates that any deactivation (or activation) has occurred before the catalyst has been on line for 20 min. The copper neither increased nor decreased the rate of deactivation of the ruthenium catalysts for the ethane hydrogenolysis reaction.

Figure 2 shows the activity (rate per total ruthenium) of the catalysts as a function of the copper atom fraction at a number of different temperatures. The sensitivity of our analytical procedure coupled with the limitations imposed on the reactor to ensure comparable conditions for all runs limited the range of catalyst compositions that could be studied at a given temperature. At the lowest temperatures the high copper content catalysts were too inactive to allow accurate rate determination. As can be seen, the addition of copper leads to a significant decrease in the activity of the catalyst, confirming that the copper and ruthenium are indeed together on the silica support.

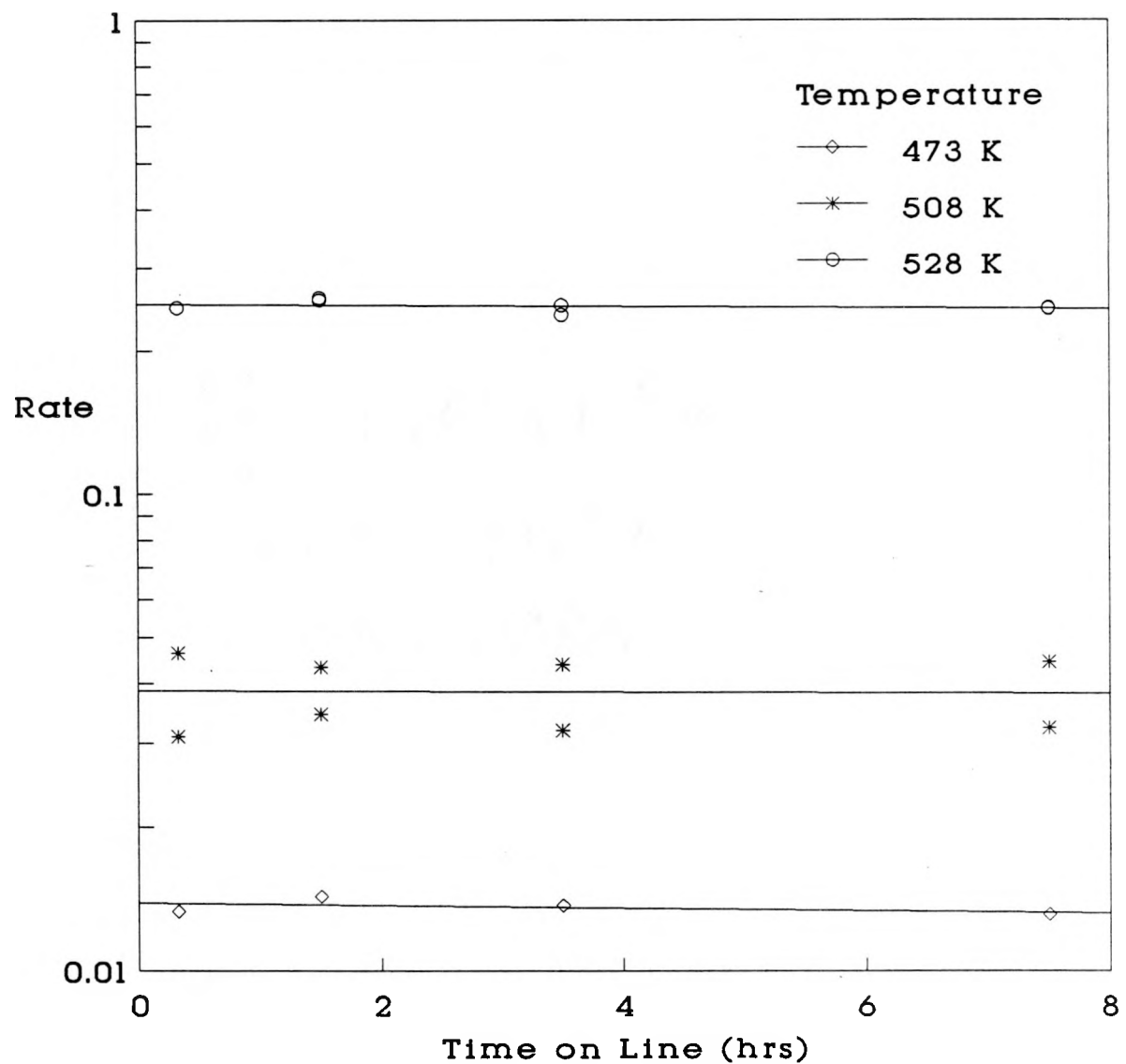


Figure 1(a). Ethane hydrogenolysis activity of the 1:9 (Cu:Ru) atomic ratio catalyst as a function of time-on-stream at various temperatures

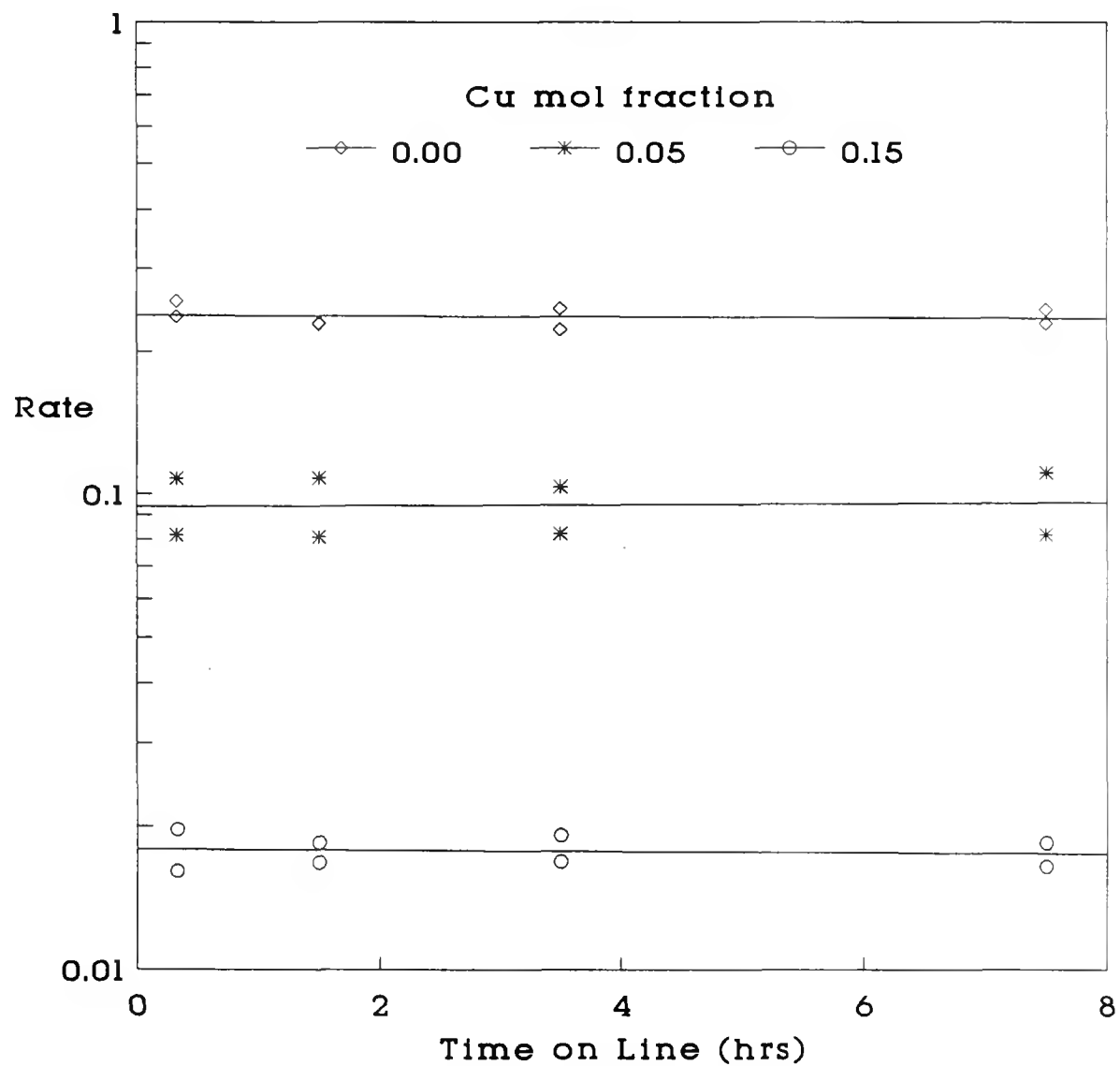


Figure 1(b). Ethane hydrogenolysis activity of silica-supported Ru-Cu catalysts as a function of time-on-stream at 508 K

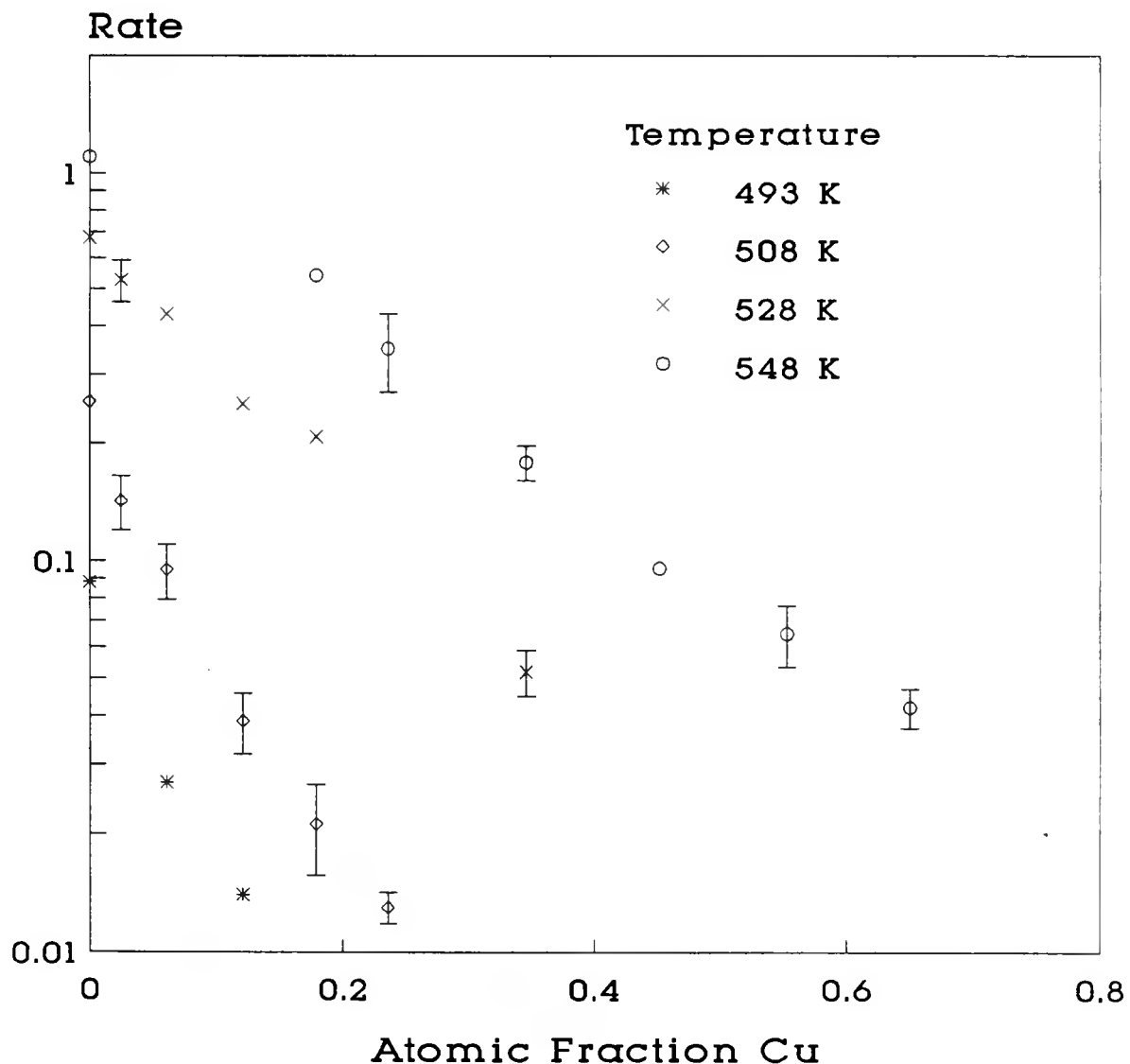


Figure 2. Rate of ethane hydrogenolysis (± 1 standard deviation) per total ruthenium atom for silica-supported Ru-Cu catalysts

Wu et al. (21) have previously used hydrogen chemisorption and NMR to characterize the same silica-supported ruthenium-copper catalysts used in these reaction studies. The catalysts were placed in an NMR tube attached to the adsorption apparatus and were reduced at 723 K in flowing hydrogen for 2 h. Then chemisorption measurements were carried out to measure the apparent dispersion of each catalyst. Subsequently, the samples were sealed and proton NMR of the adsorbed hydrogen atoms was used to elucidate the proportion of ruthenium atoms in the sample that were exposed at a surface. As can be seen in Table 1, the two methods for measuring the ruthenium dispersion of the catalyst apparently give strikingly different results. The reason is that the hydrogen chemisorbs not only on surface ruthenium atoms but also on surface copper. Hydrogen chemisorption measures both because of the hydrogen spillover effect, where the hydrogen can dissociatively adsorb on the ruthenium surface and then migrate to the copper atoms. On the other hand, the proton NMR results give the true number of surface ruthenium atoms.

The result of using strong hydrogen chemisorption data to calculate the specific activity of the catalysts is shown in Fig. 3. Note that the activity of the catalysts appears to decrease continually as the copper content is increased. It is this phenomenon that has led to the postulation of

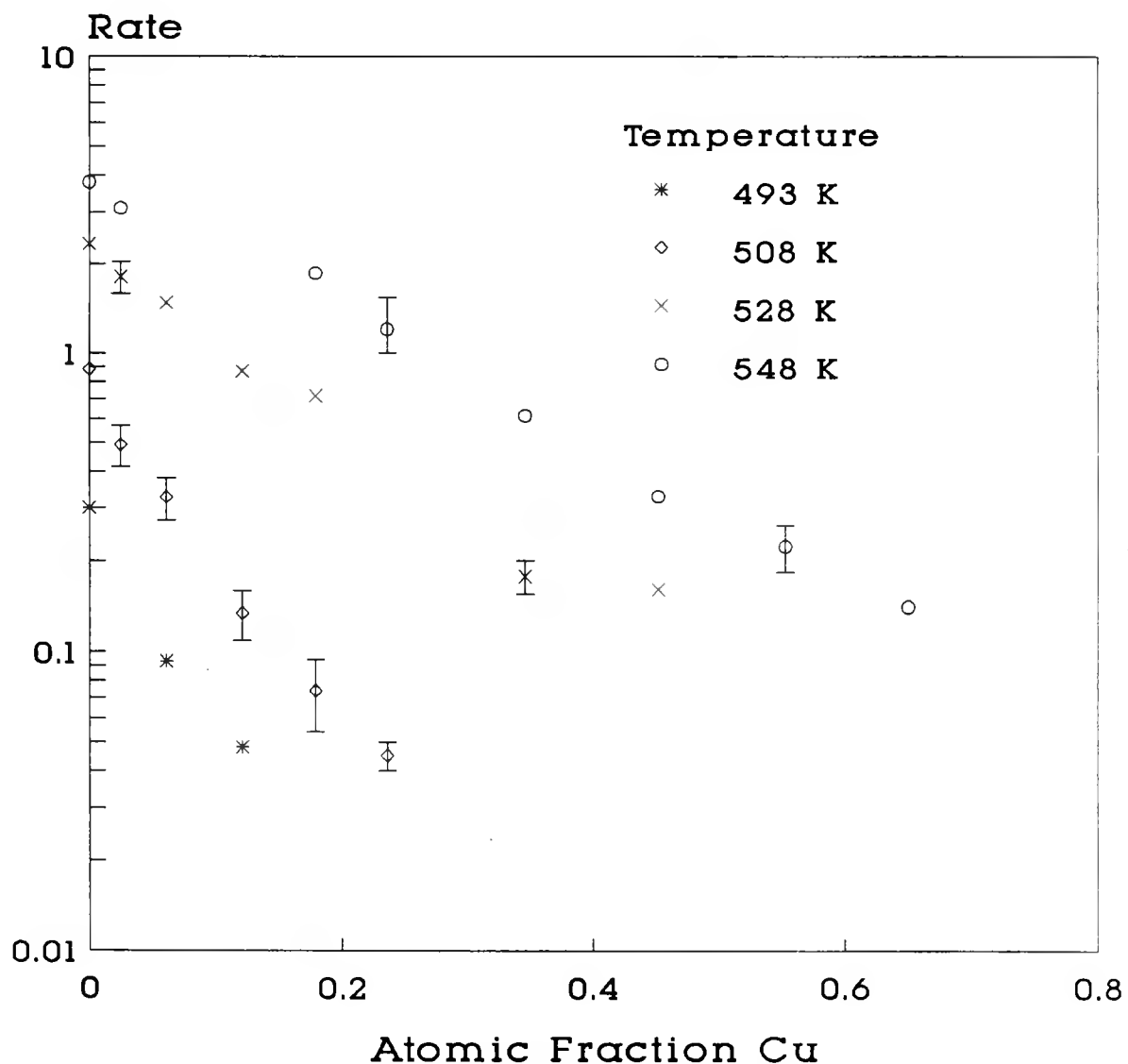


Figure 3. Rate of ethane hydrogenolysis (± 1 standard deviation) per surface ruthenium as measured by strong hydrogen chemisorption

Table 1. Ruthenium dispersion of Ru-Cu/SiO₂ catalysts measured by strong hydrogen chemisorption and NMR of protons

Cu Atom Fraction	Ruthenium Dispersion (21)	
	Chemisorption ^a	NMR
0.000	0.290	0.290
0.025	0.293	0.258
0.061	0.296	0.233
0.121	0.297	0.161
0.179	0.296	0.070
0.235	0.290	0.039
0.346	0.300	0.024
0.452	0.300	0.018
0.553	0.303	0.009
0.650	0.323	0.003

^aAssumes hydrogen strongly adsorbs only on ruthenium.

geometric effects being important in these catalysts. However, this approach over-counts the surface ruthenium atoms because of hydrogen spillover (8,9).

When the dispersion of ruthenium is measured with NMR spectroscopy of adsorbed protons (21), the calculation of

turnover frequency gives dramatically different results. As can be seen from Fig. 4, the specific activity or turnover frequency of the catalysts decreased rapidly at low temperatures as small amounts of copper were added to the system. However, after the Cu:Ru ratio exceeded about 1:9, there was no further decrease in rate per surface ruthenium atom. At higher temperatures the turnover frequency either remained constant over the range of compositions studied or increased at low copper content and then remained constant.

The difference in behavior of the catalysts at different temperatures suggests that investigating the apparent activation energy as a function of copper content of the catalyst should assist our interpretation of the system. Figure 5 shows the results of plotting turnover frequency versus inverse temperature over the 478 K - 548 K region for the pure ruthenium and 18% copper catalysts. We see that the two curves intersect in the 515 K - 540 K temperature range.

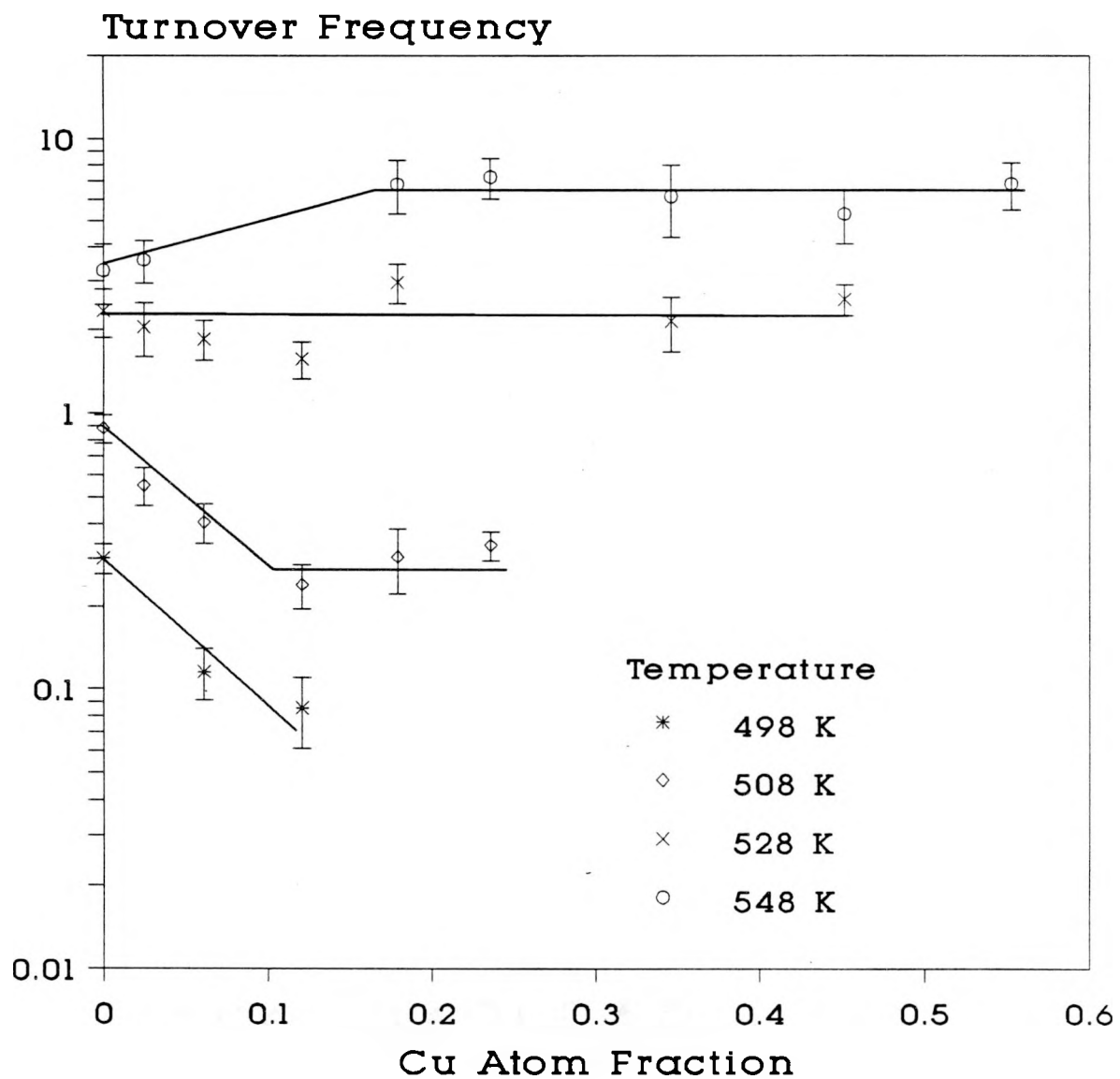


Figure 4. Rate of ethane hydrogenolysis (\pm 1 standard deviation) per surface ruthenium as measured by proton NMR

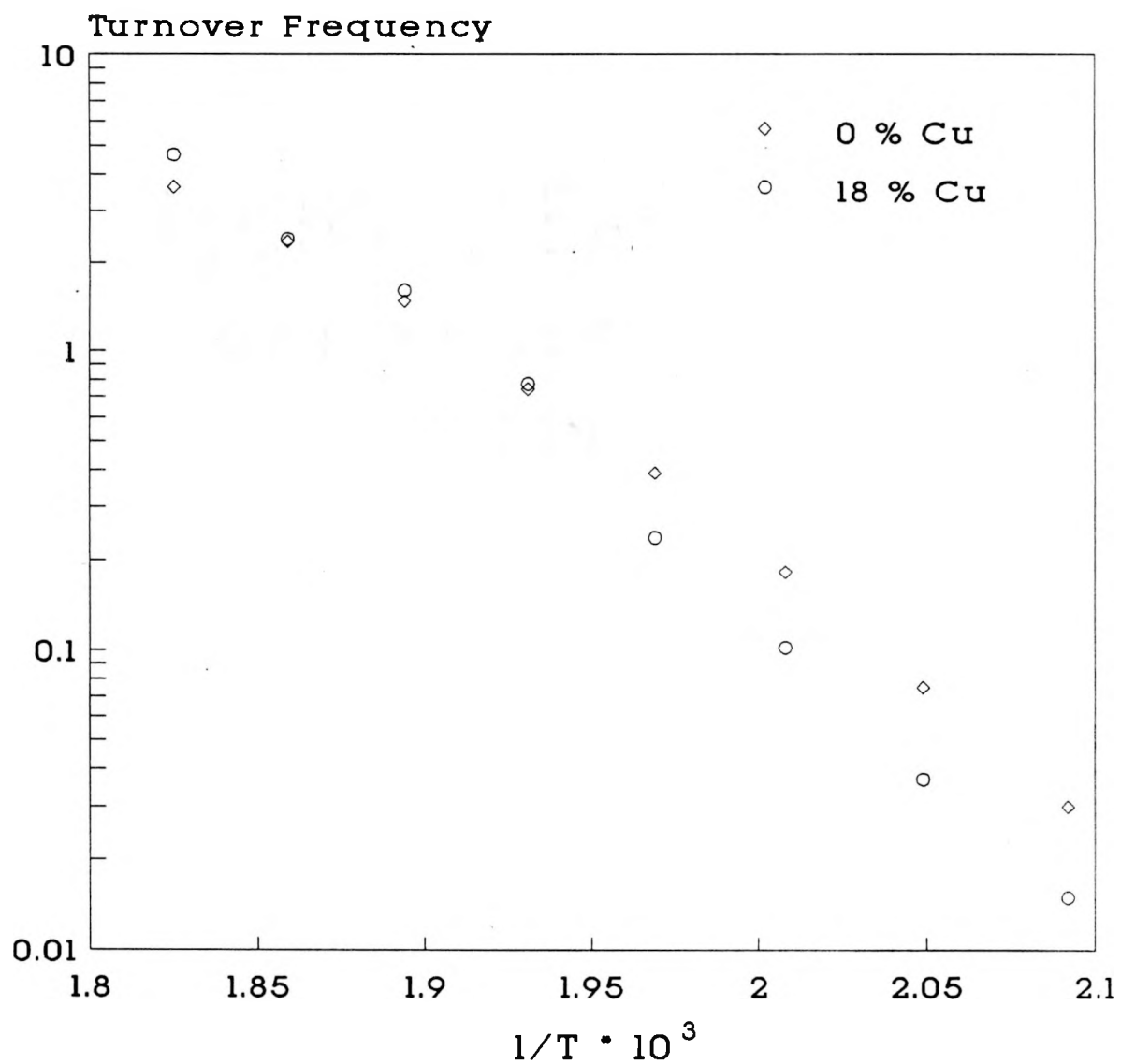


Figure 5. Arrhenius plots for Ru/SiO_2 and Ru-Cu/SiO_2 catalysts

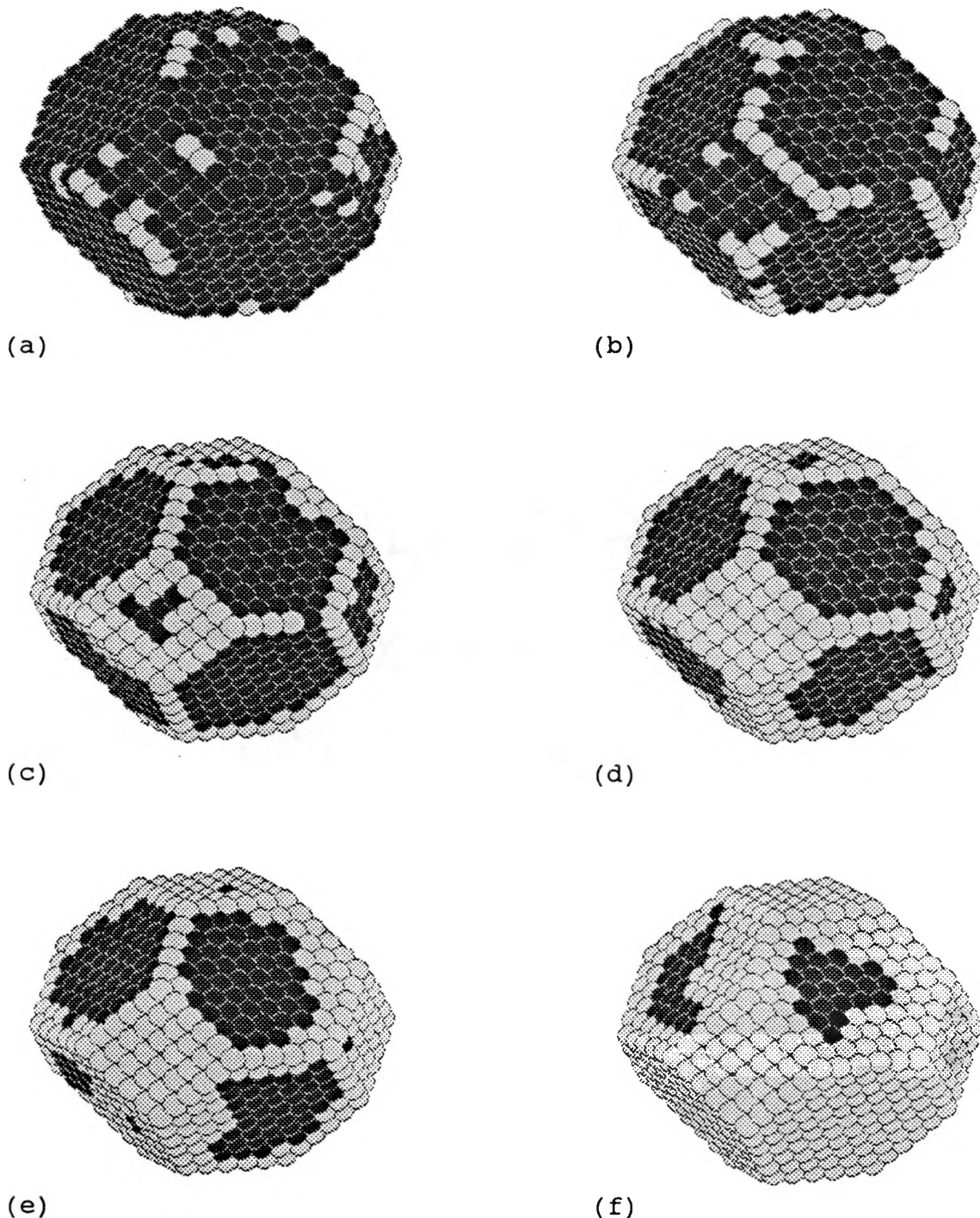


Figure 6. Monte Carlo simulation results for Ru-Cu/SiO₂ catalysts with a total metal dispersion of 30%; (a) 2% Cu, (b) 5% Cu, (c) 10% Cu, (d) 15% Cu, (e) 20% Cu, (f) 30% Cu

DISCUSSION

In order to visualize what the reaction data means in terms of the catalyst morphology, we find it useful to have a model of the bimetallic crystallites in the catalyst. The Monte Carlo simulation procedure developed previously (15, 22) was used to model ruthenium-copper catalysts. While the model used is not strictly accurate because it was written for a face-centered cubic crystal and ruthenium has a hexagonal close-packed structure, it will serve to give a good approximation of the equilibrium state of the metal crystallites.

The Monte Carlo simulation results indicate that when a small amount of copper is added to a ruthenium catalyst, it tends to preferentially populate the defect-like edge and corner sites of the metal crystallite (Figs. 6a-c). As indicated in Figs. 6d-f, further addition of copper leads to two-dimensional clustering on the low index plane surfaces of the particle. The model suggests that the copper does not disperse over the basal planes to break up ruthenium ensembles. This result is consistent with various observations (9,11,17-20) showing that copper forms large two-dimensional islands on ruthenium single-crystal surfaces. On the other hand, all the edge and corner positions are occupied by copper by the time the Cu:Ru ratio has reached about 1:9. The simulation procedure used a truncated

octahedron as the initial configuration, although this is free to change throughout the simulation. It should be noted, however, that other studies starting with different configurations give essentially the same results (15,22). Octahedral structures have indeed been observed experimentally for supported catalysts (23,24), leading us to believe that the simulations are at least qualitatively reasonable.

The Monte Carlo simulations suggest that these catalysts will never show geometric effects because the copper does not intermix with ruthenium on the low-index-plane facets of the crystallites. Therefore, even if the active site for the ethane hydrogenolysis reaction were to consist of an ensemble of ruthenium atoms, we would not expect to observe geometric effects with the ruthenium-copper catalyst series.

If we consider the reaction results for the high copper-loading catalysts, it is apparent that we are, indeed, observing no evidence for geometric effects. Instead, the rate-per-surface ruthenium atom remains constant, which is in agreement with the results of Goodman and Peden (11-13) on single crystal catalysts. This observation is not surprising because the results of the Monte Carlo simulations show that at higher copper loadings, the catalyst is essentially composed of single crystal-like facets with copper and ruthenium remaining unmixed.

At the low Cu:Ru ratios, however, a different effect seems to be important. For these catalysts, the activity per surface ruthenium atom, at least at the lower temperatures studied, decreases rapidly. The decrease in activity coincides with the loss of ruthenium from defect-like edge and corner lattice positions predicted by the simulations. After the low coordination sites are filled with copper, additional copper masks the basal planes by formation of two-dimensional islands that grow from the edges of the crystallites. Thus, it seems that the edge and corner atoms of the catalyst crystallite are responsible for a different activity than the basal planes. This supposition is supported by the observation that the specific activity of the catalyst no longer decreases with copper addition after the copper content reaches the point that the model indicates all edge and corner positions are occupied by copper.

It is interesting to note that our value for the specific rate of the supported catalyst is within a factor of four of that extrapolated from the results of Peden and Goodman (14) for a ruthenium (001) single crystal surface using the pressure dependencies they reported.

Comparison of the Arrhenius curves for the pure ruthenium and 18% copper catalysts indicates a sharp divergence around 510 K. It is conceivable that this change in intrinsic rate may be due to edge and corner sites

exhibiting a different intrinsic rate than found on the single crystal surfaces. Indeed, previous studies of the ethane hydrogenolysis reaction over different catalyst systems (3,5) have reported a lower activation energy for more open sites. In addition, Engstrom, Goodman and Weinberg (26) have suggested that the ethane hydrogenolysis reaction may proceed through different intermediates on different iridium single-crystal surfaces. They also show Arrhenius plots that curve in a very similar manner to our results for the silica-supported pure ruthenium catalyst.

An alternative hypothesis is that at the lower temperatures studied, there are some adsorbed species that are blocking sites on the Ru-Cu catalyst more effectively than on the pure ruthenium catalyst. At the higher temperatures studied, this blocking species would desorb, leaving both catalysts with roughly the same specific activity. This would account for the sharp transition over a small temperature range. A possible candidate for the blocking species is hydrogen, which was present in great excess during our experiments. It has previously been reported that the apparent order of reaction with respect to hydrogen for ethane hydrogenolysis is negative for a large number of catalysts (25), the value given for a silica-supported ruthenium catalyst being -1.3. Engstrom et al. (26) attribute the curve in the Arrhenius plots they observed for

hydrogenolysis over single crystal iridium to desorption, as the temperature was increased, of surface hydrogen, which tends to block sites at lower temperatures. It seems possible that for our supported Ru-Cu catalysts the copper at the edge and corner sites is inhibiting desorption of hydrogen from the bimetallic crystallites at the lower temperatures studied, leading to an increased blocking of the active sites (Ru) for hydrogenolysis. At the higher temperatures, copper is no longer inhibiting hydrogen desorption, so the copper is not affecting the specific activity of the catalyst. This interpretation suggests that the edge and corner sites are not sites for the hydrogenolysis step but instead serve as a location where hydrogen can recombine and desorb more effectively than from the basal planes. Besnasetz and Somorjai (27) have shown that platinum high-index planes are considerably more active than low-index planes for hydrogen-deuterium exchange, and they postulate that H-D formation occurs at step sites.

One can take the data of Feulner and Menzel (28) for the activation energy, the pre-exponential, and the sticking probability for desorption of hydrogen on a Ru(001) surface as a function of coverage and use them to determine the temperature at which the surface hydrogen desorbs at the pressure of the results shown in this work (1 atm.). The

temperature at which significant desorption occurs at equilibrium ($\theta < 0.5$) is around 505 K to 540 K.

CONCLUSION

Investigation of the ruthenium-copper system must make allowance for the well-documented hydrogen spillover phenomenon. When hydrogen spillover is considered, the interpretation of the behavior of these catalysts for the ethane hydrogenolysis reaction is very different from the interpretation when hydrogen spillover is not considered.

At the lower temperatures studied we have observed a decrease in the specific activity of the ruthenium catalysts as copper is added until a Cu:Ru ratio of 1:9 is reached. Adding more copper to the system does not change the specific activity of the catalyst. At the higher temperature the specific activity either remains constant over the entire composition range or increases somewhat over the low copper content region until a constant activity is attained. The Arrhenius plots for a pure ruthenium catalyst and 18% copper catalyst are almost coincident in the 510 K to 540 K range. Below this temperature the curves diverge sharply. These results lead us to the conclusion that the presence of defect-like sites in silica-supported ruthenium catalysts can greatly affect the activity of the catalyst. This may be due to an inherent difference in activity of defect sites as compared to single crystal surfaces or due to the two types of sites having a different ability to allow hydrogen

desorption. It is evident, however, that the morphology of the catalyst crystallite plays an important role.

Modeling of silica-supported ruthenium-copper catalysts suggests that the copper does not break up surface ruthenium ensembles. In this case, we would not expect to be able to observe geometric effects with this system; indeed, no geometric effects were observed.

ACKNOWLEDGMENT

This work was supported by the U.S. Department of Energy, Office of Energy Sciences, Contract Number W-7405-ENG-82.

REFERENCES

1. Hansen, M., and Anderko, K., "Constitution of Binary Alloys." 2nd Ed. McGraw-Hill, New York, 1958.
2. Sinfelt, J. H., J. Catal. **29**, 308 (1973).
3. Goodman, D. W., Surf. Sci. Lett. **123**, L679 (1982).
4. Guczi, L., and Gudkov, B. S., React. Kinet. Catal. Lett. **9**, 343 (1978).
5. Kane, A. F., and Clarke, J. K. A., J. Chem. Soc., Faraday Trans. I **76**, 1640 (1980).
6. Sinfelt, J. H., Lam, Y. L., Cusumano, J. A., and Barnett, A. E., J. Catal. **42**, 227 (1976).
7. Sinfelt, J. H., "Bimetallic Catalysts." John Wiley and Sons, New York, 1983.
8. Hong, A. J., Rouco, A. J., Resasco, D. E., and Haller, G. L., J. Phys. Chem. **91**, 2665 (1987).
9. Goodman, D. W. and Peden, C. H. F., J. Catal. **95**, 321 (1985).

10. King, T. S., Wu, X., and Gerstein, B. C., J. Am. Chem. Soc. **108**(19), 6056 (1986).
11. Peden, C. H. F., and Goodman, D. W., Ind. Eng. Chem. Fundam. **25**, 58 (1986).
12. Peden, C. H. F., and Goodman, D. W., J. Catal. **100**, 520 (1986).
13. Goodman, D.W., and Peden, C. H. F., J. Chem. Soc., Faraday Trans. I **83**, 1967 (1987).
14. Peden, C. H. F., and Goodman, D. W., ACS Symp. Ser. **288**, 185 (1985).
15. Strohl, J. K., and King, T. S., J. Catal. **116**, 540 (1989).
16. Kim, K. S., Sinfelt, J. H., Eder, S., Markert, K., and Wandelt, K., J. Phys. Chem. **91**, 2337 (1987).
17. Yates, J. T., Jr., Peden, C. H. F., and Goodman, D. W., J. Catal. **94**, 576 (1985).

18. Goodman, D. W., Yates, J. T., Jr., and Peden, C. H. F., Surf. Sci. **164**, 417 (1986).
19. Houston, J. E., Peden, C. H. F., and Goodman, D. W., Surf. Sci. **167**, 427 (1986).
20. Houston, J. E., Peden, C. H. F., Feibelman, P. J., and Hamann, D. R., Phys. Rev. Lett. **56**, 375 (1986).
21. Wu, X., Gerstein, B. C., and King, T. S., J. Catal. Submitted for publication.
22. Strohl, J. K., Ph.D. diss. Iowa State University, 1988.
23. Dominguez, J. M., and Yacaman, M. J., J. Catal. **64**, 213 (1980).
24. Yacaman, M. J., and Dominguez, J. M., J. Catal. **64**, 223 (1980).
25. Sinfelt, J. H., Catal. Rev. **3**, 175 (1969).
26. Engstrom, J. R., Goodman, D. W., and Weinberg, W. H., J. Am. Chem. Soc. **110**, 8305 (1988).

27. Besnasetz, S. L., and Somorjai, G. A., J. Chem. Phys.
62(8), 3149.

28. Feulner, P., and Menzel, D., Surf. Sci. **154**, 465 (1985).

SECTION II

KINETICS OF ETHANE HYDROGENOLYSIS OVER
SILICA-SUPPORTED RUTHENIUM-GROUP IB
METAL CATALYSTS

KINETICS OF ETHANE HYDROGENOLYSIS OVER
SILICA-SUPPORTED RUTHENIUM-GROUP IB
METAL CATALYSTS

Mark W. Smale

Terry S. King

Department of Chemical Engineering and Ames Laboratory
Iowa State University
231 Sweeney Hall
Ames, Iowa 50011

ABSTRACT

We have studied the effect of adding copper and silver to a silica-supported ruthenium catalyst. We measured specific activities as a function of the fraction of group IB metal at a number of temperatures. In addition, the effect of changing the ratio of hydrogen to ethane in the feed gas was used to measure apparent orders of reaction as a function of temperature and group IB metal added. At the lower temperatures studied we found that the effect of adding copper or silver to the catalyst was virtually the same, the differences being attributed to the greater affinity of copper for defect-like sites on the ruthenium crystallites. At higher temperatures, copper and silver acted differently; copper seemed to be active for the removal of site-blocking hydrogen from the active ruthenium surface, while silver merely blocked the ruthenium sites most active for the removal of hydrogen from the surface. We postulate that the defect-like sites of supported ruthenium crystallites are most active for the desorption of hydrogen and the low-index planes are active for the breaking of carbon-carbon bonds. The increase in specific activity observed as the dispersion of the catalyst decreased was attributed to the increase in relative number of carbon-carbon bond-breaking sites. This

effect overcame the detrimental repercussions of decreasing the proportion of sites active for the removal of site-blocking hydrogen.

INTRODUCTION

The cleavage of a carbon-carbon bond in saturated hydrocarbons represents one class of reactions that is important in the petrochemical industry. An example of this class of reactions is the catalytic hydrogenolysis of ethane over transition metal catalysts, which has been studied for over fifty years [1] and remains an active area of research. Ethane hydrogenolysis is commonly used as a model reaction when studying carbon-carbon bond cleavage since the analysis is not complicated by simultaneous reactions forming products other than methane. For example, Pruski et al. [2] have used nuclear magnetic resonance to study ^{13}C -enriched ethane adsorbed on a silica-supported ruthenium catalyst. Only ethane and methane were observed on the surface, suggesting that no products other than methane were formed. In contrast, when ethylene was adsorbed on this catalyst a multitude of hydrocarbon species, including surface species containing more than two carbon atoms, were seen.

Kinetic parameters for the ethane hydrogenolysis reaction over a large number of silica-supported metal catalysts were reported by Sinfelt [3]. The apparent order of reaction with respect to ethane is between 0.6 and 1.0 for a wide range of metals. For many systems, the apparent order of reaction with respect to hydrogen is strongly negative, as low as -2.5, though there is a wide variation among the

different metal catalysts. Iron and rhenium are notable exceptions, with the activity of the catalyst increasing as hydrogen pressure is increased.

The mechanism for this reaction is generally accepted to involve adsorption of ethane, dehydrogenation of the adsorbed di-carbon species, cleavage of the carbon-carbon bond and, finally, hydrogenation of the adsorbed fragments to produce methane, which then desorbs [3-5]. For example, the hydrogenolysis and deuterium exchange of ethane over the Pt(111) surface has been studied by Zaera and Somorjai [4]. They found that deuterium exchange occurred three orders of magnitude more rapidly than hydrogenolysis, producing a product distribution with maxima corresponding to exchange of one and six hydrogens. A mechanism was postulated that involved the adsorption of ethane onto the surface while a single C-H bond was broken. This species may then associatively desorb together with a hydrogen (or deuterium) atom from the surface. Alternatively, further dehydrogenation occurs to form an ethylidyne species. Breaking of the C-C bond of the adsorbed ethylidyne to form two adsorbed C-H fragments is then postulated to be the rate-limiting step for hydrogenolysis. Subsequent addition of hydrogen (or deuterium) then occurs rapidly to form the product methane.

Engstrom et al. [5] studied the mechanism of ethane hydrogenolysis over the Ir (111) and (110)-(1*2) surfaces. They found that the intermediate di-carbon species (prior to carbon-carbon bond cleavage) was a function of the orientation of the metal surface; for the (111) surface the di-carbon intermediate was proposed to be C_2H_4 , whereas on the (110)-(1*2) surface the more highly dehydrogenated C_2H_2 species was suggested to be the intermediate. One difference between this work and that of Zaera and Somorjai [4] is that competitive adsorption of hydrogen and ethane was considered in the analysis. Engstrom et al. [5] point out that neglecting to include this factor would lead to the overestimation of the extent of dehydrogenation of the intermediate di-carbon species by one hydrogen atom.

The hydrogenolysis reaction has often been suggested to be structure-sensitive; the activity of the catalyst depends on its morphology [5-16]. One of the most commonly studied features of structure sensitivity is the variation of catalytic activity with metal dispersion. For example, Carter et al. [6] studied the effect of crystallite size on the activity for the ethane hydrogenolysis reaction for nickel supported on silica-alumina. The dispersion of a 10-wt-% nickel catalyst was varied from 4% to 10% by sintering in a hydrogen atmosphere. These catalysts exhibited a systematic decrease in specific activity as the dispersion

decreased, though it appeared that for the least dispersed catalysts the specific activity of the catalysts was almost constant.

The effect of particle size on the ethane hydrogenolysis reaction has also been investigated for both unsupported and silica-supported rhodium catalysts by Yates and Sinfelt [7]. In this study the dispersion of the supported catalyst was varied by changing the metal loading between 0.1 wt % and 10 wt %. One of the supported catalysts was also calcined at various temperatures to obtain large supported crystallites. For all the catalysts studied the apparent order with respect to ethane was around 0.8. For the uncalcined supported catalysts the apparent order of reaction with respect to hydrogen was -2.1 in contrast to values of -1.4 for the supported catalyst calcined at 1073 K and -1.6 for the unsupported catalyst. The authors did not offer any explanation for these differences. However, the uncalcined supported catalysts will have significantly more edge, corner, and similar low-metal coordination sites than the other catalysts, so it seems reasonable to attribute the difference in apparent orders of reaction with respect to hydrogen to the presence of these defect-like sites. The authors noted an optimal dispersion to obtain the maximal specific activity for ethane hydrogenolysis. The supported catalysts with metal loadings in the 1 to 10-wt-% range were

most active. The least active catalysts were the supported catalysts with a metal loading below 1 wt %, the unsupported catalyst, and the catalysts that had been calcined at high temperatures.

Brunelle et al. [8] have studied the hydrogenolysis and isomerization of n-pentane over silica-supported platinum catalysts prepared by ion-exchanged and impregnated catalysts. The dispersion of the catalysts was varied by calcining at different temperatures. They found that the rate of hydrogenolysis decreased as particle size increased, whereas the rate of isomerization was not a function of dispersion.

Guczi and Gudkov [9] reported that the turnover frequency for ethane hydrogenolysis increases as the dispersion increases for the silica-supported platinum catalyst they studied. This catalyst was prepared by an ion exchange method to attain dispersions between 2% and 40%. Schay and Guczi have also obtained values of the apparent orders of reaction with respect to ethane and hydrogen for ethane hydrogenolysis over silica-supported platinum catalysts [10]. They reported values of 1 with respect to ethane and -2.1 with respect to hydrogen in the 3 to 30 Pa pressure range. Hydrogen to ethane ratios in this work were varied between 3:1 and 30:1.

In contrast to the observations of Guczi and Gudkov, Barbier et al. [11] observed that the specific activity of alumina-supported platinum catalysts for ethane hydrogenolysis decreased as the dispersion increased for a series of catalysts where the dispersion was varied by varying the metal loading. This was also true when the dispersion of a constant metal-loading-supported catalyst was changed by calcination at different temperatures. However, when the dispersion was varied by sintering constant metal-loading catalysts in a hydrogen atmosphere, an opposite trend was observed. In all cases, the apparent orders of reaction were around 1.1 with respect to ethane and between -1.9 and -2.5 with respect to hydrogen. All the catalysts used were prepared from chloroplatinic acid, and residual chlorine was observed in at least some of the catalysts, which may have affected the results. Barbier et al. [12] used these same catalysts to study the hydrogenolysis of cyclopentane. The catalyst series in which the dispersion was varied by changing the metal loading exhibited a maximum specific activity corresponding to a crystallite size of about 60 Å. However, as was the case with the ethane hydrogenolysis reaction, changing the dispersion by sintering under hydrogen at different temperatures lead to no appreciable change in specific activity. The authors observed that crystallite size was not the only important parameter determining the

activity of these catalysts; the relative activity also depended on the method chosen to change the dispersion, though the authors did not postulate why this was so.

Barbier and Marecot [13] have investigated the effect of dispersion on the ethane hydrogenolysis reaction for alumina-supported iridium catalysts. They found that decreasing dispersion, either by increasing metal loading or by calcining the catalyst, increased the specific activity for catalysts with dispersions between 8% and 67%. Apparent orders of reaction were around 1 with respect to ethane and -1.8 with respect to hydrogen for all the catalysts studied. These catalysts were prepared by impregnating the support with solutions of chloroiridic acid, so again residual chlorine may be playing a role.

Godbey et al. [14] have studied the hydrogenolysis of ethane over rhenium on Pt(111) single crystal and platinum on Re(0001) single crystal surfaces. For both single crystals, roughening the surface by argon sputtering increased the specific activity of the catalyst. Rhenium was significantly more active for this reaction than was platinum, but the most active catalysts were those with a surface composition Re_2Pt , while a Pt(111) surface covered with two monolayers of rhenium displayed virtually the same activity as the clean Re(0001) surface. The authors postulated an electronic effect extending only to first nearest neighbors to explain

their data. It is interesting to note that the apparent order of reaction with respect to hydrogen for the Pt(111) surface covered by two monolayers of rhenium (which had the same activity as the Re(0001) surface) was -0.7, compared to a value of +0.3 reported for the silica-supported catalyst [3].

Doi et al. [15] have studied ruthenium catalysts prepared from solutions of $\text{Na}[\text{Ru}_3\text{H}(\text{CO})_{11}]$ in methanol using a number of different supports. The catalysts they studied had dispersions ranging from 23% to 55%. They found little relationship between particle size and catalytic activity for these systems. However, it may be that any contribution of dispersion is masked by the effect of using different metal oxide supports. This was also true of the investigation of ethane and propane hydrogenolysis over ruthenium reported by Galvagno et al. [16], who saw no evidence to suggest that dispersion affects the activity of the catalyst. The apparent order of reaction with respect to hydrogen for ethane hydrogenolysis was measured to be between -2.21 and -1.92 for the silica-supported ruthenium catalyst. This was somewhat more negative than the value of -1.3 previously reported by Sinfelt [3]. The difference might be associated with the use of different silica supports in these two studies.

The ruthenium-copper bimetallic catalyst is particularly interesting and has received a great deal of attention, since the two metals are virtually immiscible in the bulk [17]. However, Sinfelt and coworkers have shown that the two metals interact in the supported catalyst, forming bimetallic clusters [18,19].

Sinfelt has studied ethane hydrogenolysis over silica-supported ruthenium-copper bimetallic catalysts [18,20]. He found that the activity per hydrogen chemisorption site decreased significantly as the copper content of the system increased. This led to the suggestion that the active site for ethane over ruthenium might consist of a number of adjacent ruthenium atoms (a geometric or ensemble effect).

Rouco et al. [21] have compared the silica-supported ruthenium-copper and ruthenium-silver systems. The catalysts were prepared from aqueous solutions of nitrate salts and supported on high surface area ($600 \text{ m}^2/\text{g}$) silica. Like previous studies [18,20] Rouco et al. found that the rate per hydrogen chemisorption site for ethane hydrogenolysis over ruthenium-copper catalysts decreased rapidly as copper was added, though the decrease was not as pronounced as that reported by Sinfelt. The difference might have been related to the different combinations of metal salts and supports used. The ruthenium-silver catalysts showed a modest decrease in specific activity for ethane hydrogenolysis as

the silver content was increased, but no significant change in apparent activation energy was observed. It was postulated that the silver was present predominantly as islands on the surface of the ruthenium.

Peden and Goodman [22,23] have investigated the effect of adding copper to Ru(001) single-crystal catalysts for the ethane hydrogenolysis reaction, among others. No geometric effects were observed; instead they found that the effect of adding copper was simply to block active sites on a one-to-one basis. For the pure ruthenium catalyst the apparent order of reaction with respect to ethane was found to be 0.85, in good agreement with values found for the silica-supported catalysts [3]. The apparent order with respect to hydrogen was found to be a function of hydrogen partial pressure, changing from positive to negative as the hydrogen pressure rose above 25 torr.

A supported catalyst crystallite will contain a significant number of edge and corner sites, which will have no analog on a defect-free low-index plane single crystal surface. Apparently these sites are important for many different catalyst systems. Strohl and King [24] have modeled ruthenium-silver catalysts and other segregating systems similar to ruthenium-copper. They found that the segregating element tended to preferentially populate low-coordination, defect-like edge and corner sites of the

supported metal crystallites. Once nearly all the edge and corner sites have been filled, two-dimensional islands were seen to form on the low Miller index surfaces of the particles. Kim et al. [25] have used photoemission studies of physisorbed xenon to show that copper does indeed tend to segregate to defect sites on ruthenium surfaces. Other experimental work [26,27] has shown that copper does form two-dimensional islands on Ru(0001) surfaces after annealing at 300 K. Wu et al. [28] have used nuclear magnetic resonance of chemisorbed hydrogen to show that silver does not interact with ruthenium as strongly as copper. They found that in order to cover a given fraction of a supported ruthenium crystallite, much more silver than copper was required.

The Ru-Cu and Ru-Ag catalysts also have different behaviors with respect to hydrogen chemisorption. It is well established that hydrogen can dissociatively chemisorb on ruthenium surfaces and migrate to copper (the spill-over effect) both in the case of single crystal surfaces [29,30] and for the supported catalysts [29, 30, 31, 32]. However, for ruthenium-silver catalysts, this does not occur [28, 32].

It is clear that the morphology of a catalyst can affect its activity for ethane hydrogenolysis. Since hydrogen plays an integral part in hydrogenolysis reactions, it seems likely that the interaction of a catalyst surface with hydrogen will

also affect the ethane hydrogenolysis reaction. We have investigated the silica-supported ruthenium-copper and ruthenium-silver systems, emphasizing morphology and hydrogen effects in attempt to elucidate their joint contributions towards the specific activity of these catalysts for ethane hydrogenolysis.

METHODS

The catalysts used were all supported on Cab-O-Sil HS-5 amorphous fumed silica with a surface area of $300\text{m}^2/\text{g}$ as measured by the BET method, and all the bimetallic catalysts contained 4% ruthenium (by weight). We used the incipient wetness technique to co-impregnate the support with an aqueous solution of the metal salts. The catalyst precursors for the catalysts were $\text{Ru}(\text{NO})_6(\text{NO}_3)_3$, $\text{Cu}(\text{NO}_3)_2$, and AgNO_3 . Using these salts allowed us to avoid contaminating the catalysts with chlorine.

A series of monometallic catalysts with metal loadings of 1 to 12% ruthenium (by weight) was prepared using the same method to allow us to investigate the effect of dispersion. In addition, an unsupported ruthenium powder was prepared by reduction of RuO_2 to give us a catalyst of very low dispersion.

Characterization of the catalysts was done using hydrogen chemisorption and nuclear magnetic resonance of adsorbed hydrogen, as described elsewhere [28, 32]. We carried out reaction studies using a continuous tubular reactor system, details of which have been previously reported [33]. Crystalline silica was mixed with 10 to 300 mg of catalyst to provide a bed volume of 3 cm^3 , and the catalyst was reduced in-situ for two hours while hydrogen flowed at a rate of 500 sccm through the reactor. After the

reduction step the catalyst bed temperature was lowered at a controlled rate, generally around 40 K h^{-1} , to the desired reaction temperature, during which time we continued to flow hydrogen through the reactor. Once the initial reaction temperature had been achieved, the feed was switched to the reactant mixture and samples of the product were taken and analyzed as previously reported [33]. Specific activities were calculated in terms of rate of disappearance of ethane per surface ruthenium atom per second.

The activities of the Ru-Ag/silica catalysts were measured as a function of silver content using a 10:2:1 molar ratio of hydrogen, ethane and argon. The argon was used as an internal standard for the gas chromatographic analysis. Typically, two measurements of activity at different temperatures were obtained from each catalyst load, each separated by 10 K. Some of the activity data for the hydrogenolysis of ethane of the Ru-Cu/silica catalysts reported here consisted of the data we have previously reported [33]. Additional experiments with the Ru-Cu/silica catalysts were conducted to determine the kinetic variations with the hydrogen to ethane ratio as explained later.

In addition to measuring activity for the ethane hydrogenolysis reaction as a function of group IB metal loading, we have determined apparent orders of reaction with respect to hydrogen and ethane as a function of temperature

for Ru/silica, Ru-Cu/silica, and Ru-Ag/silica catalysts. These values were obtained by changing the hydrogen to ethane ratio of the feed gas. If we assume a kinetic expression of the form

$$\text{rate} = k[H_2]^m[C_2H_6]^n$$

it can be shown that this can be transformed into the form

$$\text{rate} = k'R^m(1+R)^{-(m+n)}$$

where R is the molar ratio of hydrogen to ethane and k' is a function of temperature, total pressure, and the partial pressures of any diluent species (i.e., argon). This equation can be linearized, resulting in a linear expression in two variables (which are not independent). We fit the linearized expression to our data using a least squares regression to obtain values for the apparent orders of reaction with respect to hydrogen and ethane. This form of kinetic expression can be used to draw implications about the mechanism [3,7,10,11,13,14]. The independence of the results from any mechanistic assumptions is useful in comparing data from different groups.

RESULTS

Ruthenium dispersions of the catalysts used in this study are given in Table 1. Figure 1 shows the turnover frequency (rate per surface ruthenium) for ethane hydrogenolysis as a function of copper loading for a number of different temperatures. We see that the behavior of the system as copper was added depended strongly on the temperature. At the lower temperatures studied, addition of small amounts of copper lowered the turnover frequency dramatically. At copper atomic fractions above 10 to 15%, however, the addition of copper appeared to have little effect. At intermediate temperatures, addition of copper did not change the specific activity of the catalyst, while at the highest temperature studied, addition of small amounts of copper appeared to increase the turnover frequency until a plateau was reached at about 10 to 15% copper.

In contrast to the Ru-Cu catalysts, the Ru-Ag/silica catalysts showed an initial decrease in specific activity as silver was added at all temperatures studied (Fig. 2). The turnover frequency did not level off dramatically at the higher temperatures studied, though some leveling of the turnover frequency versus silver loading curves at the lowest temperatures shown did appear.

The Arrhenius plots for the Ru/silica and Ru-18%Cu/silica catalysts (Fig. 3) show an interesting trend.

Table 1. Ruthenium dispersion of catalysts

Cu Atom Fraction	Ruthenium Dispersion ^a
0.000	0.290
0.025	0.258
0.061	0.233
0.121	0.161
0.179	0.070
0.235	0.039
0.346	0.024
0.452	0.018
0.553	0.009
0.650	0.003
Ag Atom Fraction	Ruthenium Dispersion ^b
0.000	0.290
0.136	0.232
0.200	0.205
0.300	0.172
0.400	0.114
0.500	0.072
Wt% Ruthenium	Ruthenium Dispersion ^b
100	0.016
12	0.190
8	0.230
4	0.260
1	0.300

^a From NMR of chemisorbed hydrogen.

^b From strong hydrogen chemisorption.

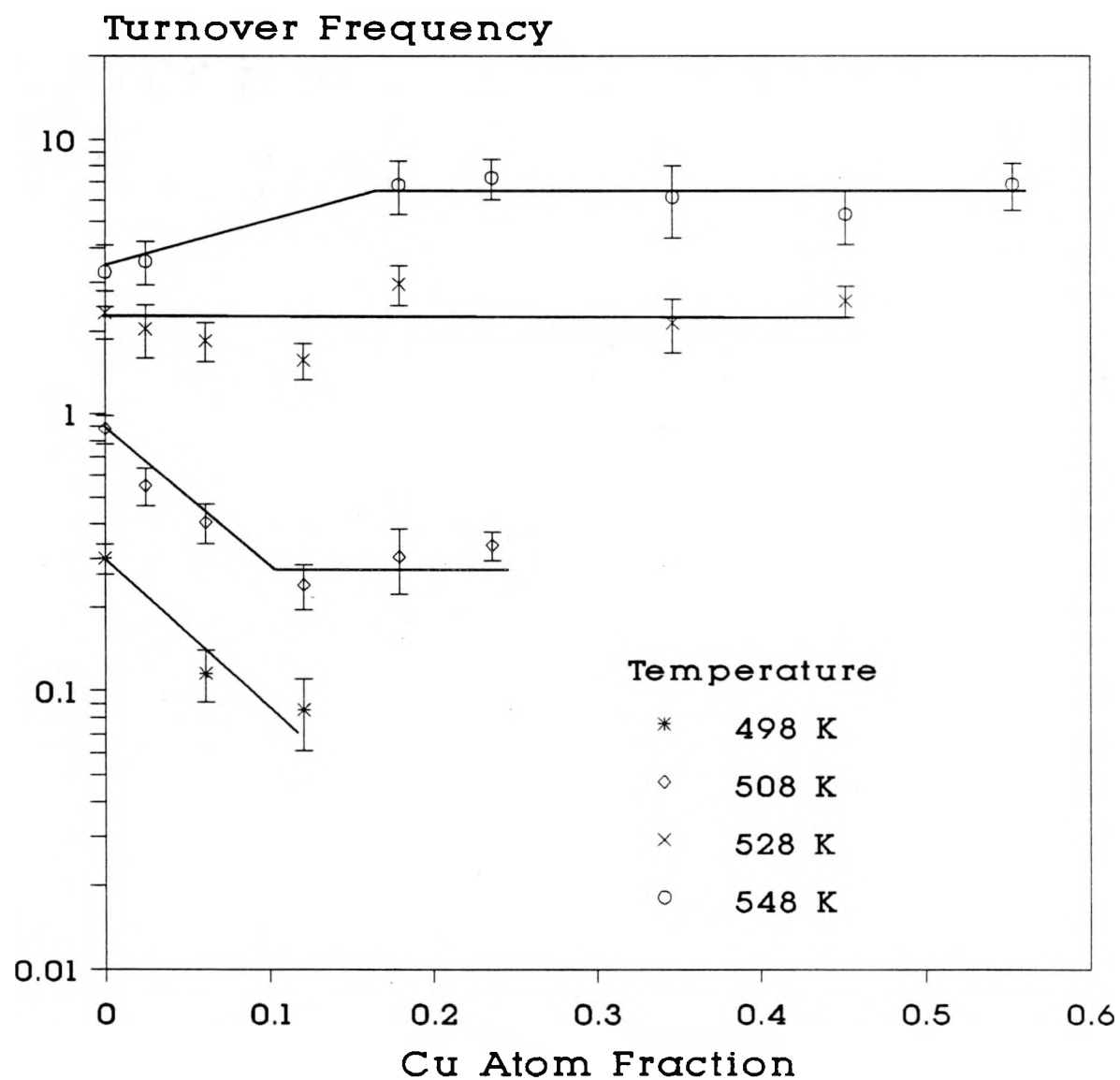


Figure 1. Rate of ethane hydrogenolysis (± 1 standard deviation) per surface ruthenium as measured by proton NMR for Ru-Cu/SiO₂ catalysts

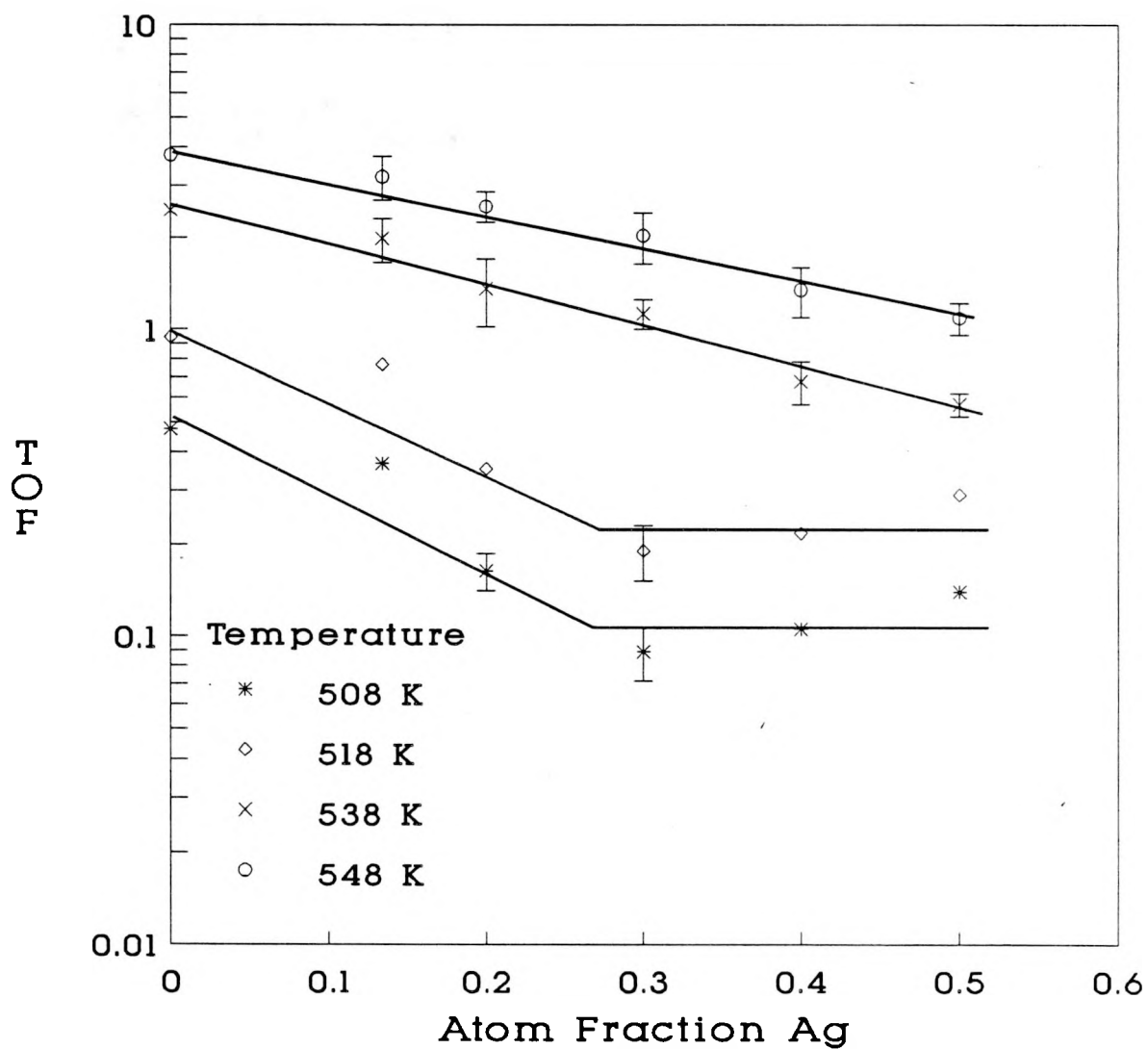


Figure 2. Rate of ethane hydrogenolysis (± 1 standard deviation) per surface ruthenium as measured by strong hydrogen chemisorption for Ru-Ag/SiO₂ catalysts

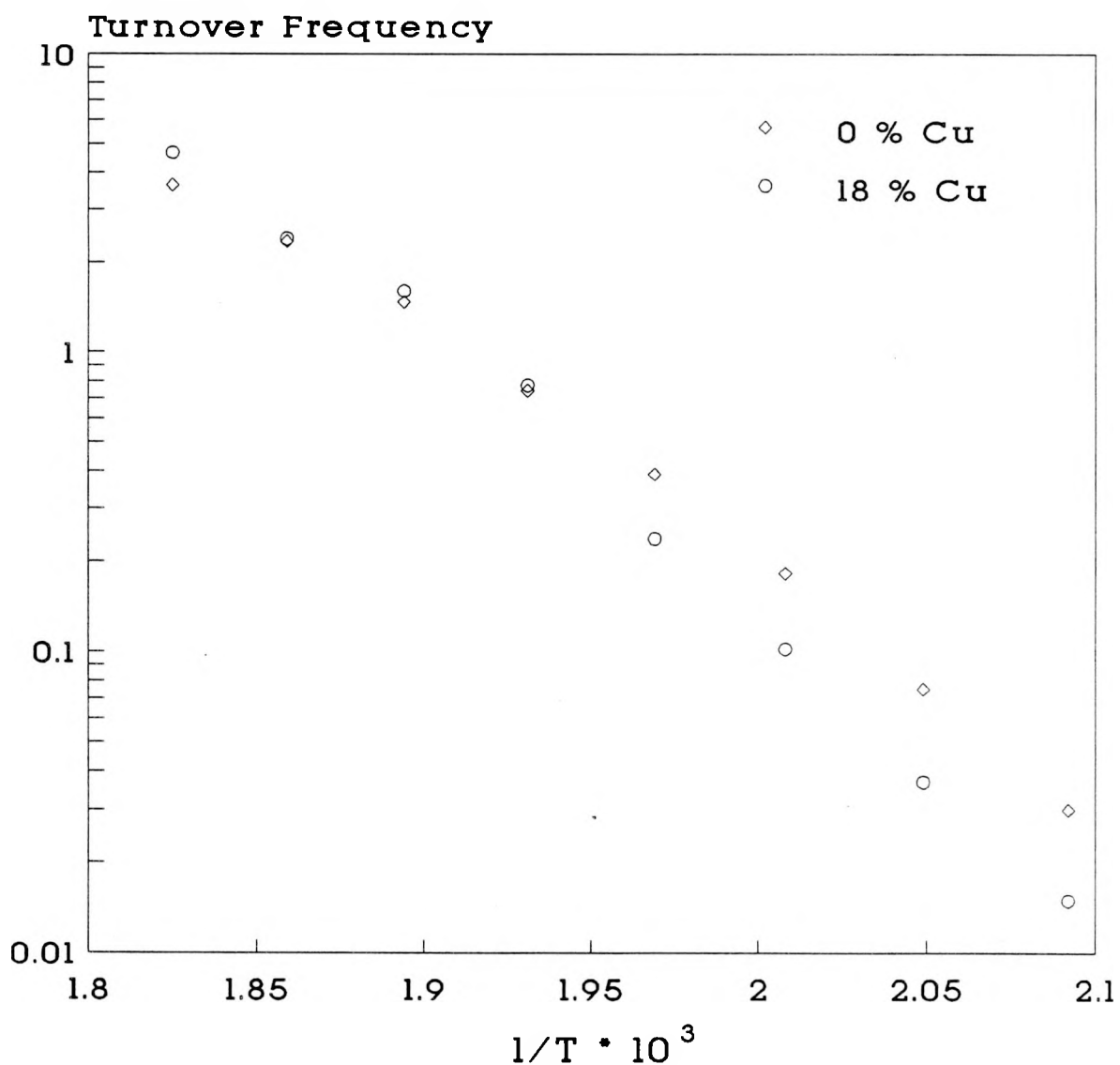


Figure 3. Arrhenius plots for Ru/SiO₂ and Ru-Cu/SiO₂ catalysts

At a temperature of 515 K the two curves intersected. Below 515 K the two curves suddenly diverged, with the pure ruthenium catalyst activity being substantially above that of the Ru-Cu catalyst. Above 515 K the order was reversed, in that the Ru-Cu was more active than the pure ruthenium. The Arrhenius plots for the Ru-Ag/silica catalysts (Fig. 4) did not exhibit this behavior. Instead, all the curves were nearly parallel throughout the temperature range we have studied. The Ru-Ag catalyst was less active than the pure ruthenium at all temperatures studied.

An example of the curve fit used to obtain the apparent order of reaction data is given in Fig. 5. As can be seen, the expression fit the data well over the entire range of hydrogen to ethane ratios at both temperatures studied. The values obtained for the apparent orders of reaction for ethane hydrogenolysis over Ru/silica, Ru-18%Cu/silica, and Ru-40%Ag/silica are given in Table 2 and are graphically presented in Figs 6a-b. These group IB metal fractions were chosen because Monte Carlo simulations suggested that nearly all edge and corner sites of the supported crystallites would be occupied by the group IB metal [34]. We see that the apparent order with respect to hydrogen for both the pure ruthenium and the ruthenium-silver bimetallic catalysts did not change significantly from 508 K to 548 K. For the pure ruthenium catalyst the order with respect to hydrogen

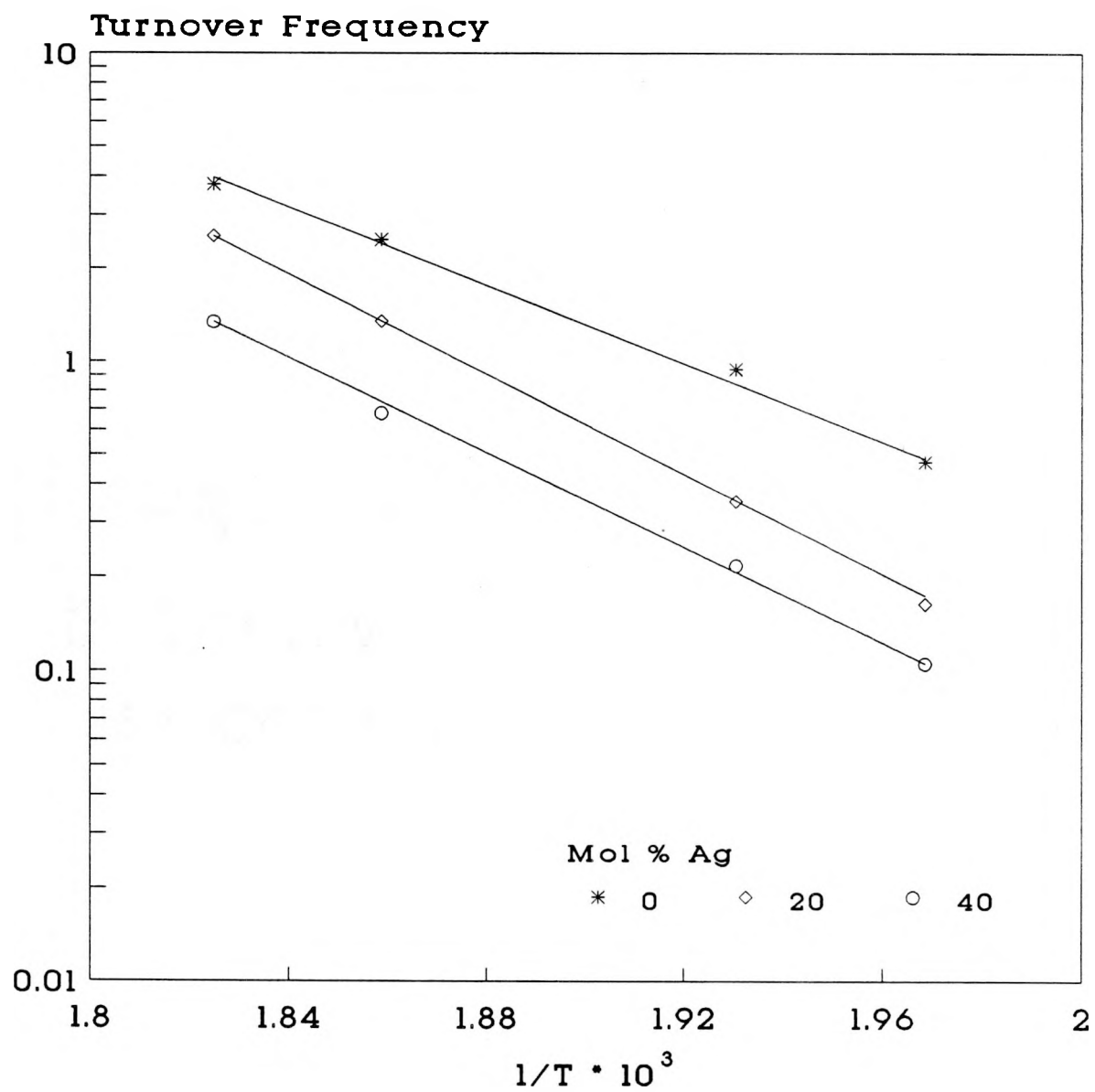


Figure 4. Arrhenius plots for Ru-Ag/SiO₂ catalysts

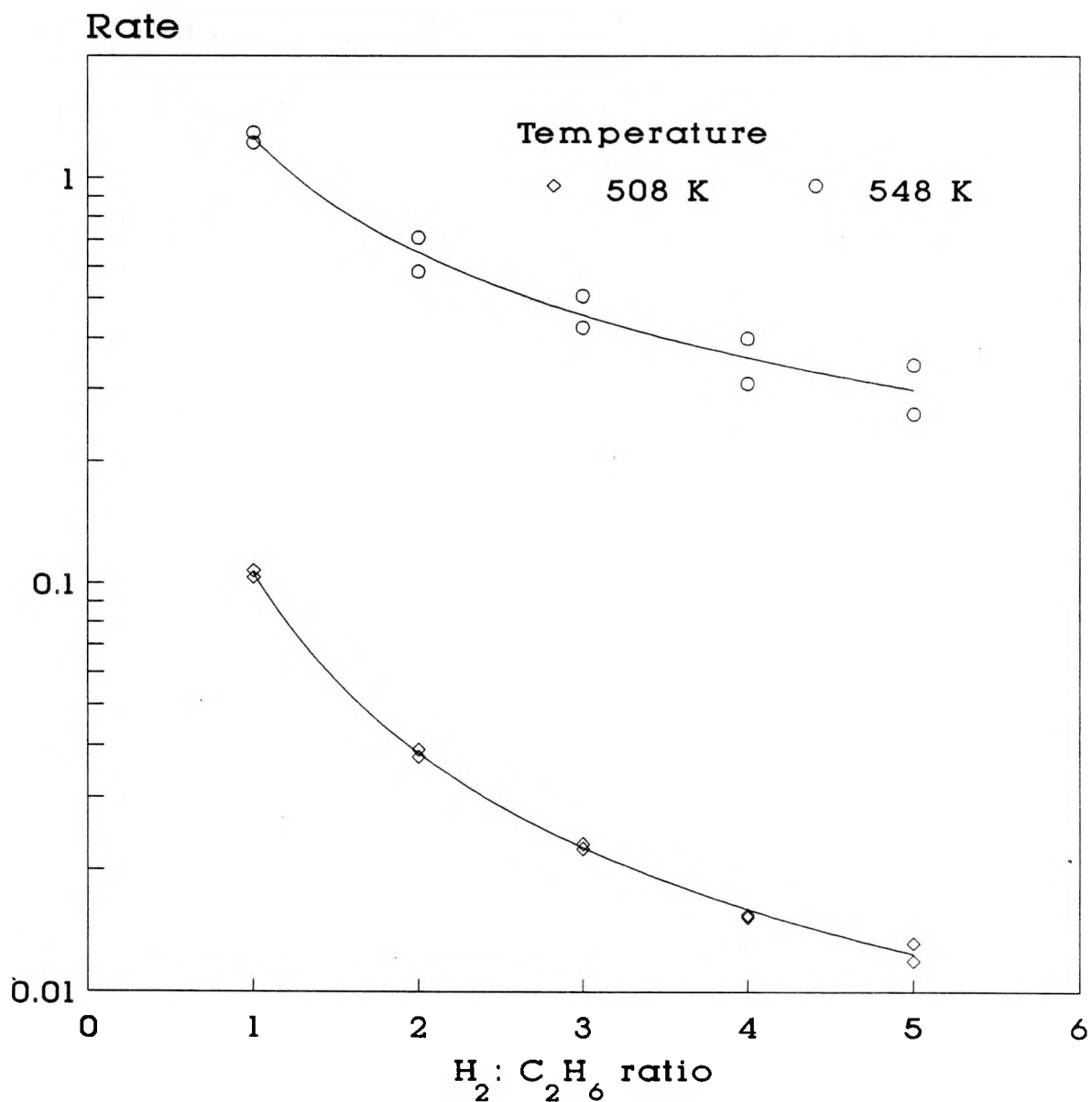


Figure 5. Rate of ethane hydrogenolysis as a function of $H_2 : C_2H_6$ ratio for Ru-18%Cu/SiO₂ catalyst fitted by expression used to calculate apparent orders of reaction

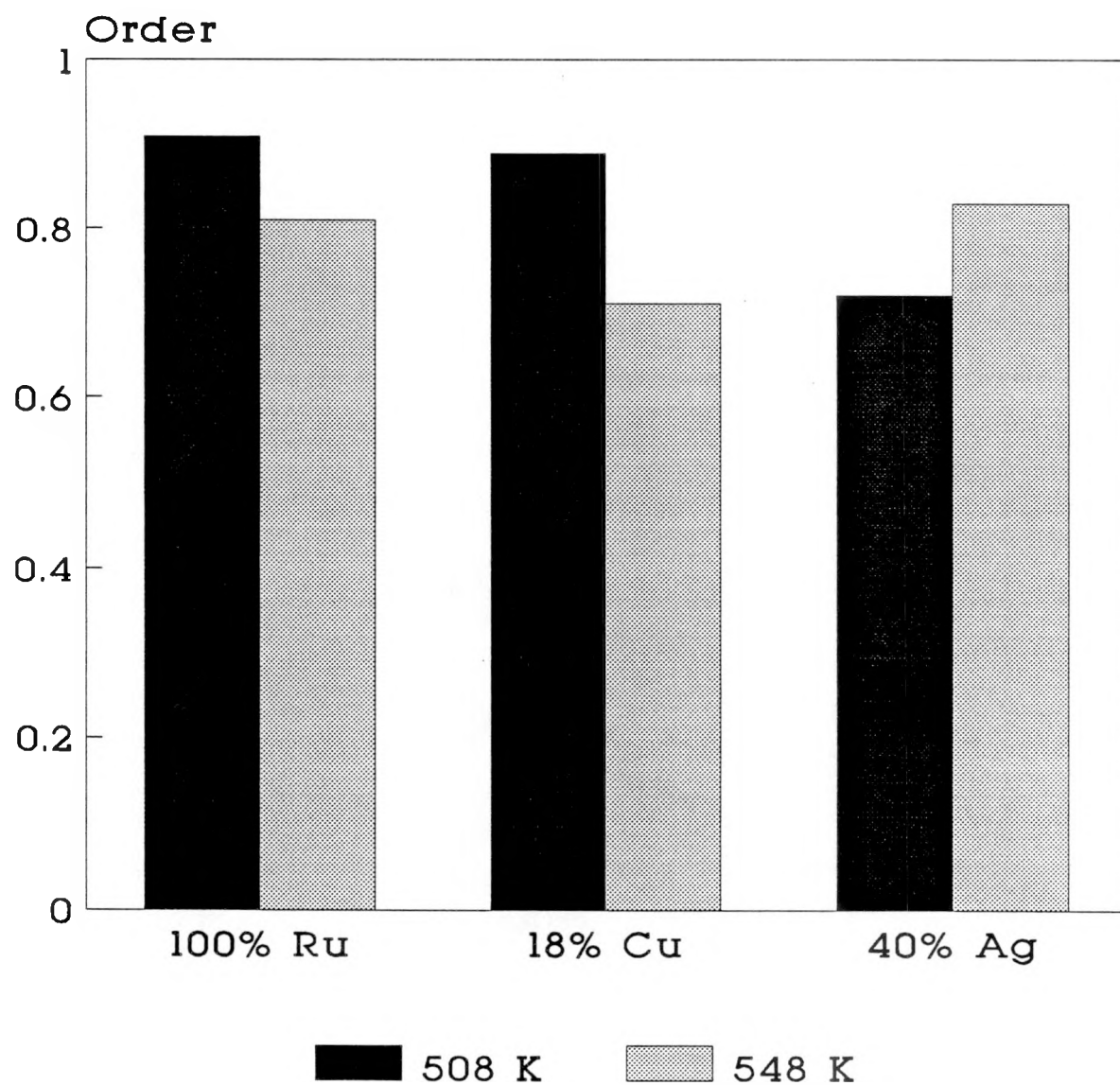


Figure 6(a). Apparent order of reaction with respect to ethane for Ru/SiO_2 , $\text{Ru}-18\%\text{Cu}/\text{SiO}_2$, and $\text{Ru}-40\%\text{Ag}/\text{SiO}_2$ catalysts at 508 K and 548 K

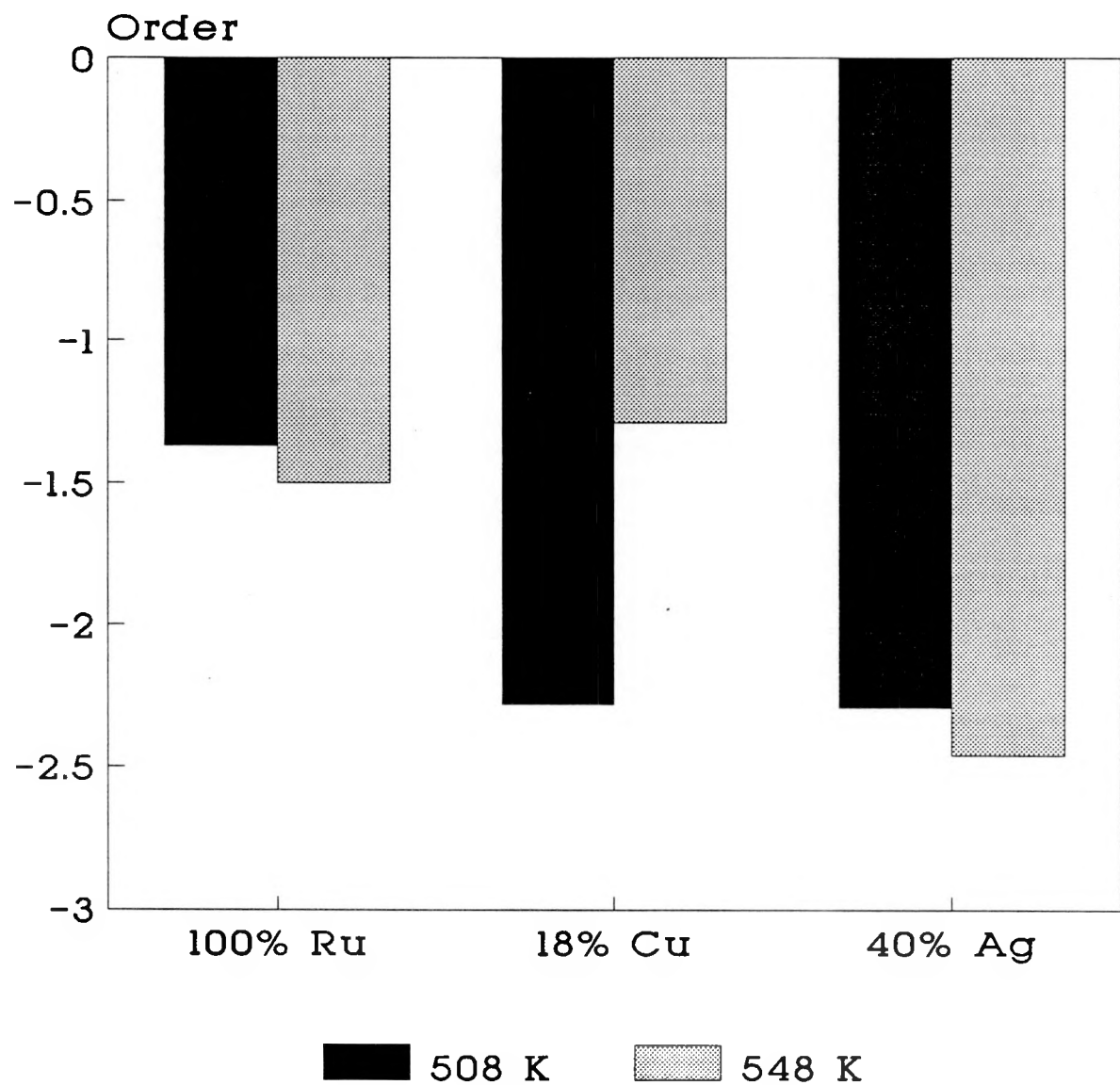


Figure 6(b). Apparent order of reaction with respect to hydrogen for Ru/SiO_2 , $\text{Ru}-18\%\text{Cu}/\text{SiO}_2$, and $\text{Ru}-40\%\text{Ag}/\text{SiO}_2$ catalysts at 508 K and 548 K

Table 2. Apparent order of reactions for ethane
hydrogenolysis with respect to ethane and hydrogen

Catalyst	Temp. (K)	Order w.r.t.	
		Ethane	Hydrogen
100% Ru	508	0.91	-1.37
	548	0.81	-1.50
18% Cu	508	0.89	-2.28
	548	0.71	-1.29
40% Ag	508	0.72	-2.29
	548	0.83	-2.46

remained at about -1.4 and in the case of the ruthenium-silver bimetallic the value was around -2.4. In contrast, the ruthenium-copper bimetallic showed a significant change in the apparent order of reaction with respect to hydrogen between the two temperatures studied. At 508 K, the measured value of -2.28 was almost identical to that for the ruthenium-silver bimetallic, while at 548 K the apparent order of reaction with respect to hydrogen was -1.29, close to the value of -1.5 found for the pure ruthenium catalyst. We also noted that the apparent order of reaction with

respect to ethane for all the catalyst and temperature combinations studied was around 0.8.

The activity of the series of pure ruthenium catalysts with different metal loadings is shown as a function of the dispersion of the catalysts in Fig. 7. The ruthenium powder was reduced at 573 K to ensure that it was not sintered. The supported catalysts were all reduced at 723 K. We also made runs for the highest and lowest metal-loading supported catalysts where the reduction temperature was 573 K. The activity of the supported catalysts was not a function of reduction temperature. As can be seen, generally the specific activity decreased as the dispersion increased, though at the lowest dispersions the effect of changing dispersion was minimal.

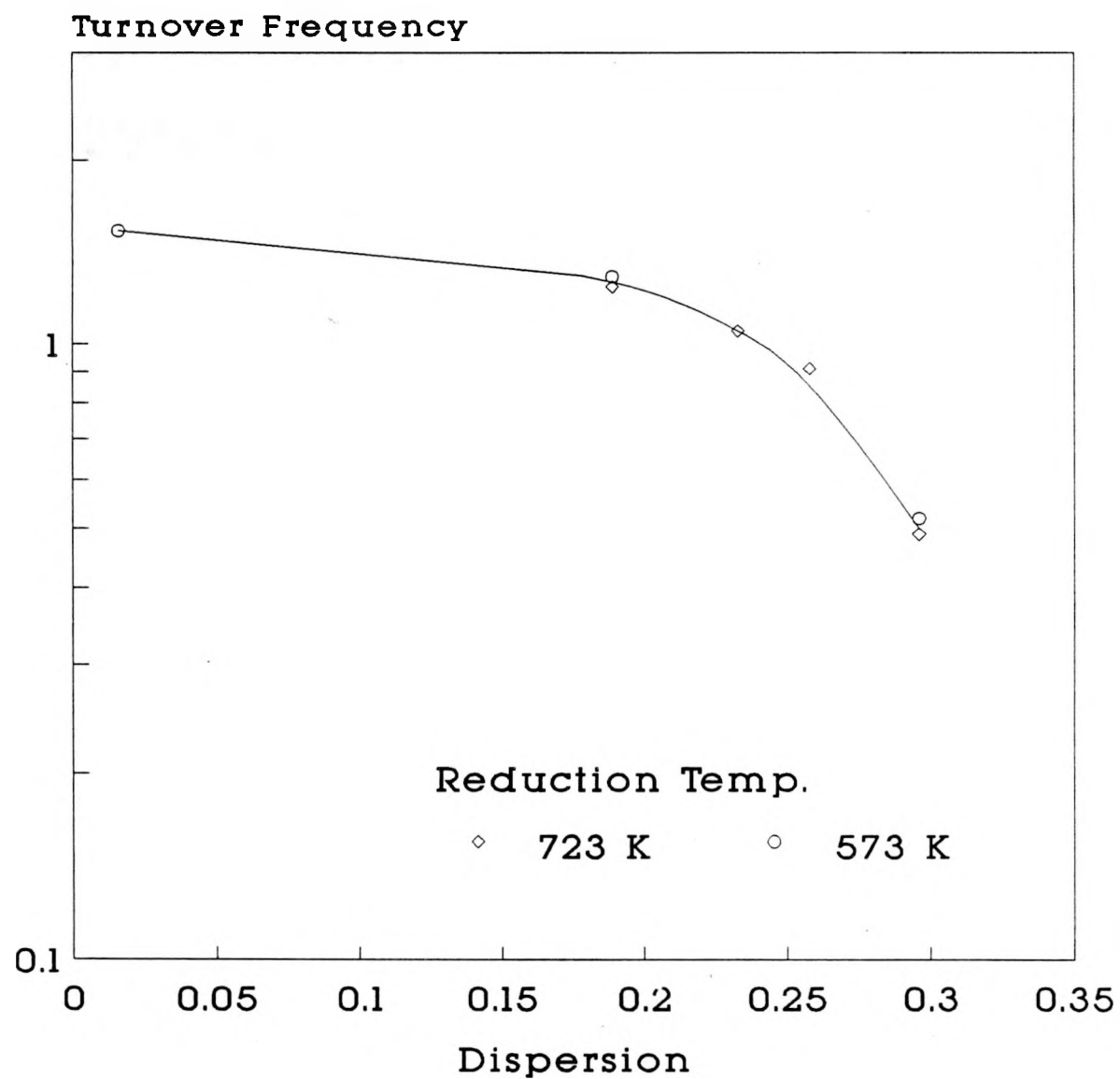
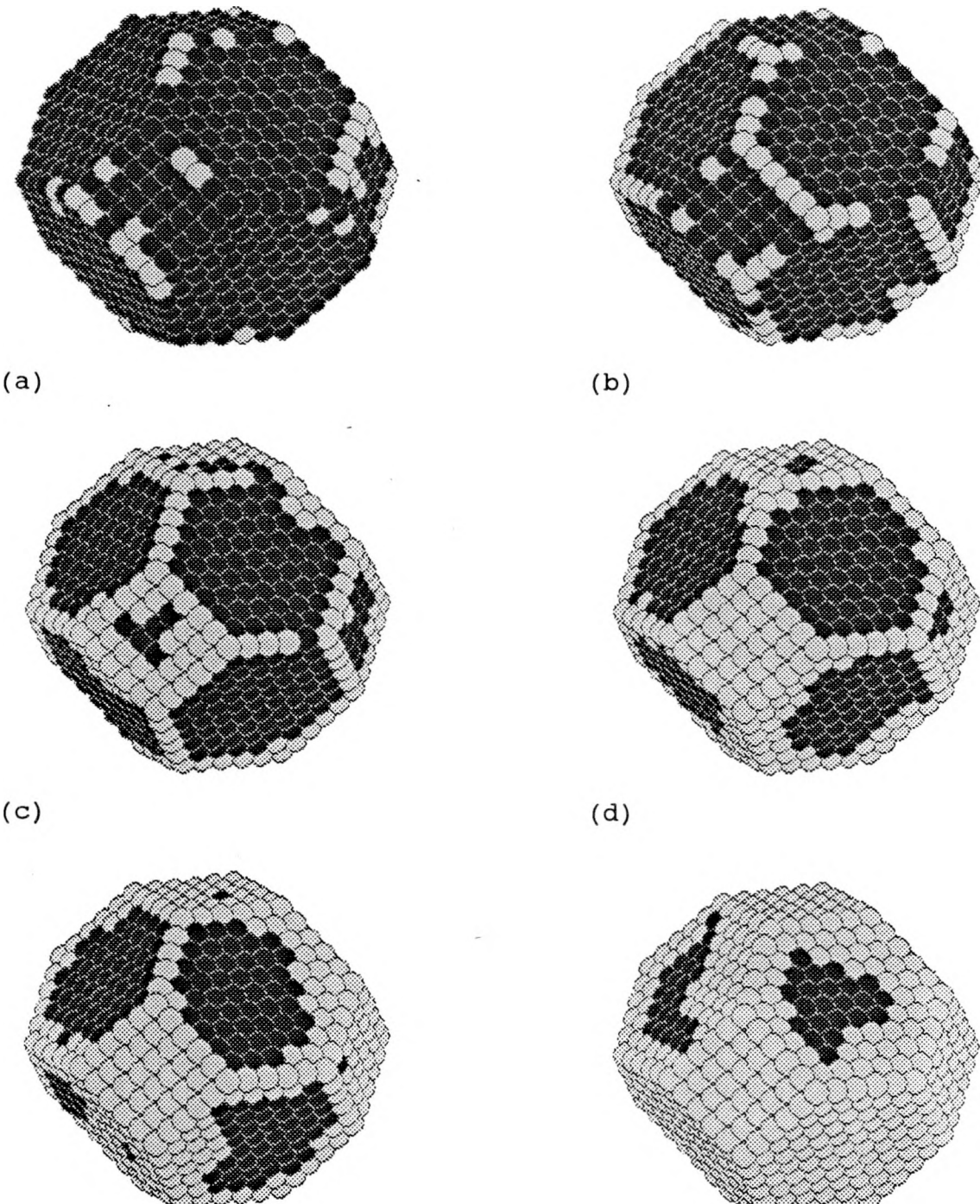


Figure 7. Specific activity of monometallic Ru catalysts as a function of dispersion



(e) (f)
Figure 8. Monte Carlo simulation results for Ru-Cu/SiO₂ catalysts with a total metal dispersion of 30%;
(a) 2% Cu, (b) 5% Cu, (c) 10% Cu, (d) 15% Cu,
(e) 20% Cu, (f) 30% Cu

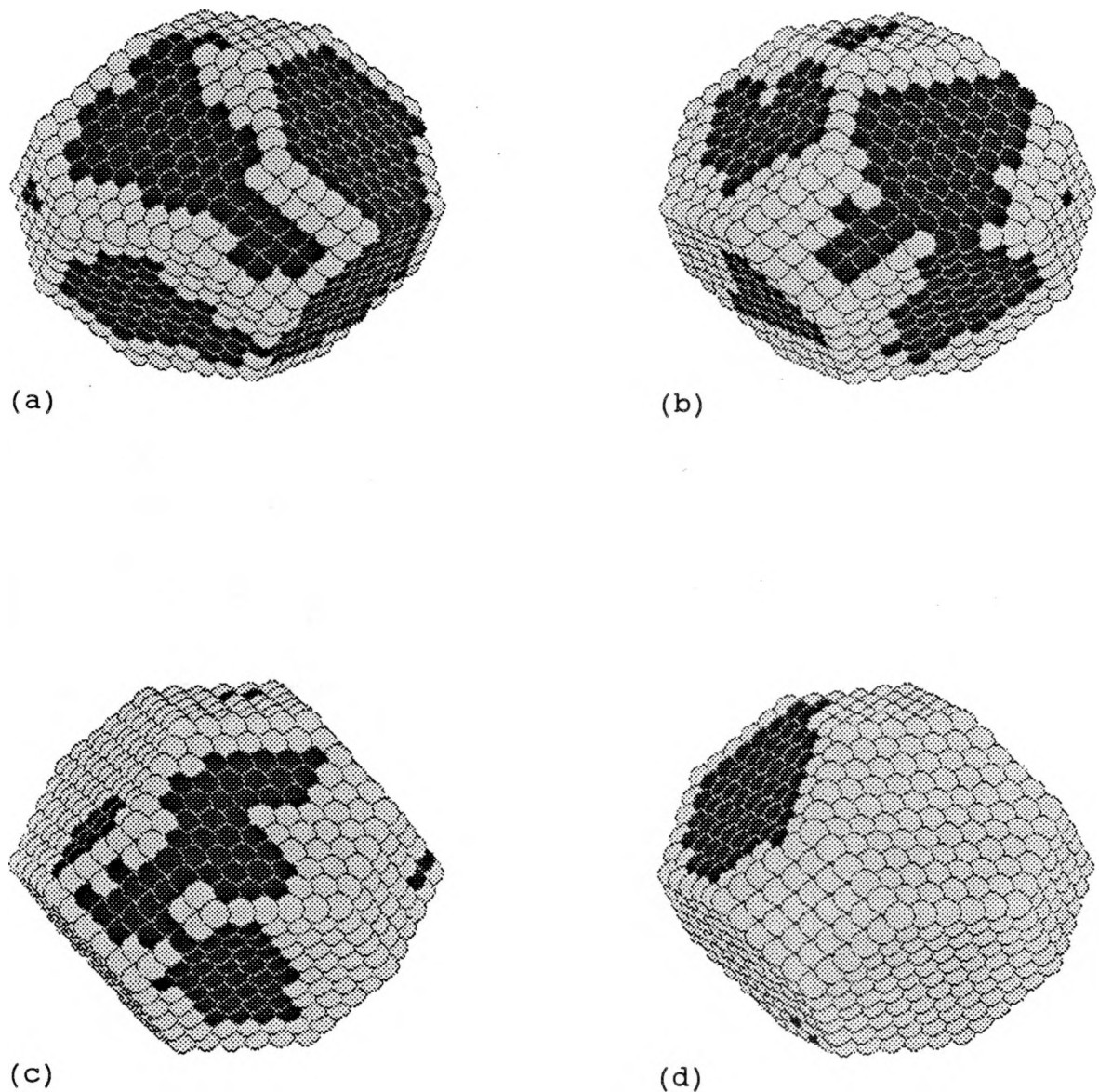


Figure 9. Monte Carlo simulation results for Ru-Ag/SiO₂ catalysts with a total metal dispersion of 30%:
(a) 13% Ag, (b) 20% Ag, (c) 30% Ag, (d) 40% Ag

DISCUSSION

We find it useful while attempting to explain our reaction data to have a model of the bimetallic crystallites on the catalyst support. The use of a Monte Carlo simulation technique to model ruthenium-group IB metal catalysts has been previously described [24,33]. As with all simulation procedures, we should be aware of limitations to the technique. The output from the simulation is an equilibrium solution and as such does not take the kinetics of the formation of the bimetallic crystallites into account. Given a sufficiently long reduction step for our catalysts, this should not be a restriction to our use of the model. In addition, the simulations do not, in general, allow for modification of the catalyst surface due to adsorbed species. However, simulations have been reported that allow for an adsorbed species such as hydrogen or carbon monoxide [24]. It was found that the presence of an adsorbate did not significantly change the calculated crystallite morphology in cases where the metal-metal bond is much stronger than the metal-adsorbate bond. A final limitation of the simulations is that they are done with a rigid lattice. The crystal structure used in the simulation is a face-centered cubic lattice while ruthenium has a hexagonal close-packed structure. Since ruthenium does not mix with either silver or copper, but merely provides a surface for the second metal

to form aggregates, the general results are not significantly influenced by this limitation. Given these restrictions, we believe that the simulations can give useful qualitative results for an average particle size that can be used to assist our understanding of the systems we have studied.

The Monte Carlo simulation results suggested that when a small amount of copper was added to a ruthenium catalyst, it preferentially populates the edge and corner sites of the bimetallic crystallites (Fig. 8a-c). Only when these sites were filled with copper were the low-index planes covered with copper (Fig. 8d-f). We notice that the simulation suggested that the copper tends to form two-dimensional rafts on the low-index ruthenium planes, as has been observed experimentally [26,27]. Copper was occupying all the edge and corner sites of the crystallite at Cu:Ru ratios as low as 1:9.

Modeling of the ruthenium-silver catalysts gave results similar to those observed for the ruthenium-copper case (Fig. 9a-d). This system, however, required significantly more of the group IB metal before there was no longer any ruthenium at the edge and corner sites of the catalyst crystallite. In fact, for a particle with a total metal dispersion of 30%, it was not until over 30 to 40% of the particle was made up of silver that all the edge and corner sites were occupied by the silver. Experimental results have confirmed that silver

is less inclined to cover the surface of ruthenium crystallites than copper [28, 32].

Figure 1 shows that at the lower temperatures studied, the addition of a small amount of copper to the ruthenium catalyst caused a dramatic decrease in specific activity. For copper to ruthenium atomic ratios above 1:9, however, there appeared to be no change in specific activity as copper was added to the system. This breakpoint coincided with the point at which the Monte Carlo simulation predicts that all the edge and corner sites of the bimetallic particles were occupied by copper, suggesting that these sites play a special role in the reaction. At the intermediate temperature studied, no change occurred in specific activity as the copper content of the catalyst was increased. At the highest temperature studied, we observed a reversal in behavior, as the addition of a small amount of copper to the system appeared to increase the turnover frequency for ethane hydrogenolysis. Again, a breakpoint was observed at a copper to ruthenium ratio of 1:9, above which the addition of copper did not change the specific activity of the catalyst. This change in trend at higher temperatures suggested that the relative importance of the defect sites and low-index planes might be changing.

In contrast to the results for ruthenium-copper, we can see in Fig. 2 that the specific activity of the ruthenium

catalyst decreased as silver was added to the system at all temperatures studied. The Monte Carlo simulations predicted that copper was much more efficient at covering defect-like sites than silver. If the ethane hydrogenolysis reaction is structure-sensitive, occurring more rapidly on defect-like sites than on the basal planes of the supported ruthenium crystallite, it would therefore be expected that the effect of adding silver would be less pronounced than adding copper. Moreover, if the group IB metals played no part in the reaction, we might expect that the effect of covering a given fraction of edge and corner sites with silver or copper would be the same. The fact that copper and silver appeared to affect the catalyst in different ways suggests that either or both of the group IB metals may be actively participating in the reaction, at least at one of the extremes of the temperature range we have studied. Since hydrogen, which of course takes part in the reaction, is known to migrate from ruthenium to copper, both on single-crystal catalysts [29, 30] and silica-supported catalysts [29, 30, 31], we suspected that the copper might be playing a role in the reaction. In addition, hydrogen does not spill over from ruthenium to silver in the Ru-Ag/silica catalysts [28, 32] and, therefore, silver merely occupies surface sites. We ruled out the possibility of an electronic effect since the

Arrhenius plots for pure ruthenium and ruthenium-silver catalysts are virtually parallel.

The Arrhenius plots for a pure ruthenium catalyst and one in which 18% of the metal atoms are copper showed interesting differences. At temperatures above 515 K the two curves were coincident except at the very highest temperature studied. Below 515 K the curve for the pure ruthenium catalyst was higher than that for the 18% copper catalyst. However, at these lower temperatures, the two curves were still running parallel to each other, suggesting that the apparent activation energy at any given temperature was identical for the two catalysts. This suggested to us that the cleavage of the carbon-carbon bond of a dehydrogenated di-carbon species probably remained the rate-limiting step [4, 24, 5] as copper was added to the catalyst. Since copper tends to populate the edge and corner sites of a supported ruthenium crystallite preferentially, the implication was that either the mechanism for ethane hydrogenolysis on these defect-like sites was no different than that on the low-index planes or that the role of the edge and corner sites was not in the facilitation of the carbon-carbon bond cleavage.

In our attempts to explain the disparate behaviors of the silica-supported Ru, Ru-Cu, and Ru-Ag catalysts, it became obvious that investigation of the apparent orders of

reaction for these catalysts at the two extremes of temperatures studied could give enlightening results. The values we measured are given in Table 2. Our choice of copper and silver atomic fractions of 0.18 and 0.40, respectively, was dictated by the results of Monte Carlo simulations, which suggested these fractions of the group IB metals would nearly cover all the edge and corner sites of the ruthenium crystallites. We saw that the apparent order of reaction with respect to ethane was essentially constant at around +0.8 for all six catalyst and temperature combinations we used. This is in good agreement with published results for both supported and single crystal ruthenium catalysts [3,22].

The behavior of the apparent order with respect to hydrogen, however, was much more interesting. For the pure ruthenium catalyst, the apparent order of reaction with respect to hydrogen did not change appreciably between the two temperatures studied, with the mean value, -1.44, in good agreement with that of Sinfelt, who reported a value of -1.3 for a silica-supported ruthenium catalyst at 461 K.

For the case of the Ru-Ag catalyst we also saw no significant difference in the apparent order of reaction with respect to hydrogen at the two temperatures studied. However, for this bimetallic catalyst the value obtained, around -2.4, was considerably more negative than that found

for the pure ruthenium catalyst. Such a large negative value is not unprecedented. Apparent orders of reaction with respect to hydrogen for the ethane hydrogenolysis reaction of around -2.4 have been reported for systems such as silica- or alumina-supported platinum [3,11]. In comparison with ruthenium, silver had negligible activity for the hydrogenolysis of ethane, and hydrogen spillover from ruthenium to silver did not occur [28, 32]. It therefore seemed likely that silver was acting as an inert site blocker. The composition of the Ru-Ag catalyst was chosen such that we expected all the defect-like sites to be occupied by silver, so that any difference observed between the pure ruthenium and Ru-Ag catalysts was due to the presence of these edge and corner sites in the pure ruthenium catalysts. The decrease in specific activity of these catalysts as the proportion of silver increased, together with the more negative order of reaction with respect to hydrogen of the silver-containing catalyst led us to the hypothesis that the low-coordination ruthenium sites were important in removing hydrogen from the surface.

The hydrogen was generated in part from the dissociative chemisorption of hydrogen in the feed gas. However, though the ethane hydrogenolysis reaction is a net consumer of hydrogen, the intermediate species were highly dehydrogenated [3-5]. It is probable that the hydrogen removed from the

ethane to form the dehydrogenated fragments on the surface was itself adsorbed onto the metal catalyst, further adding to the pool of adsorbed hydrogen. Absence of the sites most active for the removal of hydrogen therefore led to the blocking of active sites on low-index ruthenium surfaces by hydrogen. Therefore, the low-coordination and high-coordination sites each played a different role in the reaction. High-coordination sites were predominantly active for the carbon-carbon bond cleavage. Hydrogen may adsorb on these sites directly or first dissociate on the edge and corner sites and move onto the high-coordination sites, blocking adsorption and subsequent reaction of ethane. Hydrogen may migrate from high- to low-metal coordination sites, which were more active for the associative desorption of hydrogen than the highly coordinated ruthenium surface atoms.

The concept that the interaction of hydrogen with a metal surface depends on the coordination of the metal atoms is not unprecedented. Wu et al. [28, 32] have shown, using nuclear magnetic resonance of adsorbed hydrogen, that there were two different hydrogen adsorption sites on a supported ruthenium crystallite. They found that increasing the number of edge and corner sites in the supported metal particle allowed more weakly adsorbed hydrogen to be present on the surface.

A number of groups have studied hydrogen adsorbed on platinum single-crystal surfaces. Christmann et al. [35] investigated hydrogen on the Pt(111) surface. For a well-annealed surface they observed two adsorption states. When there were defects in the surface a third, more strongly adsorbed, state was noted. Hydrogen-deuterium exchange reaction studies suggested that hydrogen was adsorbed dissociatively on the platinum surface.

Bernasek and Somorjai [36] found that at low pressures the stepped Pt(997) and Pt(553) surfaces were significantly more active for hydrogen-deuterium exchange than the Pt(111) surface. They attributed this to an enhanced activity for dissociating hydrogen (or deuterium) at the step sites. Associative desorption on the surface was the predominant mechanism at lower temperatures; at temperatures above 600 K, exchange between a gas-phase molecule and an adsorbed atom was observed. Poelsema et al. [37] have also studied hydrogen adsorbed on the Pt(997) surface. They observed that desorption of hydrogen occurred via second-order kinetics, as might be expected. Two distinct sites for the adsorption of hydrogen were seen, with heats of adsorption of 22 and 19 kcal/mole being attributed to step edge sites and terrace sites, respectively. The authors noted that the surface hydrogen atoms were mobile, adsorbing on terraces and migrating to step edges.

Salmeron et al. [38] have studied the hydrogen-deuterium exchange reaction as a function of the approach angle of the reactant over the Pt(332) and Pt(553) single-crystal surfaces. They found that reaction probability was greatest when the reactants approached the open side of the step directly. Measurements using a Pt(111) single-crystal surface indicated that there was a small activation energy barrier (>0.4 kcal/mole) for adsorption of hydrogen, whereas adsorption onto the Pt(332) surface was not activated. Later work by the same authors [39] confirmed that hydrogen adsorption onto the Pt(111) surface was activated, with an activation energy of 0.5 to 1.5 kcal/mole, and that there was no activation energy barrier for the adsorption of hydrogen onto the stepped Pt(332) surface. The authors found that surfaces of differing roughness, which were indistinguishable from their LEED patterns, had significantly different activities for hydrogen-deuterium exchange. Analysis of the data led to the conclusion that recombination of adsorbed atoms was the rate-limiting step. A number of different unspecified pathways were postulated to be important, the same mechanisms being important for both the Pt(111) and Pt(332) surfaces. One mechanism was observed over the entire temperature range studied (298 K to 1073 K). Activation energies for this mechanism were calculated to be 13.0 kcal/mole for the Pt(332) surface and 15.6 kcal/mole for the

Pt(111) surface. At temperatures below 573 K, a second pathway was postulated, acting in series with the first; above 573 K a third mechanism was suggested, this time acting in parallel with the first mechanism.

Smith et al. [40, 41] have proposed that edge sites of supported platinum and palladium catalysts are significantly more active for dissociative hydrogen chemisorption than the low-index planes. Moreover, the addition of hydrogen to unsaturated surface species occurred at sites on the low-index planes by hydrogen that migrated from the defect-like sites.

Given the hypothesis that the defect-like sites are most active for the dissociation and association of hydrogen while the low-index planes are most active for hydrogenolysis, the ruthenium-copper system becomes even more interesting. This is a system where the group IB metal segregates to the low coordination sites of the supported crystallites even more strongly than does silver. At the same time, we have the well-documented phenomenon of hydrogen spillover for this system [29-31]. Thus, even though copper is essentially inactive for the hydrogenolysis reaction, it could be active as source or sink for hydrogen. Therefore, since it appears that hydrogen acts to inhibit the hydrogenolysis reaction, the role of copper in the catalyst may be more than that of simply blocking active sites.

At the lower temperature studied, the apparent order of reaction with respect to hydrogen of the ethane hydrogenolysis reaction was essentially the same as that for the Ru-Ag catalyst. It would appear that at low temperatures, therefore, copper, like silver, simply acted to block hydrogen desorption sites. At the higher temperature studied, however, a dramatic change took place. For this case, the apparent order of reaction with respect to hydrogen of the pure ruthenium and Ru-Cu bimetallics were almost the same, considerably less negative than the value obtained for the Ru-Ag bimetallic. It would appear that at this higher temperature the copper at the low-coordination sites was effective in removing hydrogen from the surface of ruthenium. This explains why, at the highest temperatures studied, the specific activity of the ruthenium catalyst appeared to increase as a small amount of copper was added to the system.

At these lowest copper loadings, the copper was populating edge and corner sites exclusively. These sites were much less active for carbon-carbon bond cleavage than the low index planes. Hydrogen chemisorption onto copper is known to be an activated process, with an activation energy around 5 kcal mol⁻¹ [42], so we would expect that the desorption process is also activated. At the highest temperatures studied, therefore, we suggest that hydrogen can be removed from the surface by copper at defect-like sites.

Thus, at high temperatures, addition of copper changed neither the absolute rate of carbon-carbon bond cleavage nor the absolute rate of hydrogen desorption compared to the monometallic ruthenium catalyst. However, the proportion of the surface occupied by ruthenium decreased, while the overall activity was not changed, leading to an increase in the rate per surface ruthenium atom. That is, the edge and corner atoms were not sites for the hydrogenolysis reaction.

The activity of the ruthenium-copper system did not continue to increase as copper was added beyond the point at which it occupied all the high-index sites. This indicated that the dominant effect beyond this point was to block the ruthenium sites that were active for the carbon-carbon bond cleavage. This could be done without decreasing the number of sites available for desorption of the site-blocking hydrogen. It is also possible that the copper on the ruthenium surface may be mobile at the highest temperatures studied. For a number of reasons we do not believe that this is happening. Silver has a lower melting point than copper but the Ru-Ag catalyst shows no evidence for silver mobility. Since we were operating at only about 28% of the mean melting point of ruthenium and copper, it seemed unlikely that the copper mobility was significantly affecting our catalysts.

The behavior of the monometallic ruthenium catalyst as a function of dispersion was opposite to that observed for

platinum catalysts [8,9], though in some cases optimal dispersions have been observed [7]. In fact, the specific activity of iridium catalysts was seen to decrease as dispersion was increased [13], the same trend that we observed for our ruthenium catalysts. Note that the apparent order of reaction with respect to hydrogen for silica-supported iridium and ruthenium catalysts was quite similar, at -1.6 and -1.3, respectively [3], while that for platinum catalysts was -2.5 [3]. These apparently contradictory results may be reconciled by considering the competing effects of increasing the proportion of edge and corner sites and increasing the proportion of highly coordinated surface atoms. Increasing the proportion of highly coordinated surface atoms would increase the relative number of sites active for the breaking of carbon-carbon bonds. At the same time, however, the relative number of sites for associative desorption of hydrogen atoms would decrease, thereby increasing the effect of hydrogen poisoning. It would therefore be expected that for systems where the apparent order of reaction with respect to hydrogen was highly negative, decreasing the proportion of defect-like sites would be more detrimental than for systems where the order was less negative. Indeed, eventually the activity-enhancing effect of increasing the proportion of sites active for carbon-carbon bond cleavage would overcome the detrimental

effect of decreasing the proportion of sites most active for the removal of hydrogen from the surface. This suggested that there should be an optimal crystallite size, which would be a function of the system and ethane to hydrogen ratio used. We extrapolated the single-crystal data of Peden and Goodman [22] from the 20:1 $H_2:C_2H_6$ ratio they used to the 5:1 ratio used in this work and found a specific activity of 0.4, lower than the activity of the lowest dispersion catalyst we used. This suggested that there may indeed be an optimal ratio of defect-like to low-index sites, though for the case of ruthenium this optimal ratio would be very low. It must be noted, however, that the single-crystal work was done at substantially lower total reactant pressures than our studies, so the extrapolation may not be valid.

It would appear, therefore, that the dominant effect of adding a group IB metal to a silica-supported ruthenium catalyst was to change the rate of hydrogen desorption from the surface. Desorption occurred fastest on the low coordination sites that were preferentially populated by the group IB metals. These were not as active for hydrogen desorption at low temperatures as was ruthenium. At higher temperatures, however, copper appeared to have a significant ability to remove hydrogen from the low-index ruthenium planes.

CONCLUSION

At the lower temperatures studied, adding copper or silver to our silica-supported ruthenium catalysts had virtually the same effect in kind, though the effect in degree of adding copper was much more pronounced. We think that this is because both group IB metals tended to block the low-coordination sites of the supported ruthenium crystallites preferentially; however, copper is much more effective at doing so. We postulate that these edge and corner sites of the particles play an important part in removing hydrogen from the surface, which would otherwise tend to inhibit the ethane hydrogenolysis reaction. At the higher temperatures studied, the silver continues to act in the same way. However, at these higher temperatures we propose that copper is active in the removal of hydrogen from the surface.

ACKNOWLEDGMENT

This work was supported by the U.S. Department of Energy, Office of Energy Sciences, Contract Number W-7405-ENG-82. Development of the code used in the Monte Carlo simulations was supported by the National Science Foundation under Grant CPE-8307959.

REFERENCES

1. Morikawa, K., Benedict, W. S., and Taylor, H. S., J. Am. Chem. Soc. **58**, 1795 (1936).
2. Pruski, M., Kelzenburg, J. C., Gerstein, B. C., and King, T. S., J. Am. Chem. Soc., submitted for publication.
3. Sinfelt, J. H., Catal. Rev. **3**, 175 (1970).
4. Zaera, F., and Somorjai, G. A., J. Phys. Chem. **89**, 3211 (1985).
5. Engstrom, J. R., Goodman, D. W., and Weinberg, W. H., J. Am. Chem. Soc. **110**, 8305 (1988).
6. Carter, J. L., Cusumano, J. A., and Sinfelt, J. H., J. Phys. Chem. **70**, 2257 (1966).
7. Yates, D. J. C., and Sinfelt, J. H., J. Catal. **8**, 348 (1967).
8. Brunelle, J.P., Sugier, A., and Le Page, J. F., J. Catal. **43**, 273 (1976).

9. Guczi, L., and Gudkov, B. S., React. Kinet. Catal. Lett. **9**, 343 (1978).
10. Schay, Z., and Guczi, L., J. Chem. Research (S), 66 (1980).
11. Barbier, J., Morales, A., and Maurel, R., Bull. Soc. Chim. Fr. I 1-2, 32 (1978).
12. Barbier, J., Marecot, P., Morales, A., and Maurel, R., Bull. Soc. Chim. Fr. I 7-8, 309 (1978).
13. Barbier, J., and Marecot, P., Nouv. J. Chim. **5**, 393 (1981).
14. Godbey, D. J., Garin, F., and Somorjai, G. A., J. Catal. **117**, 144 (1989).
15. Doi, Y., Miyake, H., and Soga, K., J. Mol. Catal. **48**, 123 (1988).
16. Galvagno, S., Schwank, J., Gubitosa, G., and Tauszik, G. R., J. Chem. Soc., Faraday Trans. I **78**, 2509 (1982).

17. Hansen, M., and Anderko, K., "Constitution of Binary Alloys." 2nd Ed. McGraw-Hill, New York, 1958.
18. Sinfelt, J. H., J. Catal. **29**, 308 (1973).
19. Helms, C. R., and Sinfelt, J. H., Surf. Sci. **72**, 229 (1978).
20. Sinfelt, J. H., "Bimetallic Catalysts." John Wiley and Sons, New York, 1983.
21. Rouco, A. J., Haller, G. L., Oliver, J. A., and Kemball, C., J. Catal. **84**, 297 (1983).
22. Peden, C. H. F., and Goodman, D. W., ACS Symp. Ser. **288**, 185 (1985).
23. Peden, C. H. F., and Goodman, D. W., Ind. Eng. Chem. Fundam. **25**, 58 (1986).
24. Strohl, J. K., and King, T. S., J. Catal. **116**, 540 (1989).
25. Kim, K. S., Sinfelt, J. H., Eder, S., Markert, K., and Wandelt, K., J. Phys. Chem. **91**, 2337 (1987).

26. Goodman, D. W., and Peden, C. H. F., J. Chem. Soc., Faraday Trans. I **83**, 1967 (1987).
27. Houston, J. E., Peden, C. H. F., Feibelman, P. J., and Hamann, D. R., Phys. Rev. Lett. **56**, 375 (1986).
28. Wu, X., Gerstein, B. C., and King, T. S., J. Catal. submitted for publication.
29. Hong, A. J., Rouco, A. J., Resasco, D. E., and Haller, G. L., J. Phys. Chem. **91**, 2665 (1987).
30. Goodman, D. W., and Peden, C. H. F., J. Catal. **95**, 321 (1985).
31. King, T. S., Wu, X., and Gerstein, B. C., J. Am. Chem. Soc. **108**(19), 6056 (1986).
32. Wu, X., Gerstein, B. C., and King, T. S., J. Catal., submitted for publication.
33. Smale, M. W., and King, T. S., J. Catal., in press.
34. Kelzenberg, J. C., and King, T. S., J. Catal., submitted for publication.

35. Christmann, K., Ertl, G., and Pignet, T., Surf. Sci. **54**, 365 (1976).
36. Bernasek, S. L., and Somorjai, G. A., J. Chem. Phys. **62**, 3149 (1975).
37. Poelsema, B., Mechtersheimer, G., and Comsa, G., Surf. Sci. **111**, 519 (1981).
38. Salmeron, M., Gale, R.J., and Somorjai, G. A., J. Chem. Phys. **67**, 5324 (1977).
39. Salmeron, M., Gale, R. J., and Somorjai, G. A., J. Chem. Phys. **70**, 2807 (1979).
40. Smith, G. V., Notheisz, F., Zsigmond, A. G., Ostgard, D., Nishizawa, T., and Bartòk, M., Proc. 9th Int. Congr. Catal., Calgary, 1066 (1988)
- .
41. Smith, G. V., Bartòk, M., Notheisz, F., Zsigmond, A. G., and Pàlinkò, I., J. Catal. **110**, 203 (1988).
42. Balooch, M., Cardillo, M. J., Miller, D. R., and Stickney, R. E., Surf. Sci. **46**, 358 (1974).

SECTION III

NMR STUDIES OF HIGH COVERAGES OF ETHYLENE ADSORBED
ON SILICA-SUPPORTED PLATINUM CATALYSTS

NMR STUDIES OF HIGH COVERAGES OF ETHYLENE ADSORBED
ON SILICA-SUPPORTED PLATINUM CATALYSTS

M. W. Smale¹

M. Pruski²

B. C. Gerstein³

T. S. King¹

¹Department of Chemical Engineering and Ames Laboratory
231 Sweeney Hall
Iowa State University

²Ames Laboratory
230 Spedding Hall
Iowa State University

³Department of Chemistry and Ames Laboratory
229 Spedding Hall
Iowa State University
Ames, Iowa 50011

ABSTRACT

Ethylene on Pt/SiO₂ has been studied using a number of Nuclear Magnetic Resonance (NMR) techniques, including cross-polarization with magic angle spinning (CP/MAS), CP/MAS with dipolar dephasing and direct excitation of ¹³C nuclei with and without proton decoupling. NMR has proved to be a useful tool for studying high coverages of molecules on supported catalysts.

The evolution of the system as the samples are heated has been studied and a number of both strongly and weakly adsorbed species have been identified. Weakly adsorbed species present at various stages in the treatment of the samples include ethylene, ethane, methane and both cis- and trans-but-2-ene. After treatment at the higher temperatures C_nH_m fragments and finally coke have been observed strongly adsorbed on the catalyst surface. The coke present after the final heat treatment at 673 K has been characterized as consisting of aromatic rings with an overall stoichiometry of C_{2.4}H.

INTRODUCTION

Nuclear Magnetic Resonance (NMR) spectroscopy is now recognized as an important method for studying species adsorbed on a metal surface and has been used to study many systems [1,2] using, for example, ^{13}C [3], ^1H [4,5] or both [6] as probe nuclei. One of the main advantages of NMR is that it is non-invasive and low-powered, so is unlikely to perturb the system being studied. However, this also means that the sensitivity of the technique is rather low and requires a large number of nuclei present to obtain an acceptable signal-to-noise ratio in a reasonable amount of time. Supported-metal catalysts are therefore good candidates for studying surface species using NMR since the number of surface metal atoms in a given volume of catalyst is typically rather large compared to the number in a single-crystal sample.

Wang et al. [7] have studied sub-monolayer coverages of ^{13}C -labelled ethylene adsorbed on alumina-supported platinum clusters. The dispersion of the samples studied was 51% as measured by hydrogen chemisorption. After adsorption of ethylene at room temperature a number of ^{13}C spin echo experiments were carried out with different pulse separations. The frequency of the observed "slow beats" gave a fitted C-C bond length of 1.49 ± 0.02 Å, compared to values of 1.54 Å for a C-C single bond and 1.34 Å for a C=C double

bond. Further experiments indicated that the ratio of protonated to non-protonated ^{13}C nuclei was around 1:1 and indicated the presence of CH_3 groups rotating around a C-C bond. Wang et al. [7] therefore concluded that the surface species observed after adsorption of ethylene at room temperature is ethyldyne ($\equiv\text{C}-\text{CH}_3$). The effect of temperature on these sealed samples was also studied. Carbon-carbon bond cleavage was observed to occur between 400 K and 470 K, the predominant product being unprotonated carbon atoms together with a small amount of adsorbed CH_3 .

Ethylene adsorbed on supported platinum catalysts has also been studied by Gay [8]. Chlorine-free and chlorine-containing alumina- and silica-supported catalysts were used in this work. The dispersion of the catalysts was measured using hydrogen chemisorption, and singly ^{13}C -enriched ethylene was adsorbed to saturation at room temperature onto the surface of the catalysts. The amount of ethylene adsorbed at saturation corresponded to a coverage (C_2H_4 molecules per surface platinum atom) of approximately 0.25 in all cases. The cross-polarization / magic-angle spinning (CP/MAS) technique was used to obtain spectra. In addition some spectra were obtained from direct observation of ^{13}C nuclei in a static sample. Broad features were observed in the CP/MAS spectra, shifted between -100 and +300 ppm with respect to TMS. These features disappeared when a 50 μs

dipolar dephasing time was introduced before acquisition of the free induction decay. In general, the dipolar dephasing experiment attenuates the signal from carbon nuclei strongly coupled to protons. However, the signal from the CH_3 group, where the rotation around the $\text{H}_3\text{C-X}$ bond reduces the effect of the dipolar dephasing, can still be observed. A delay of 50 μs has been shown [9] to almost completely destroy the signal from rigid CH_n groups ($n = 1$ or 2). The signal from carbon nuclei not directly bonded to protons is almost unaffected. Thus, the result of Gay's experiment [8] indicated that there were no unprotonated carbon atoms on the surface of the catalysts. On the chlorine-free silica-supported catalysts Gay observed only a wide feature shifted between 70-90 ppm with respect to TMS using CP/MAS without dipolar dephasing. This was attributed to a π -bonded olefin. On the other catalysts a number of other species were suggested to occur, including σ -bonded vinyl or diadsorbed unsaturated species and alkyl groups.

Shibamura and Matsui have also studied ethylene adsorbed on platinum [10], using proton NMR. Platinum powder prepared by precipitation of H_2PtCl_6 from aqueous solution was used in their study. Ethylene was adsorbed onto the platinum surface at 182 K and 296 K with coverages of 0.21 ± 0.02 and $0.17 - 0.18$, respectively. Shibamura and Matsui [10] observed two states of ethylene observed on the platinum surface. The low-

temperature state seen at 182 K was believed to be di- σ -bonded ethylene. At 296 K a different species was observed. It was suggested, based on the observed line-shape, that both carbon atoms of this species had bonded with the platinum surface, forming a $-\text{CH}_2-\text{CH}=$ fragment. The authors found that the line-shape they observed for the high-temperature species is not consistent with its being ethyldyne.

Several other methods have also been used to study ethylene adsorbed on platinum surfaces. For example, Cruz and Sheppard [11] have used infrared spectroscopy (IR) to investigate the state of ethylene adsorbed on a 16% Pt/SiO_2 catalyst prepared from H_2PtCl_6 . The metal particle size of their catalyst was between 50 Å and 150 Å. At 189 K ethylene was observed to be π -bonded to the platinum surface and in addition a di- σ -bonded species was present adsorbed on two distinct sites. On warming the catalyst to 294 K the di- σ -bonded species adsorbed at one of the sites was converted to a fragment that was believed to be ethyldyne, while the di- σ -bonded species at the second site remained intact. The unknown species formed at around 300 K has been assigned to be ethyldyne by Skinner et al. [12] by comparison with the IR spectrum of $\text{CH}_3\text{CCo}_3(\text{CO})_9$ and its deuterated analog.

Ethylene adsorbed on the $\text{Pt}(111)$ single crystal-surface has received much attention. Sheppard [13] has reviewed the results of electron energy loss spectroscopy (EELS) applied

to ethylene adsorbed on metal single-crystal surfaces. At low temperatures ethylene is seen to adsorb on the Pt(111) surface in the di- σ -bonded state. In the presence of pre-adsorbed oxygen or carbon, a π -bonded state is observed on a number of metals, including the oxygen-contaminated Pt(111) surface. At room temperature the ethyliyne species is observed to form on a number of metal surfaces, including Pt(111), which have three-fold triangular symmetry. Avery and Sheppard [14,15] have also studied higher carbon number unsaturated species adsorbed on the Pt(111) single-crystal surface. They found that at low temperatures di- σ -bonded species are invariably observed. At about 300 K the alk-1-enes formed straight-chain alkylidynes, in the same manner that ethylene is believed to form ethyliyne.

Early work by Ibach et al. [16,17] using EELS of ethylene adsorbed on the Pt(111) single crystal surface showed that a transition between adsorbed species occurred around 260 K. At temperatures lower than 260 K ethylene was believed to be adsorbed in a π -bonded state. Above 260 K another species was observed, which was tentatively assigned to be ethyliene ($=\text{CH}-\text{CH}_3$). Further work [18] suggested that there was an intermediate CCH_2 species between these two states. The publication of data on $\text{CH}_3\text{CCo}_3(\text{CO})_9$ by Skinner et al. [12] together with data from thermal programmed desorption spectroscopy (TPD) [19] allowed a more definite

assignment of the room temperature species as ethyldyne ($\equiv\text{C}-\text{CH}_3$). In the presence of oxygen, no ethyldyne was observed. Instead H_2O and CO_2 were formed and desorbed from the surface.

Kesmodel et al. [20] have used low-energy electron diffraction spectroscopy (LEED) to study ethylene adsorbed on the Pt(111) surface in the 300 K to 350 K temperature range. They find that the intensity-voltage profiles obtained are best fit by an ethyldyne species adsorbed above a three-fold hollow. The C-C bond length was found to be 1.50 ± 0.05 Å while the C-Pt bond lengths were 2.00 ± 0.05 Å. The assignment of ethyldyne as the surface species present around room temperature has been confirmed by Salmeron and Somorjai using TPD [21], and the adsorption of other unsaturated hydrocarbons on the Pt(111) surface has also been studied [21, 22, 39]. For ethylene, propylene, and 2-butenes the surface species present at room temperature was an alkylidyne, which decomposed at temperatures between 380 K and 490 K (490 K for ethyldyne) to form C_nH species. These in turn broke down at higher temperatures to form a carbon residue on the Pt(111) surface. Godbey et al. [23] compared the kinetics of ethylene hydrogenation under ultra-high vacuum conditions with results at high pressure previously published by Zaera and Somorjai [24] and found that the

reaction proceeded by different mechanisms under the different conditions.

Ethylene adsorbed on platinum surfaces other than Pt(111) single crystals has also been studied. Beebe and Yates [25] used IR spectroscopy to show that ethyldyne was present on alumina-supported platinum catalysts containing 10% metal (by weight). Paál et al. [26] have used secondary ion mass spectroscopy (SIMS) to investigate ethylene on Pt-black. After flowing ethylene through the platinum at 633 K, clusters with a composition PtC_2H_3 were observed, which were believed to be ethyldyne strongly bonded to platinum. The ethyldyne was easily removed by heating in air.

However, not all investigations of ethylene adsorbed on platinum have concluded that the ethyldyne species is present. Hatzikos and Masel [27] have suggested that the decomposition of ethylene on platinum may be surface sensitive. EELS was used to show that at low temperatures ethylene adsorbs molecularly on both (5X20)Pt(100) and (1X1)Pt(100) surfaces. The (5X20)Pt(100) surface has open sites of three-fold symmetry similar to the Pt(111) surface, whereas the (1X1)Pt(100) surface lacks these sites. On the (5X20)Pt(100) surface, ethylene decomposed to form ethyldyne, as has been observed on the Pt(111) surface. In contrast, ethylene adsorbed on the (1X1)Pt(100) surface shows no evidence for the ethyldyne species. Instead, at

temperatures between 100 K and 350 K a vinylidene species was formed ($=\text{C}=\text{CH}_2$), most probably in the bridge-bonded form. The vinylidene species was then believed to be transformed to a quad- σ -bonded acetylene species by the time the temperature reached 450 K. It was not clear what species were present above 450 K, though LEED showed that the (1X1)Pt(100) surface was intact at 750 K, whereas a clean (1X1)Pt(100) surface normally reconstructs to form the (5X20)Pt(100) surface between 440 K and 550 K.

Windham et al. [28] have shown that ethylene does not invariably decompose to form ethylidyne even on Pt(111) surfaces. They found that the adsorption and decomposition of ethylene was contingent on the presence of ensembles of platinum atoms. The ensemble requirement for ethylene adsorption was found to be four, while an ensemble of six Pt atoms was needed to allow ethylene to decompose to ethylidyne.

A striking difference between ultra-high vacuum studies of single-crystal surfaces and the actual environment found in working catalysts is the invariable presence of a carbon overlayer in the latter [29]. In addition to simply blocking sites for adsorption and reaction of hydrocarbons, it has been suggested that the carbonaceous overlayer acts as a sink for hydrogen, which may then be incorporated into surface species [29]. It may also provide sites from which product

species can desorb more readily than from the surface of the metal crystallites. Zaera and Somorjai [24] have investigated ethylene hydrogenation over the Pt(111) single-crystal surface using conditions where a carbonaceous overlayer is expected to form. The reaction studies were carried out in the 300 K temperature region, in which the carbonaceous overlayer was expected to consist of ethylidyne species. Zaera and Somorjai [24] found that ethylene hydrogenation took place not on the metal surface directly, but instead on top of the carbonaceous overlayer. Wang et al. [30] used NMR to investigate the carbonaceous overlayer deposited on an alumina-supported platinum catalyst. They found that heating adsorbed ethylene to 690 K led to essentially unprotonated single carbon atoms. These atoms were found to be highly mobile on the catalyst surface, with an activation energy for diffusion of 7 ± 1 kcal/mol.

It seems that the state of adsorbed ethylene on the Pt(111) single-crystal surface under ultra-high vacuum conditions is rather well characterized. However, it is not clear that the species found on single-crystal surfaces with three-fold hollow sites is necessarily that present under high pressures of ethylene on supported platinum crystallites. NMR spectroscopy does not require that the sample under investigation be under vacuum. We have

therefore chosen to study silica-supported platinum catalyst samples heavily dosed with ethylene using NMR.

EXPERIMENTAL

The catalysts used in this study were prepared by aqueous impregnation of $\text{Pt}(\text{NH}_3)_4(\text{NO}_3)_2$ into the support. The support was Cab-O-Sil HS-5 amorphous fumed silica, which had a surface area of $300 \text{ m}^2/\text{g}$ (as measured using the BET method). Following impregnation, the catalysts were dried overnight at 383 K and reduced for two hours in flowing hydrogen at 623 K prior to storage in air. All catalysts used had metal loadings of 4% (by weight) and a dispersion of 57% as measured using strong hydrogen chemisorption. Blank silica samples were prepared by soaking the support in distilled water and then drying overnight at 383 K prior to storage in air.

Samples for analysis by NMR were prepared using the multi-port glass sample preparation apparatus, which has been described previously [31]. Norell XR-55 precision NMR tubes were necked prior to introduction of the catalyst sample. This was done to facilitate the production of the symmetrical seals required when the sample is to be spun at high speeds. In general, approximately 100 mg of catalyst were loaded into the necked NMR tubes. The exception to this was when the sample was to be studied using the Bruker MSL-300 spectrometer we used for some of the NMR experiments to investigate weakly adsorbed species. In this case the probe geometry dictated the use of shorter samples containing only

about 40 mg of catalyst. After the catalyst had been introduced into the sample tube, a wad of glass wool was placed near the tube opening to prevent the possibility of the catalyst contaminating the adsorption apparatus during the first evacuation step.

The NMR tubes containing the catalyst samples were connected to the adsorption apparatus and evacuated to a pressure between 0.1 and 0.01 Torr. The samples were heated to 625 K and hydrogen was introduced to bring the pressure up to about 760 Torr. The samples were then reduced for two hours at 625 K in static hydrogen, with the sample evacuated and the hydrogen being replaced every 30 minutes. Following reduction, the samples were evacuated to below 10^{-4} Torr and labelled ethylene (either singly ^{13}C - or doubly ^{13}C -labelled) was introduced into the sample tube while the sample was held in the boil-off from a beaker of liquid nitrogen. The coverage of ethylene was generally between 10 and 20 molecules of C_2H_4 per surface platinum atom. The sample tubes were then sealed while still held in the boil-off from the liquid nitrogen.

A number of different transient techniques in NMR were employed to study the ^{13}C -labelled ethylene in the samples. All spectra were obtained at room temperature. The strongly adsorbed species could be better observed at a lower magnetic field on a home-built spectrometer, using cross-polarization

(CP) or Bloch decay measurements with magic angle spinning (MAS) and proton decoupling. A Bruker MSL-300 spectrometer was used to obtain high-resolution spectra of weakly adsorbed molecules. The details of the NMR experiments are given below.

The home-built spectrometer operating at 100.06 and 25.16 MHz for ^1H and ^{13}C , respectively, has been described, in whole or in part, previously [32, 33]. The spectrometer used a high-resolution Varian XL-100 15-inch electromagnet. The other parts were designed in our laboratory or purchased commercially. A double-tuned, single-coil probe was constructed allowing for MAS of sealed samples at rates of 4-5 kHz using an air drive. This rotation speed and resonant frequency avoids the problem of spinning sidebands of ^{13}C . The spinning assembly uses a modified design based on that published by Shoemaker and Apple [34] with the glass sample tube held in the Torlon rotor using fast-hardening glue. Most of the ^{13}C spectra were acquired using ^{13}C - ^1H cross-polarization with magic angle spinning (CP/MAS) and strong proton decoupling. In addition to standard CP/MAS experiments, dipolar dephasing was applied [35]. Rotating-frame fields were kept at 50 kHz during both the cross-polarization and proton-decoupling periods. The Hartmann-Hahn match was verified by monitoring the ^{13}C CP intensities versus the ^{13}C rf field with a static sample of adamantane.

Since no measurable effect on the impedance of the probe due to samples was detected, the center of symmetry of the matching curve observed for adamantane was taken to best represent the exact Hartmann-Hahn match. To attenuate the baseline distortion associated with rf pulse breakthrough, the proton spin temperature inversion with add-subtract of ^{13}C free induction decays was used [36]. All spectra were acquired using a 2K quadrature detection and Fourier transformed after zero filling to 8K. A dwell time of 10 μs was used in most cases, resulting in a spectral range of 50 kHz. Throughout the work, the resonance line positions were determined in ppm with respect to the ^{13}C of tetramethylsilane (TMS) as the reference, and are believed accurate to $\pm 2\text{ppm}$. All shifts are reported on the δ scale, with more positive numbers being downfield (deshielded). Only the range from 400 to -300 ppm is usually shown because no features were observed outside this region.

CP/MAS spectra were accumulated with a repetition rate between 1 Hz and 2 Hz, with up to 600,000 scans required in some cases in order to obtain acceptable signal:noise ratios. The primary mechanism for polarization transfer between ^1H and ^{13}C in our experiments is inferred to be the heteronuclear dipolar interaction. The CP technique allowed for observation of ^{13}C spectra of strongly adsorbed species which, as was verified by comparison of the "true" spectra

obtained by direct ^{13}C excitation at 25.16 MHz (Bloch decay experiment), well represented all rigid carbons in the samples. However, in most samples we were also able to observe resonances from molecules that were weakly adsorbed, or in the gas phase. For some of these species, the cross-polarization mechanism is believed to be the scalar coupling (J cross-polarization). In these cases the Hartmann-Hahn matching condition is much more critical and the kinetics of the polarization transfer is different than in solids. This cross-polarization mechanism was the subject of a more detailed study and will be described separately [33]. It is only noted here that the intensities from very mobile species are generally strongly underestimated relative to those of rigid species in the CP/MAS spectra presented in this work.

Due to the problems mentioned above, direct pulsed FT NMR (Bloch decay) experiments were carried out on samples where the CP/MAS studies suggested the presence of weakly adsorbed species represented by narrow peaks in the spectra. The aim of these experiments was only to observe mobile species, and they were performed on a Bruker MSL-300 spectrometer, operating at a ^{13}C frequency of 75.1 MHz. The spectrometer was fitted with a double resonance MAS probe which allowed spinning sealed samples at rates up to 1 kHz, after they were placed in an alumina rotor. Spinning at this rate helped to eliminate the residual line broadening

resulting from the anisotropy of magnetic susceptibility. In addition, the spectra were accumulated with and without heteronuclear decoupling. In the latter case J-splittings could be observed for the most mobile species, which assisted in the assignment of the observed resonances. The residual resolution (<0.3 ppm) at the higher field allowed differentiation between the peaks representing weakly adsorbed and gaseous states of the reaction products in the samples studied. The ^{13}C spin-lattice relaxation times were measured for weakly adsorbed species using the spin inversion recovery method.

RESULTS**Background**

We obtained CP spectra from the empty stator, after it had been in use for an extended period of time, to discover whether a significant background signal was observable. As can be seen from Fig. 1, a wide peak is present in the -50 to 250 ppm range (all positions quoted relative to TMS). This peak was unaffected by flushing the probe with solvent. We suggest two possibilities for this peak. It could be due to the adhesive used in construction of the probe or another possibility is that the house air used to drive the rotor is contaminated with oil from the compressor, and this has irreversibly impregnated the stator. In either case, the background is small compared to most of the sample signals we observe. We further carried out CP/MAS experiments on a sample consisting of the silica support. This sample had been impregnated with water and dried, but not been put through the reduction and adsorption stage before sealing in the tube. Fig. 2 shows that there is no difference seen in the signal from this sample and that of the empty stator, confirming that the silica support is not significantly contaminated with carbon species. This experiment also shows that there is no observable contribution from the rotor or the adhesive used to fix the sample tube into the rotor.

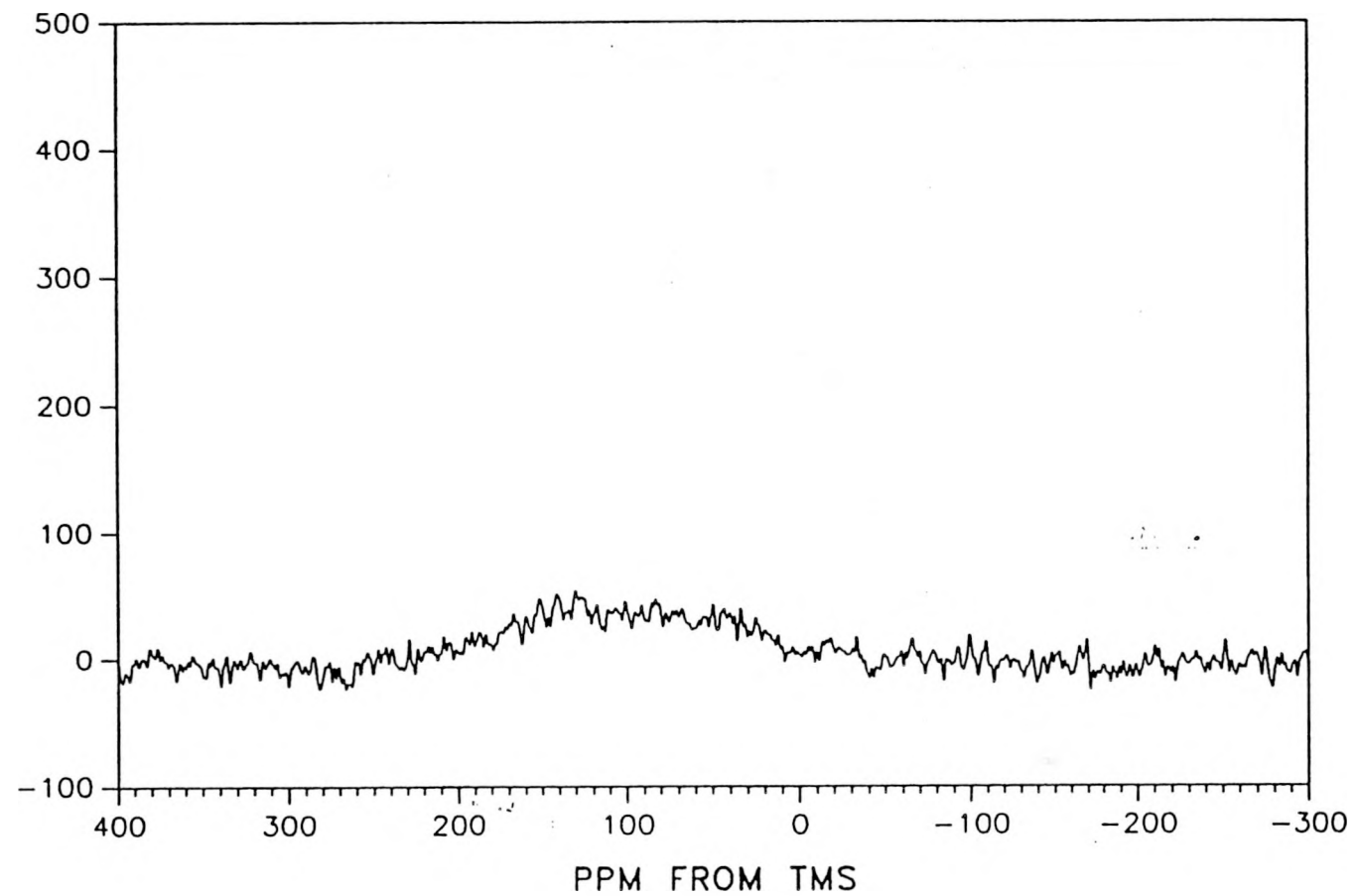


Figure 1. CP spectrum of stator background (with 100 Hz broadening function)

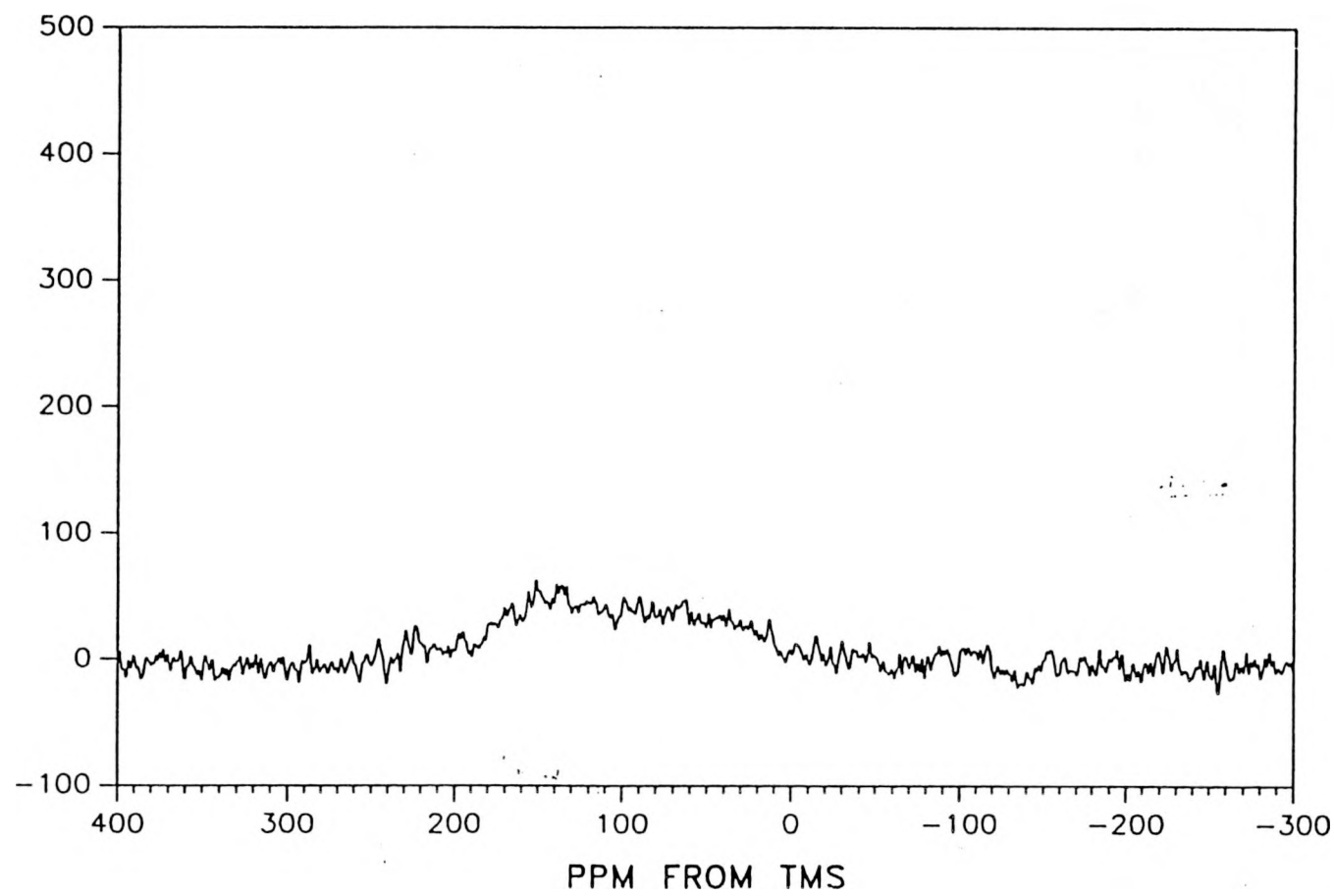


Figure 2. CP/MAS spectrum of untreated silica sample (with 100 Hz broadening)

We also used the MSL-300 spectrometer to obtain a spectrum of ethylene gas for reference purposes. A single sharp peak at about 119 ppm was observed from the Bloch decay experiment (with proton decoupling).

C₂H₄ on SiO₂

As a control experiment, we obtained CP/MAS spectra from ethylene adsorbed on pure silica support treated identically to the catalyst samples. The spectrum obtained at room temperature is shown in Fig. 3. Only a single sharp peak at 121 ppm is seen, which we attribute to ethylene either adsorbed on the silica or having restricted motion within the pores. After heating this sample to 413 K for 24 hours, a further CP/MAS spectrum was taken that had no observable difference from the first. We further obtained a spectrum by direct pulsing of the ¹³C nuclei in the 25 MHz spectrometer to confirm that there were no very weakly adsorbed species formed that the CP/MAS technique might miss. As can be seen in Fig. 4, only the single ethylene peak is observed. Further heating the sealed sample to 513 K for 24 hours had no effect on the CP/MAS spectrum obtained, as shown in Fig. 5.

The Bruker MSL-300 spectrometer was also used to obtain a spectrum from C₂H₄ on silica using direct excitation of ¹³C. A pair of peaks was observed at 120.5 ppm and 119 ppm.

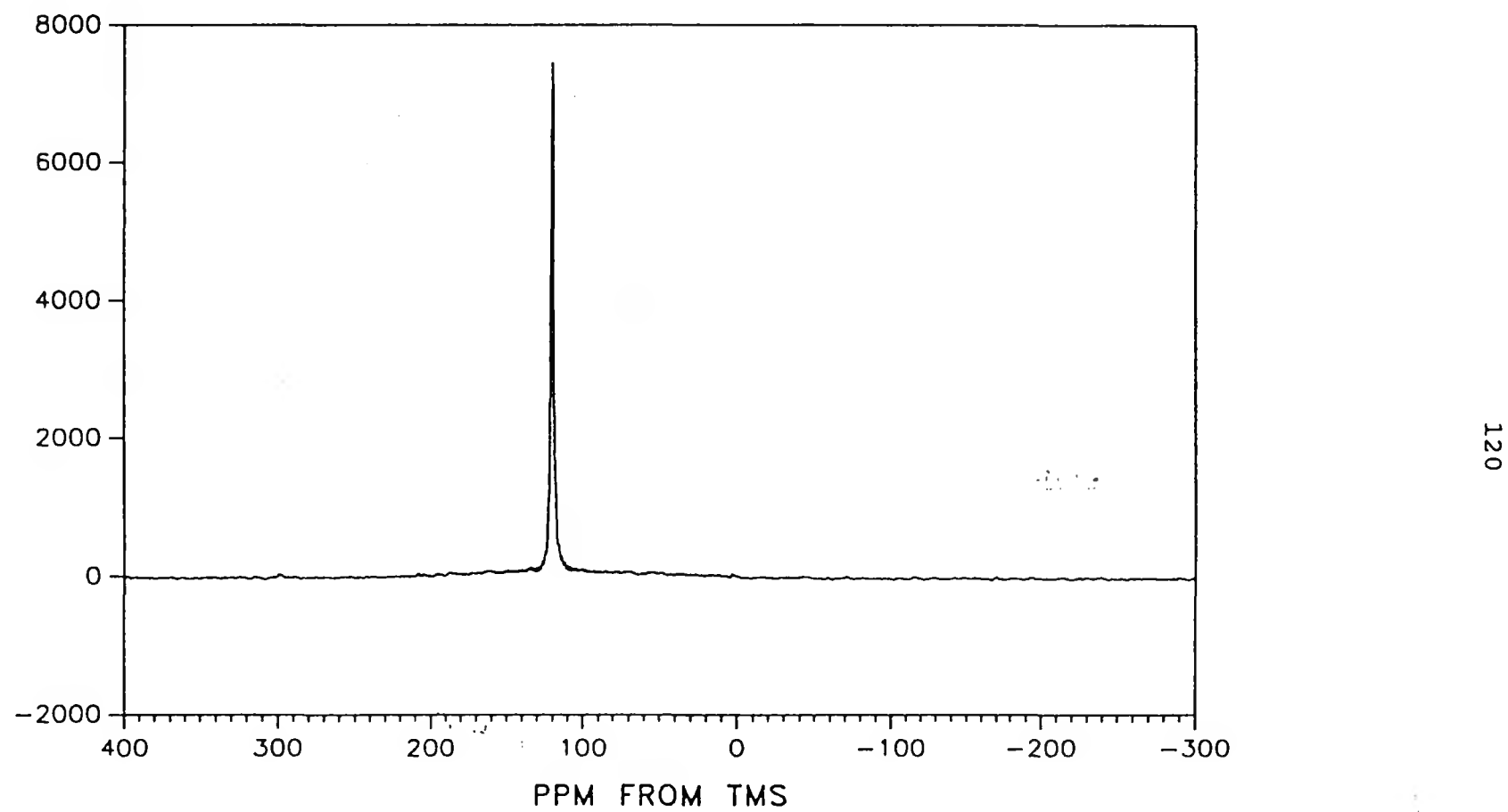


Figure 3. CP/MAS spectrum of ethylene on silica as prepared (with 100 Hz broadening)

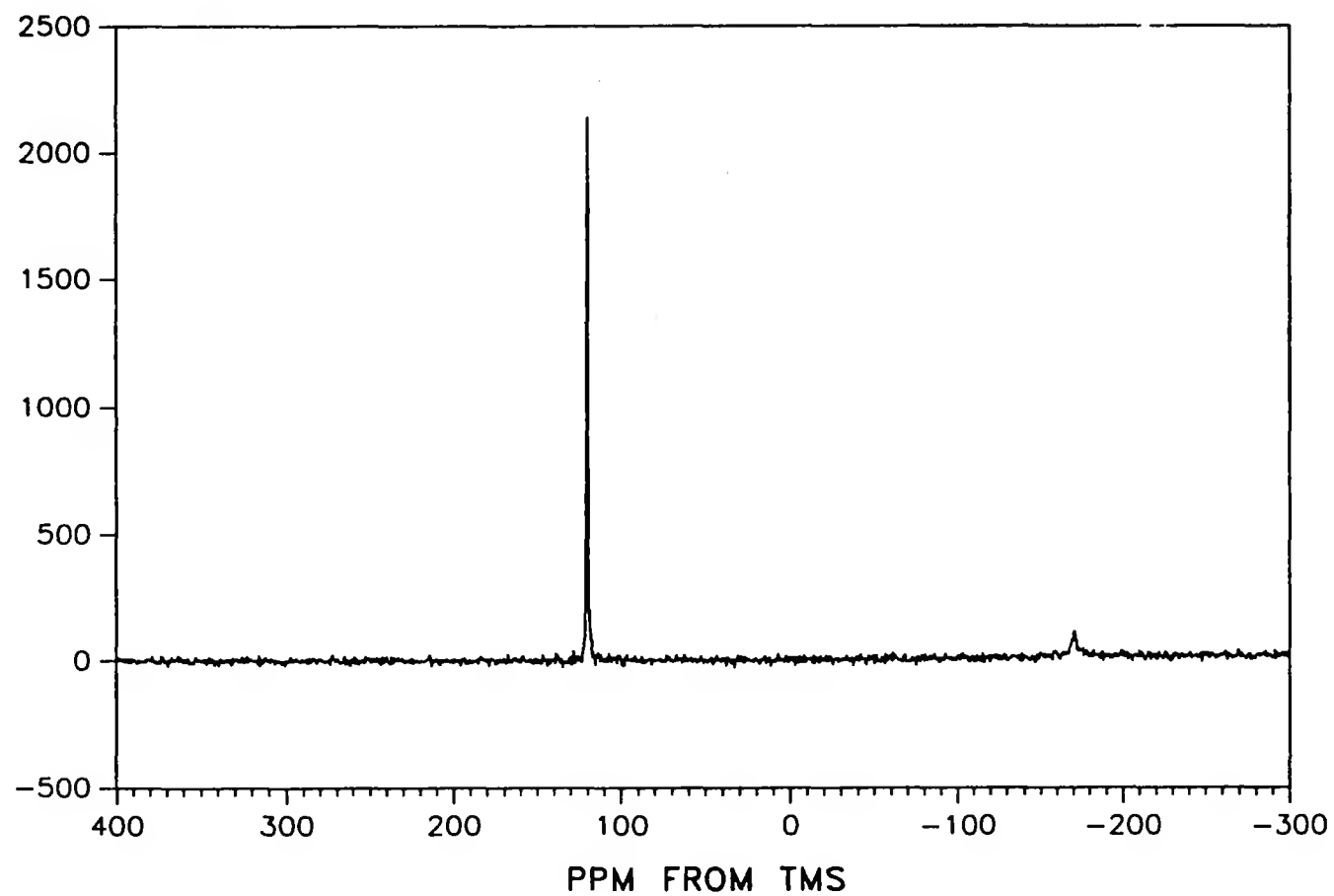


Figure 4. Bloch decay spectrum of ethylene on silica after heating to 413 K, with proton decoupling

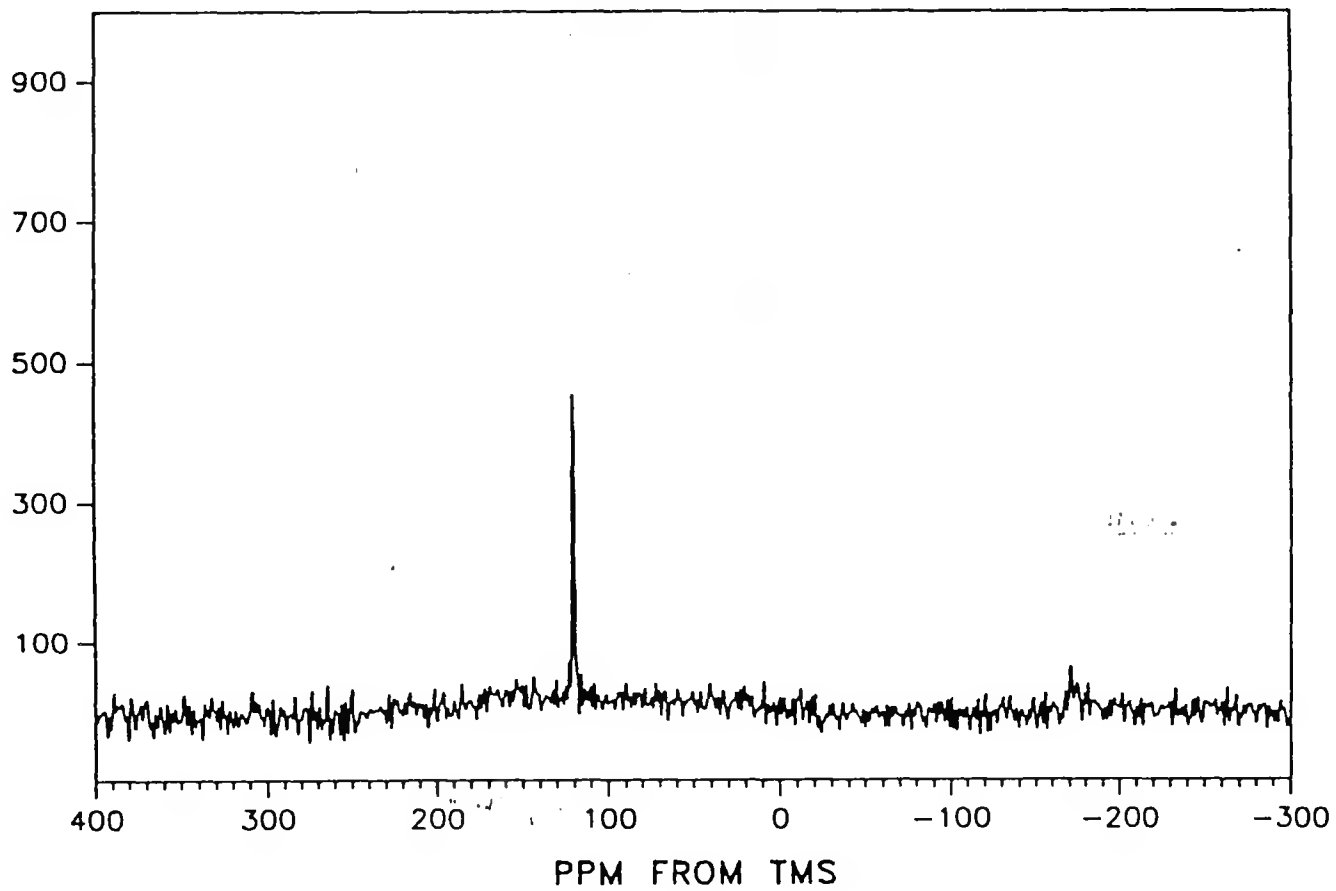


Figure 5. CP/MAS spectrum of ethylene on silica after heating to 513 K

C₂H₄ on Pt/SiO₂

Room temperature CP/MAS spectra of ethylene adsorbed on a Pt/SiO₂ catalyst show a sharp feature at around 120 ppm from TMS. In some spectra, this feature appears to be resolved into two sharp peaks, one at 119 ppm and the other shifted 1.5 ppm downfield at 120.5 ppm (Fig. 6). These peaks are attributable to molecular ethylene in two different states. The wide baseline peak is indistinguishable from the background spectrum from the empty stator. On one sample a very small peak appeared in the room temperature spectrum in a position concomitant with the presence of ethane, though it was barely distinguishable from the baseline.

After accumulating spectra at room temperature the sealed samples were heated in an oven at 413 K for 24 hours and re-examined. Again, a sharp peak is observed at about 120 ppm in the CP/MAS spectrum (Fig. 7), which we assign to be ethylene on the basis of chemical shift data. As in the case of the unheated sample, this peak may in fact be composed of two closely spaced sharp peaks, though it is difficult to be certain at the resolution of this experiment. In addition to the ethylene peak, a sharp peak is observed shifted 3 ppm from TMS. The most likely candidate for this is ethane. We have also obtained spectra using Bloch decay experiments with proton decoupling in the 25 MHz (for ¹³C) magnet to check for more mobile species (Fig. 8). In

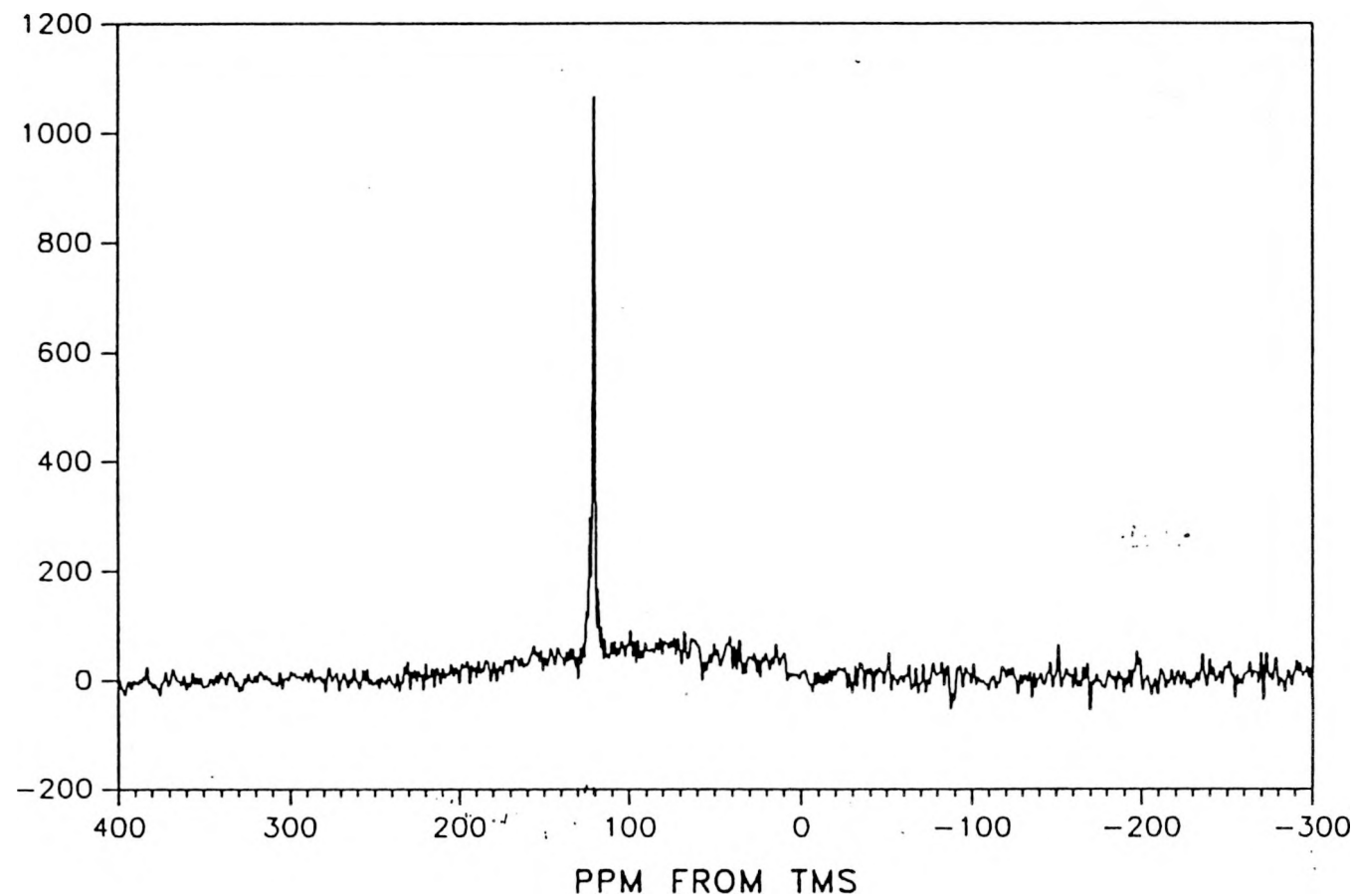


Figure 6. CP/MAS spectrum of ethylene on silica-supported platinum catalyst, as prepared

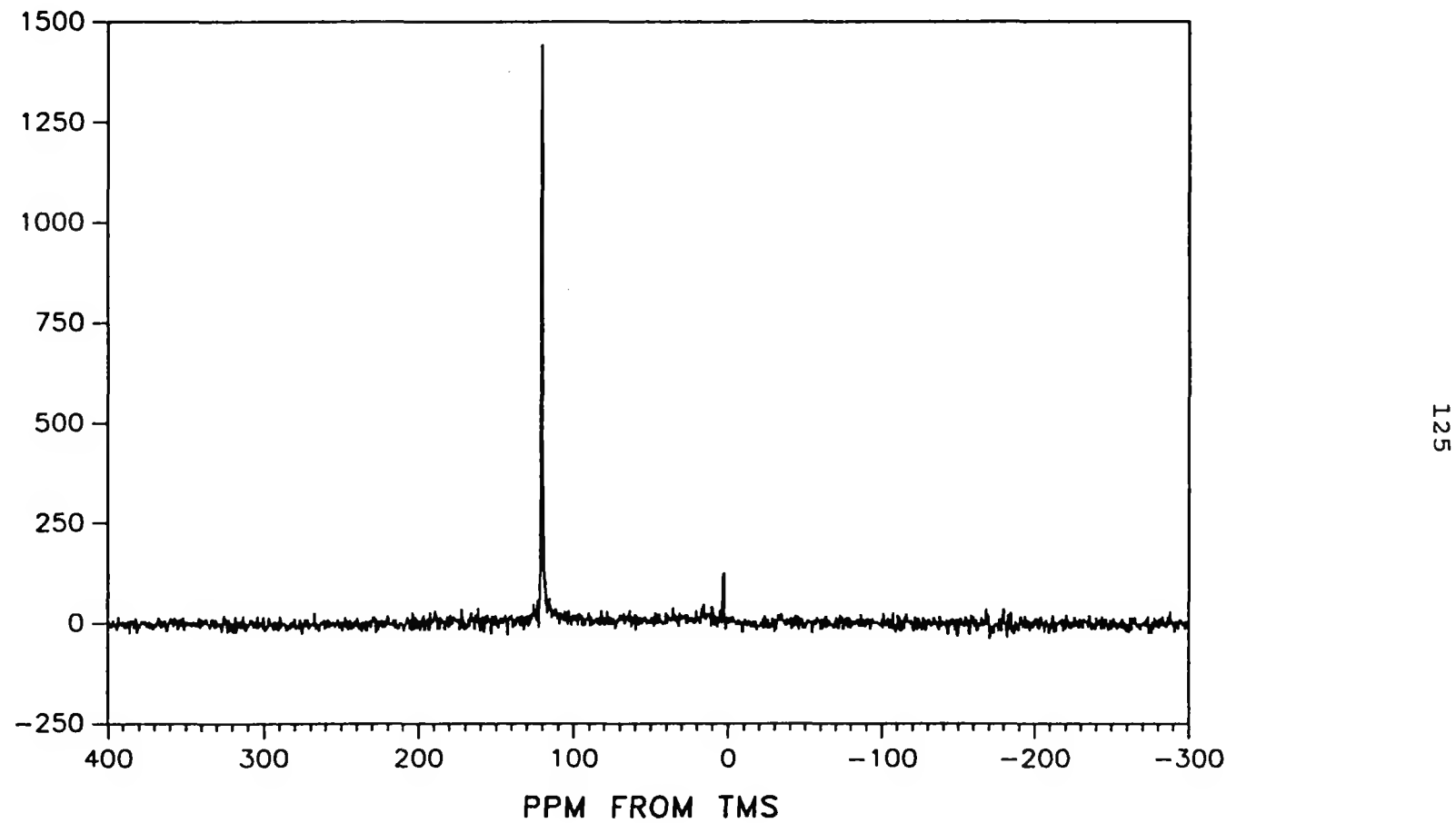


Figure 7. CP/MAS spectrum of ethylene on silica-supported platinum catalyst after heating to 413 K

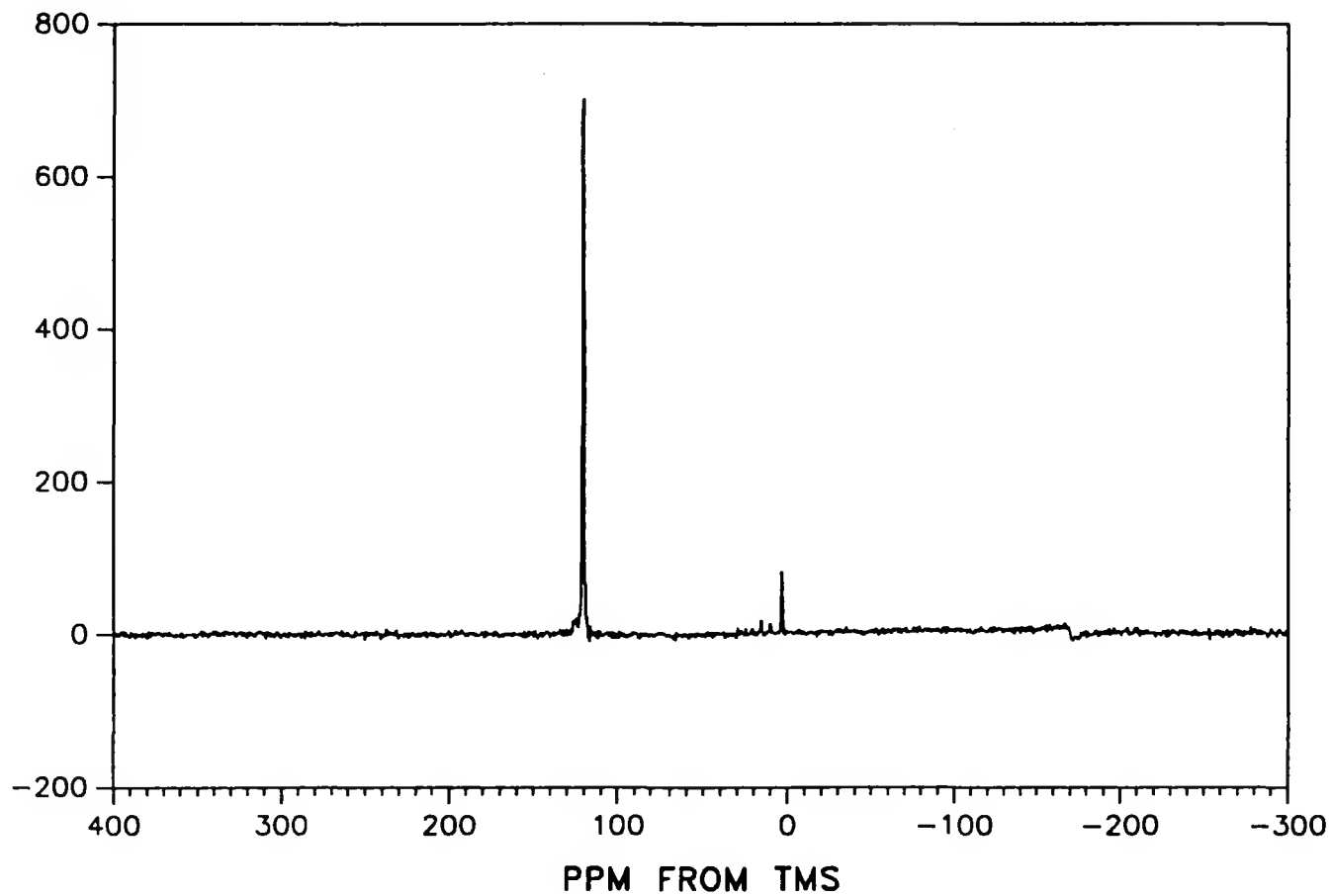


Figure 8. Bloch decay spectrum of ethylene on Pt/silica after heating to 413 K, with proton decoupling

addition to the peaks for ethylene and ethane previously observed, pairs of small peaks are seen downfield of both the ethylene and ethane peaks. On the basis of later experiments after the sample had been further heated, we suggest that these peaks are due to the cis and trans isomers of but-2-ene. The intensity of these peaks is, however, very much less than that of the ethylene and ethane peaks. Confirmation of the assignment of the ethane and ethylene peaks was obtained by obtaining Bloch decay spectra without proton decoupling (Fig. 9). A typical quartet corresponding to the CH_3 groups in ethane is seen in the upfield region, while the most prominent feature in the downfield region of the spectrum is the triplet expected from the C-H couplings in ethane. The smaller peaks associated with the ethylene triplet may be due to a second, partially obscured triplet from ethylene present in a second state.

After accumulating the previous spectra, the sealed Pt/SiO_2 samples were further heated in an oven for 24 hours at 513 K. Again CP/MAS spectra were obtained, but this time a significant change had occurred (Fig. 10). Again, a pair of sharp peaks are present at about 119 ppm and 120.5 ppm, which are attributed to molecular ethylene in different states. The sharp ethane peak is also still seen at about 3 ppm. However, this spectrum also exhibits two wide peaks that are clearly distinguishable from the baseline. The

first of these is in the 90-170 ppm region normally associated with aromatic species. The second wide peak covers the 0-60 ppm region associated with saturated (sp^3) carbon species. There also appear to be some narrow peaks superimposed onto the wide upfield peak. Repeating the CP/MAS experiment with a delayed decoupling time of 100 μ s (Fig. 11) removed most of the integrated intensity of the wide peaks. In the case of the downfield peak, this indicates that almost all of the carbon nuclei corresponding to this peak are strongly coupled to both protons and the support. The upfield peak lost intensity in its downfield portion, corresponding to strongly adsorbed CH or CH_2 groups, while the rotation of the CH_3 groups contributing to the upfield portion of this peak attenuated the dipolar dephasing, and therefore CH_3 groups are still observed.

We used the 75 MHz (for ^{13}C) spectrometer together with direct excitation of the ^{13}C nuclei with proton decoupling to better observe the weakly adsorbed peaks on the catalyst sample that had been heated to 513 K. Figure 12 shows the spectrum obtained, which exhibits a large number of peaks. The most prominent features are two pairs of peaks, one pair each in the upfield and downfield ends of the spectrum. The downfield pair of large peaks are shifted 119.2 ppm and 120.7 ppm from TMS, close to the position expected for ethylene. The largest upfield features are the two peaks at

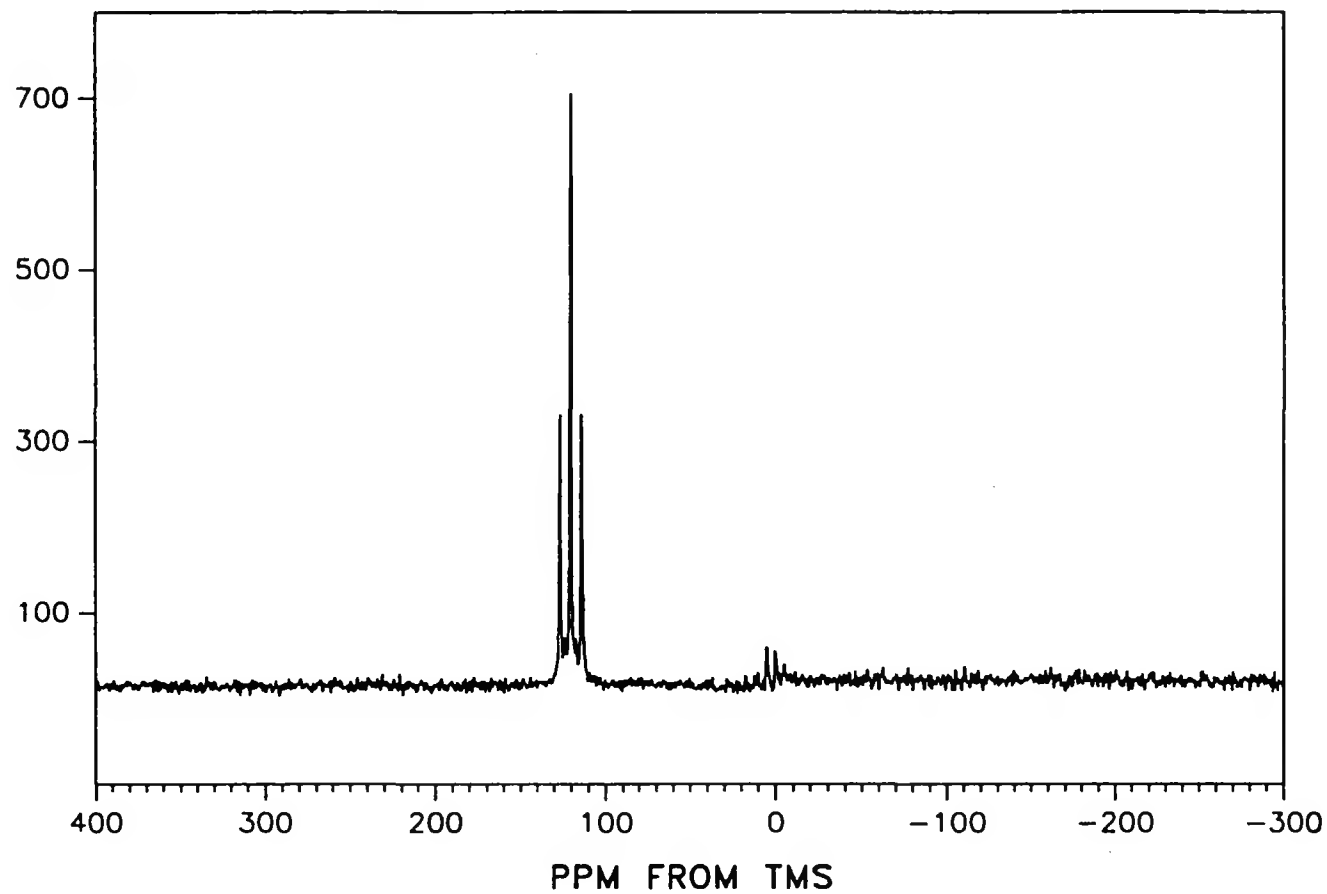


Figure 9. Bloch decay spectrum of ethylene on Pt/silica after heating to 413 K, with proton coupling

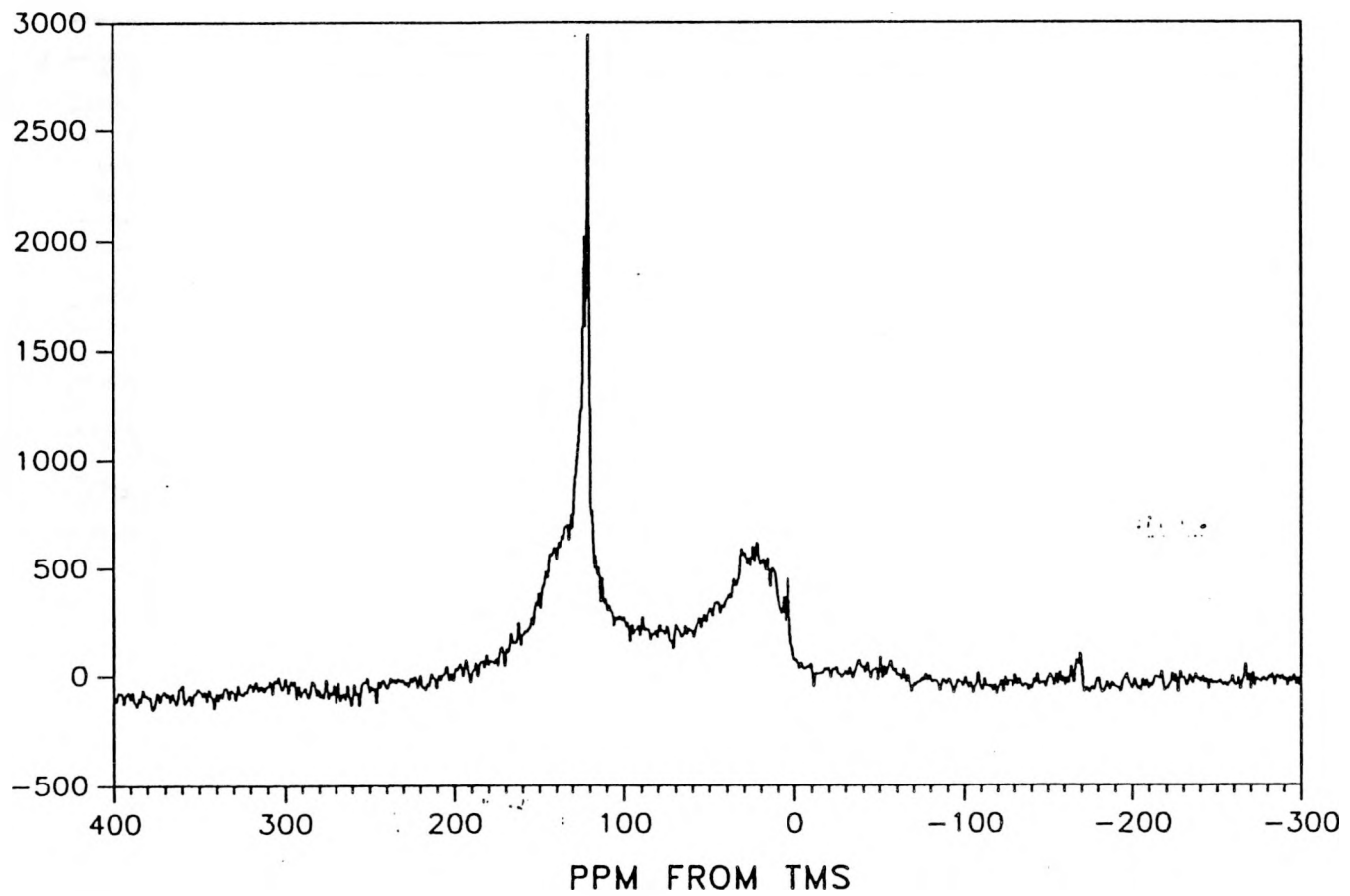


Figure 10. CP/MAS spectrum of ethylene on Pt/silica after heating to 513 K

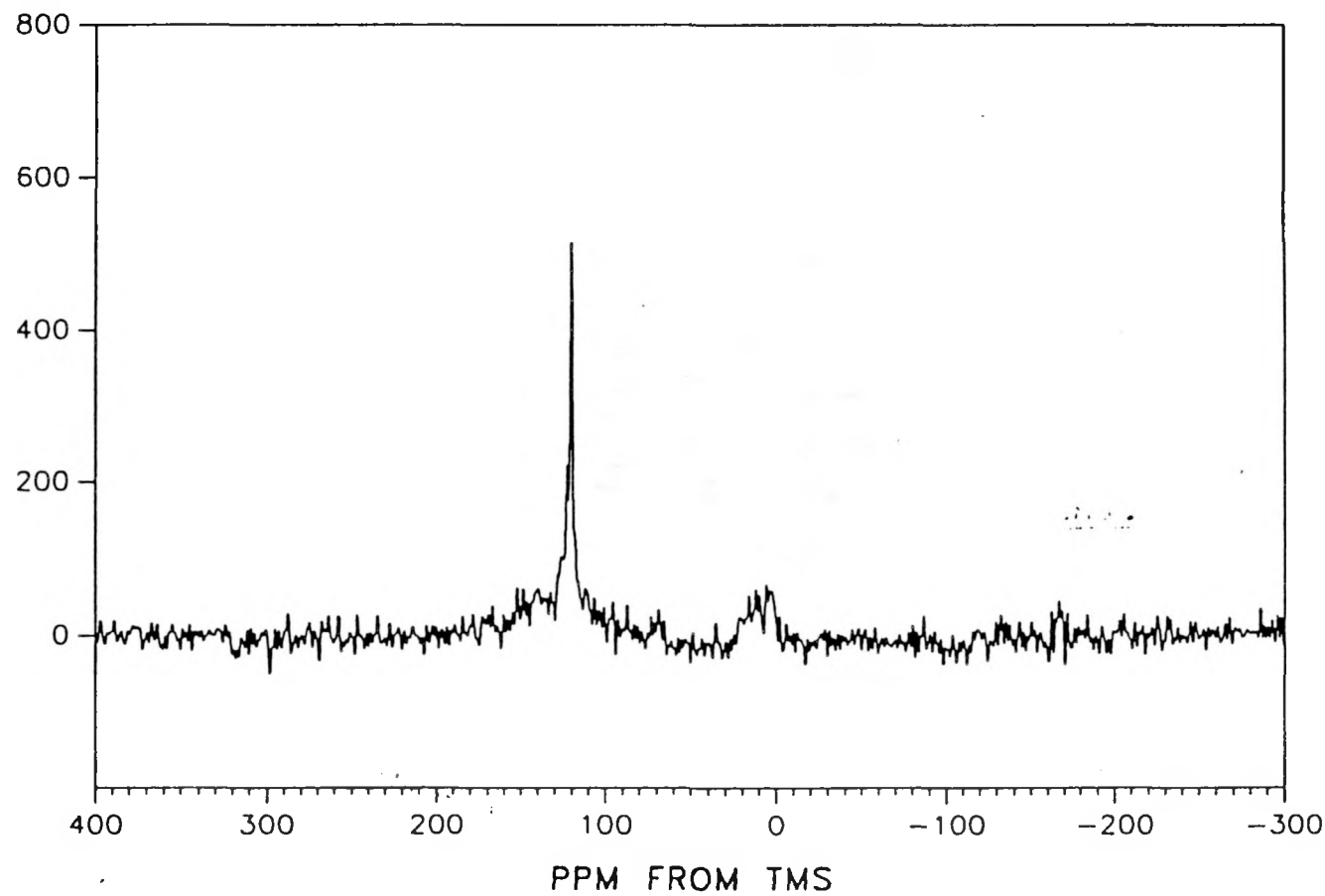


Figure 11. CP/MAS spectrum of ethylene on Pt/silica after heating to 513 K, with depolar dephasing time of 100 μ s

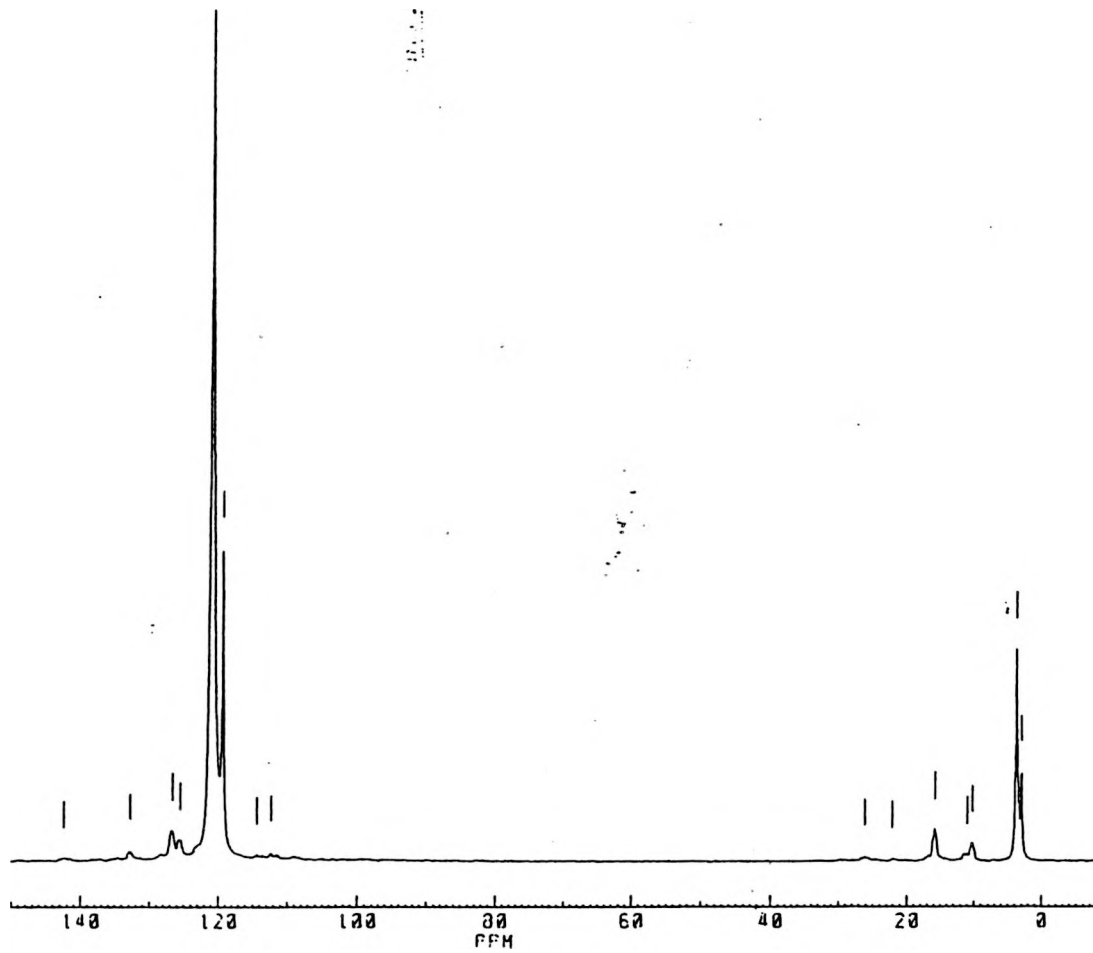


Figure 12. High-resolution ^{13}C spectrum of weakly adsorbed species formed by heating ethylene on Pt/silica at 513 K, with proton decoupling

2.8 ppm and 3.5 ppm, which are attributed to ethane. It is interesting to note that the ratio of integrated intensities of the two ethylene peaks is about 4:1, virtually the same as that of the two ethane peaks. The small peaks at 10.1 ppm and 15.7 ppm are attributed to the CH_3 groups of cis- and trans-but-2-ene, with the peaks from the $-\text{HC}=\text{CH}-$ carbons showing up at 125.3 ppm and 126.5 ppm. The peak at 132.6 ppm is a spinning sideband of the wider ethylene peak. This was confirmed by changing the spinning rate and observing that the peak position moved. In addition, when the spectrum was re-plotted on an expanded intensity scale additional spinning sidebands, equally spaced from the ethylene peak, were observed at 108.5 ppm and 142 ppm. It is possible that there are other peaks present, but the signal to noise ratio for these peaks is too small to make any realistic statements about them.

To further confirm our assignments of the peaks in the decoupled spectrum we obtained a spectrum without carrying out proton decoupling. The spectrum (Fig. 13) is somewhat complicated due to the overlapping of splittings from the different species in addition to the presence of homonuclear and long and short range heteronuclear coupling. However, the primary splitting from the proton-carbon coupling is still observable. The two upfield peaks assigned to ethane species have clearly split into the expected pair of

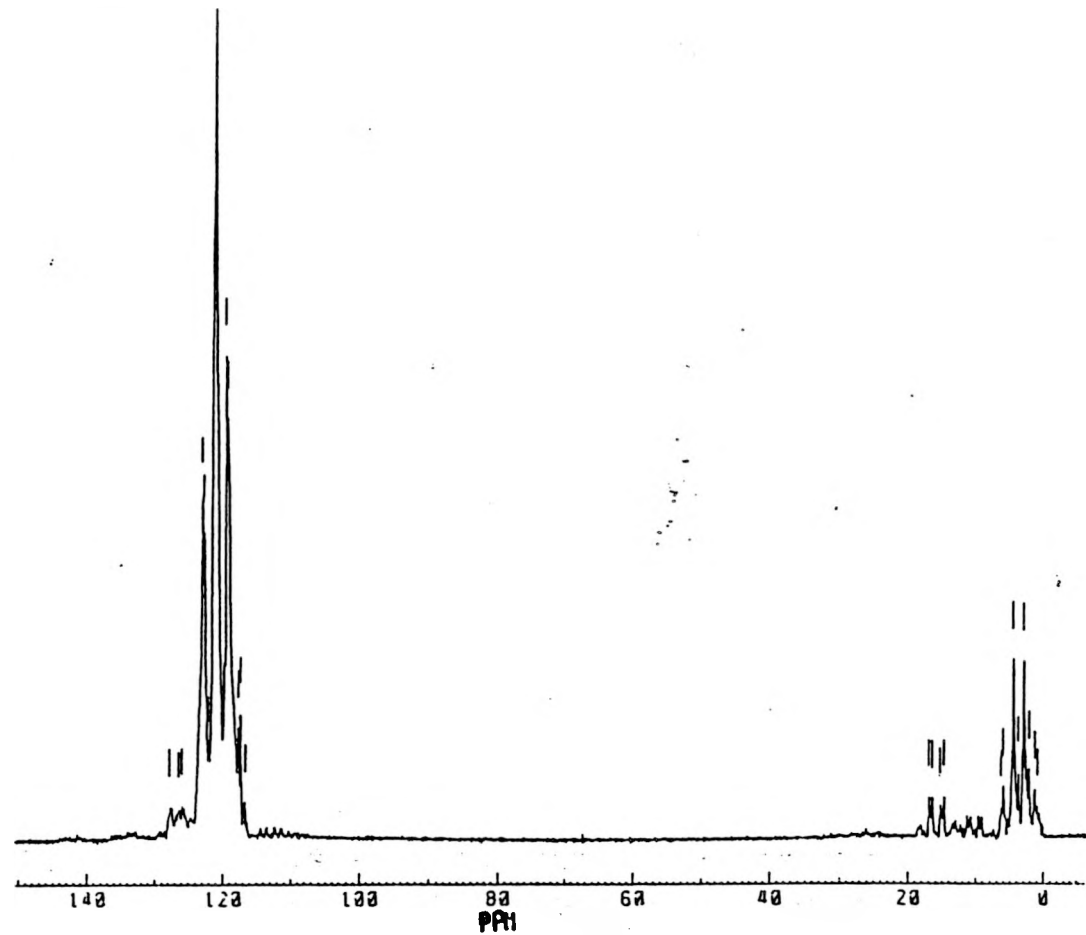


Figure 13. High-resolution ^{13}C spectrum of weakly adsorbed species formed from ethylene on Pt/silica catalyst after heating to 513 K, without proton decoupling

overlapping quartets. The larger of the two ethylene peaks has split into a triplet, with the center peak at 120.7 ppm as should be that case. The triplet from the smaller of the two ethylene peaks is almost completely obscured by that of the larger peak. The two peaks from the CH_3 groups of the cis- and trans-but-2-ene have split into the quartets expected, and it appears that the two downfield peaks from these species may have split into a pair of overlapping doublets, which is consistent with our assignment.

Relaxation times were measured for a number of the surface species at 75 MHz (for ^{13}C) using the inversion recovery technique. The larger ethylene peak at 120.5 ppm was found to have a T_1 relaxation time of 147 ms while the smaller, narrower of the two ethylene peaks had a T_1 of only 70 ms. The relaxation times of the two ethane peaks was much longer, but again the more downfield of the pair (3.3 ppm) had the longer T_1 , 773 ms compared to a value of 619 ms measured for the peak at 2.6 ppm. The relaxation times measured for the peaks attributed to the but-2-enes had yet longer relaxation times. Relaxation times were measured for two of the resonances attributed to the but-2-enes, one in the downfield and one in the upfield areas of the spectrum. The downfield T_1 measured, from the peak at 126.5 ppm, was 1.96 s while the peak at 15.6 ppm had a T_1 associated with it in excess of 4.2 s.

The sealed Pt/SiO₂ sample was finally heated at 673 K for 24 hours in a furnace. As before, CP/MAS spectra were obtained using this sample. A further definite transformation has obviously taken place (Fig. 14). There is still a wide peak in the 90-165 ppm range where aromatic species are commonly observed. This peak, centered at about 130 ppm, has definite spinning sidebands at 310 ppm and -50 ppm. There is a sharp peak coincident with this wide peak, centered at about 129 ppm. This is significantly shifted from the ethylene peaks previously observed, and is most likely attributable to weakly adsorbed benzene. The ethane peak previously observed at about 3 ppm is still present, as are the cluster of sharp features between 10 ppm and 20 ppm. It appears that a remnant of the wide upfield peak also remains in this area, though it is possible that there are simply a number of overlapping narrow peaks. For the first time there is evidence for the formation of methane, as seen in the sharp feature at around -8 ppm.

We measured the integrated intensity of the wide downfield peak (including the spinning sidebands) in the spectrum of the catalyst that had been heated to 673 K as a function of delayed decoupling time. As might be expected, the center of the peak shifted slightly downfield as the delayed decoupling time increased, reflecting the greater proportion of the peak attributable to unprotonated carbon

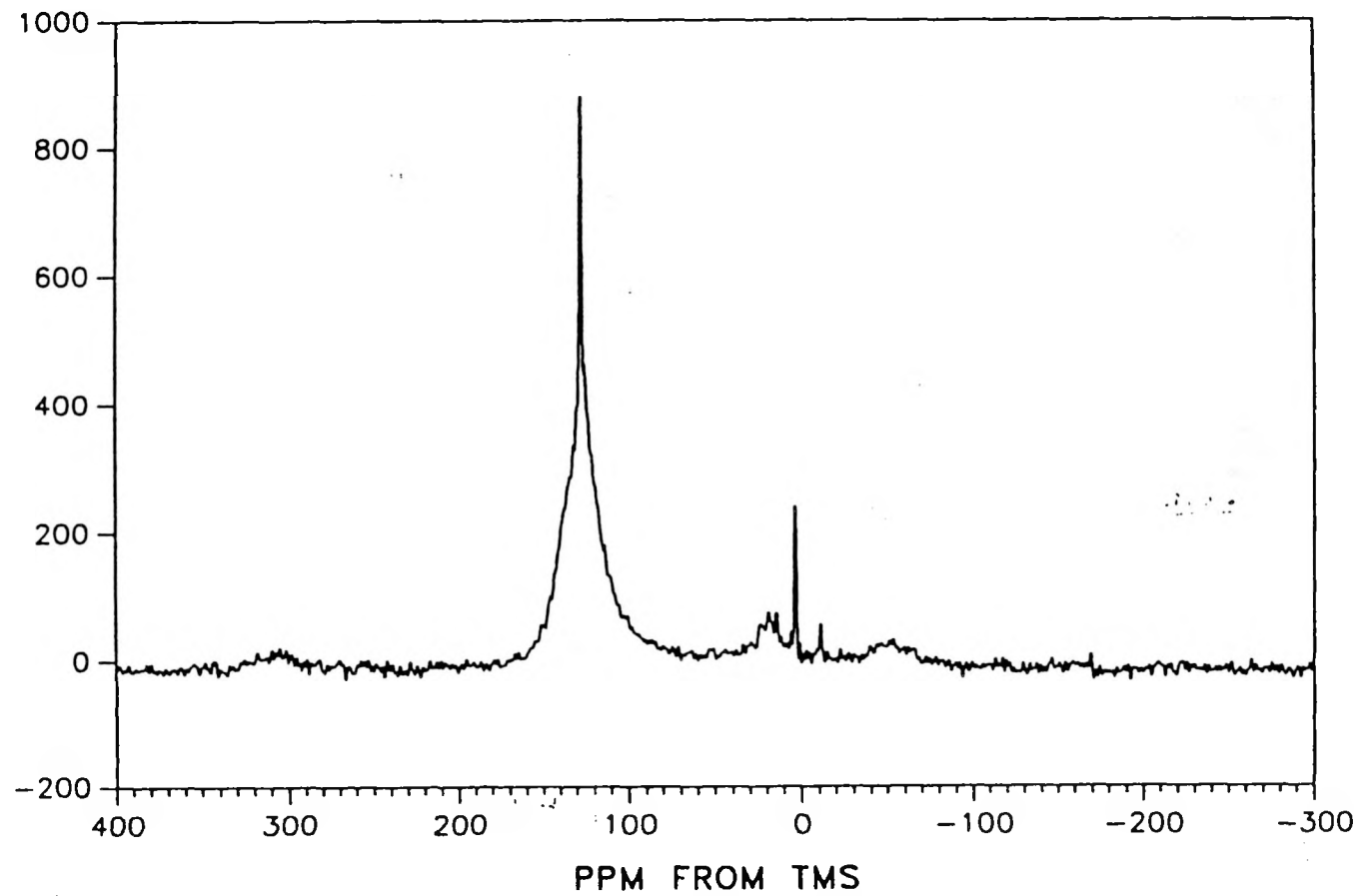


Figure 14. CP/MAS spectrum after heating ethylene adsorbed on Pt/silica to 673 K

atoms. If a wide peak is observed for a carbonaceous species, as seen in the spectra, we expect a double exponential decay in a plot of the integrated intensity of the peak versus delayed decoupling time, as has been shown for coal samples by Solum et al. [37]. The first component will be a rapid gaussian decay corresponding to the protonated carbon nuclei and the second component will be a slow lorentzian decay associated with the un-protonated carbons. The ratio of the heights at which each curve intersects the intensity axis (at zero delay time) gives the ratio of protonated to non-protonated carbon nuclei in the surface species responsible for the peak. This can then be used to put limits on the size of the carbon clusters [37]. As shown in Fig. 15, the integrated intensity versus dephasing time plot obtained was fit using a double exponential expression. The rapid initial decrease in integrated intensity was primarily due to a gaussian decay with a time constant of $30.2 \mu s$, which corresponds to the protonated carbon nuclei. The long lorentzian decay, corresponding to the unprotonated carbon nuclei, had a time constant of $402.7 \mu s$. The ratio of the intercepts of the gaussian and lorentzian curves with the integrated intensity axis at a dephasing time of zero gives the ratio of protonated to non-protonated carbon nuclei in the species responsible for the wide downfield peak. This was found to

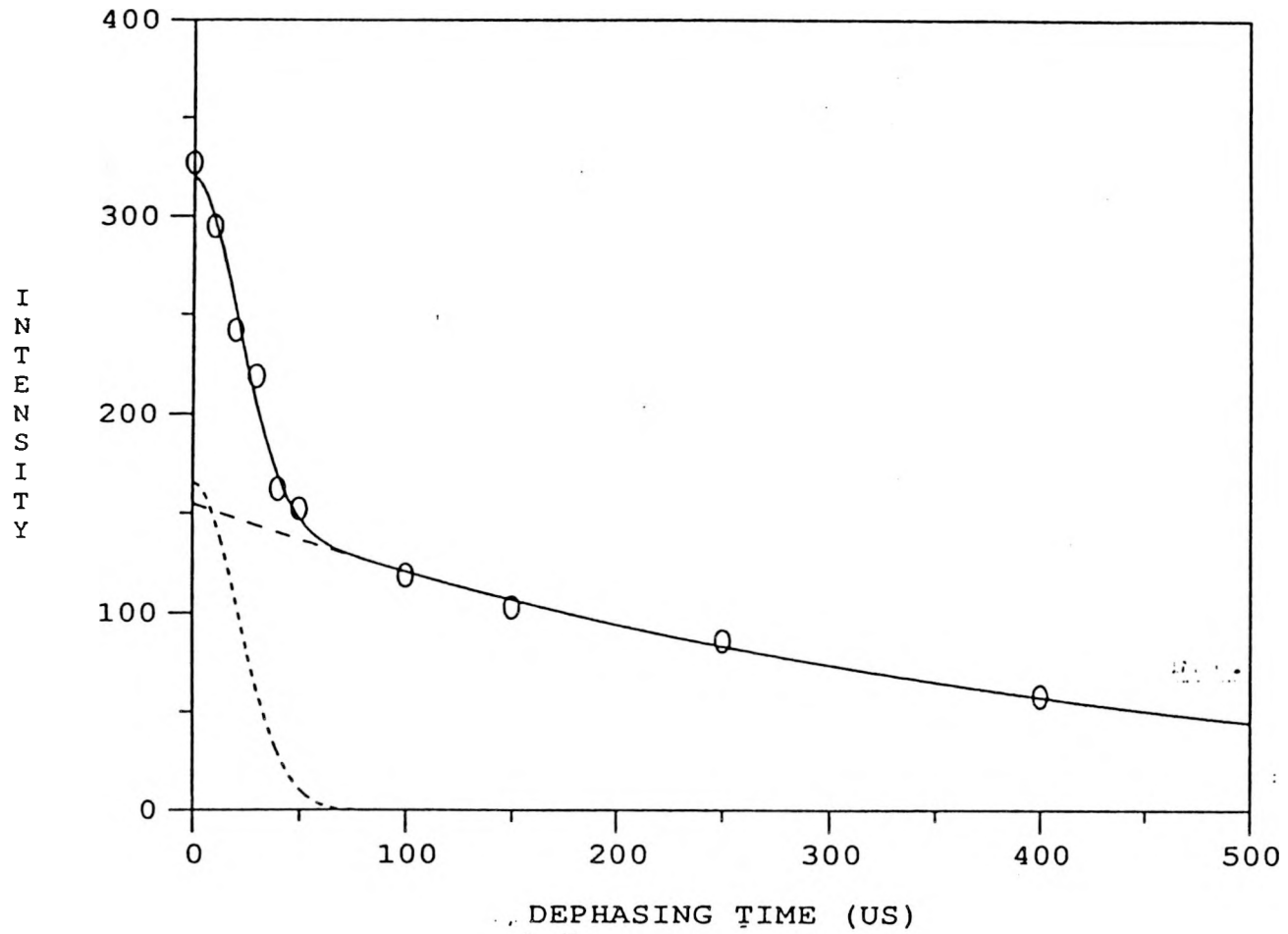


Figure 15. Integrated intensity versus dipolar dephasing time for wide downfield peak in CP/MAS spectrum after heating ethylene on Pt/silica at 673 K

be 165:155, indicating that approximately 58% of the carbon nuclei responsible for this peak are protonated.

Again, we obtained more information about the weakly adsorbed species by direct excitation of ^{13}C nuclei in the 75 MHz spectrometer both with (Fig. 16) and without (Fig. 17) proton decoupling. In the decoupled spectrum we are clearly able to detect a pair of peaks at -11.0 ppm and -11.4 ppm, which are attributed to methane both from their chemical shifts and also from the splittings in the coupled spectrum, which contains the expected overlapping pair of quintuplets. The small peak at -2.6 is a spinning sideband. Expansion of the intensity axis reveals two peaks at 2.7 ppm and 3.6 ppm corresponding to ethane. The probable reason that the ethane peaks are barely visible in this spectrum while there was clearly a peak in this position in the corresponding CP/MAS spectrum is that the sample for the direct excitation experiments contained a lower initial coverage of ethylene. Therefore, all the ethane that was produced has already been converted to other species, most likely methane which is observed in large quantities in the high resolution spectrum. The downfield portion of the decoupled spectrum contains two additional peaks in the region normally assigned to aromatic species. Comparing the coupled and decoupled spectra shows that the peak at 124.8 ppm is a non-protonated aromatic carbon atom. The other peak observed has a shift of

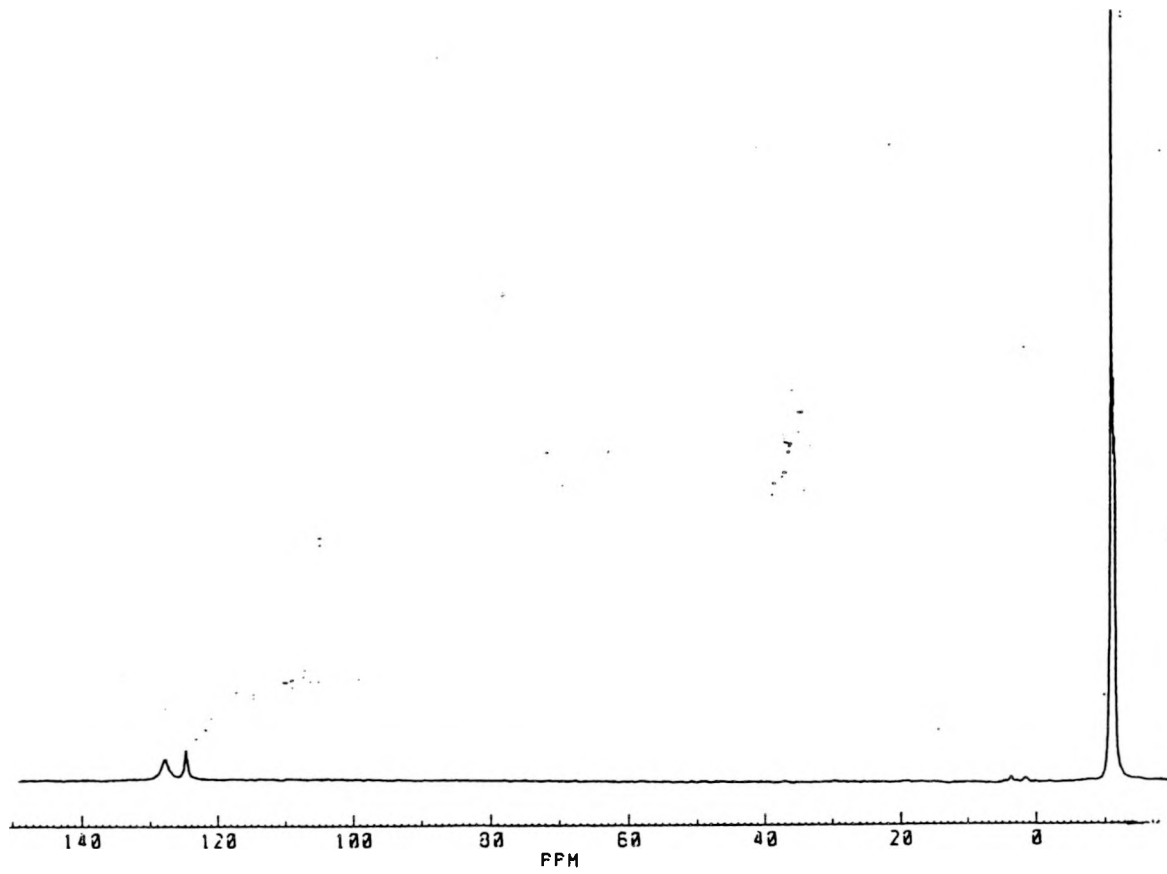


Figure 16. High-resolution ^{13}C spectrum of weakly adsorbed species formed after heating ethylene adsorbed on Pt/silica at 673 K (with proton decoupling)

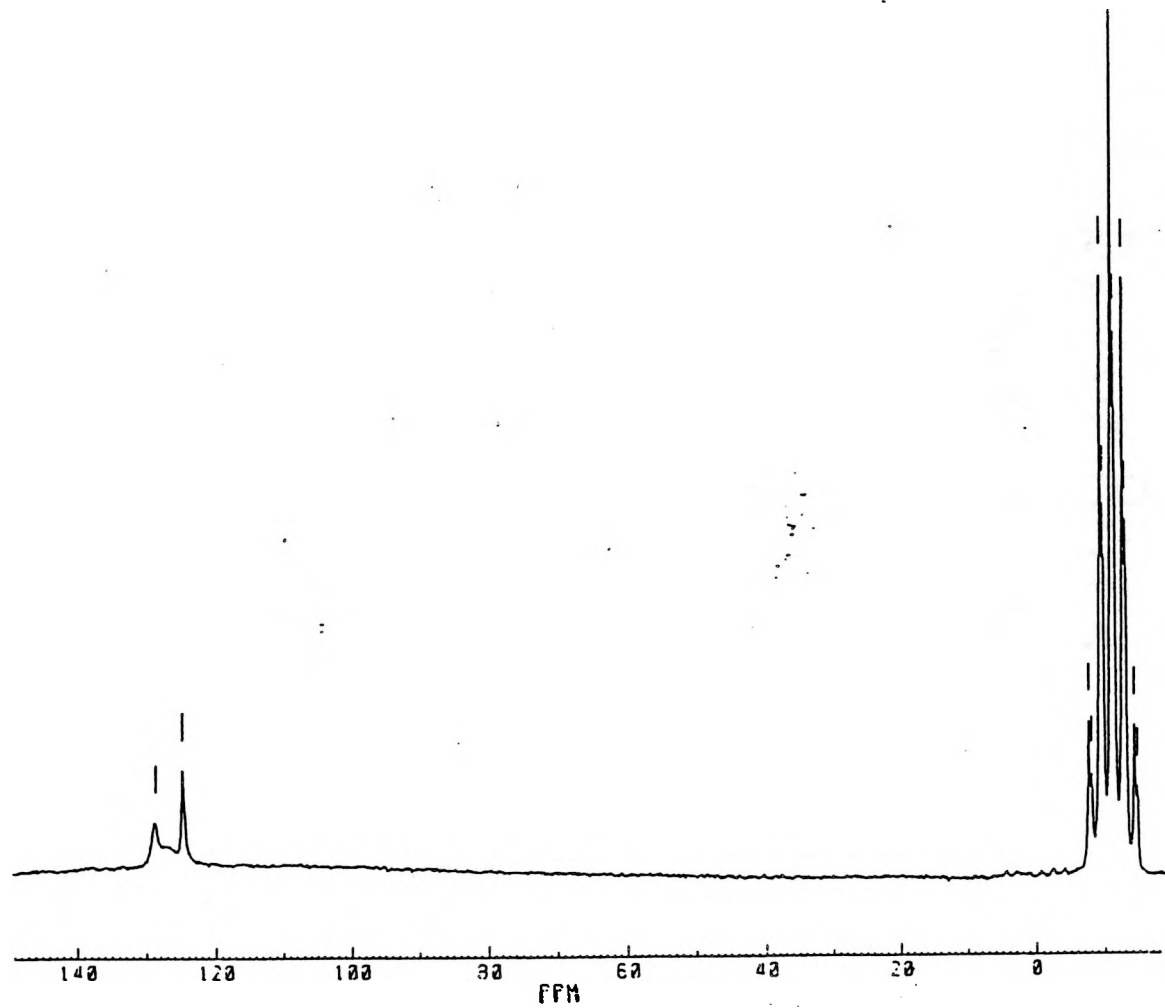


Figure 17. High-resolution ^{13}C spectrum of weakly adsorbed species formed after heating ethylene adsorbed on Pt/silica at 673 K (without proton decoupling)

127.6 ppm in the decoupled spectrum. In the spectrum taken without proton decoupling this peak appears to have split into two peaks, a sharp one centered at 128.8 ppm, and a wide peak filling the area between the sharp peaks at 124.8 ppm and 128.8 ppm. A doublet would be expected from the CH group in benzene, which the observed chemical shift suggests is the species present, but we are unable to completely explain the different forms of the two sides of the apparent doublet.

As before, we measured the T_1 relaxation times of the major peaks observed in the spectrum. The two sharp peaks in the upfield part of the spectrum had relatively fast relaxation times, 265 ms and 145 ms for the peaks at -11.0 ppm and -11.4 ppm respectively. Note that the more downfield of the pair of peaks had the longer relaxation time as was the case for the pairs of ethane and ethylene peaks after the sample was heated to 513 K. The unprotonated aromatic carbon nuclei had a T_1 of 400 ms and the aromatic CH carbon had a much longer relaxation time of 1.91 s.

DISCUSSION

The coverages of ethylene employed in this work are far greater than those typically used in the single-crystal studies, bringing us closer to the typical operating conditions of industrial catalyst systems. Use of such high coverages allows us to observe many surface species which are not seen using ultra-high vacuum spectroscopic techniques. The ability to use NMR spectroscopy at these high coverages makes the technique particularly interesting for the study of catalytic systems.

Comparison of the results for the ethylene adsorbed on SiO_2 and on the Pt/ SiO_2 catalysts after each temperature treatment shows that the peaks we observe from the catalyst samples are not due to the inherent activity of the silica support. This is an important result in light of the recent report by Chin and Ellis [38] showing that acetylene can adsorb on an alumina support and form multiple adsorbed species. It is therefore important to show that the results obtained from spectroscopic observation of adsorbed species are unique to the metal-containing catalyst.

Comparison of the spectra obtained by direct excitation of ^{13}C in C_2H_4 on silica and a sample of ethylene gas shows that we are able to detect ethylene in the gas phase in both cases. Ethylene in the gas phase resonates slightly upfield from adsorbed ethylene.

The spectra obtained before the samples were exposed to any heat treatment show no significant features due to reaction of the ethylene. We think, based on the two peaks that were observed, that ethylene is present in two molecular states, an adsorbed state and in the gas phase. We saw no evidence for any other surface species, including the ethyliyne species commonly suggested to be present on the Pt(111) single crystal surface at room temperature [11-15, 18-21]. If ethyliyne were present we would certainly expect to observe a signal in the 0 ppm to 40 ppm range from the CH_3 group. There is more question as to where the carbon attached to the platinum surface might resonate. The best analog currently available is from the work of Aime et al. [39], who have obtained ^{13}C NMR of $\text{Co}_3(\text{CO})_9\text{CCH}_3$. They found that the ethyliyne carbon attached to the three cobalt atoms resonated at 296 ppm. Evans and McNulty [40] found that the unprotonated ethyliyne carbon in $\text{Os}_3(\text{CO})_9(\mu\text{-H})_3(\mu_3\text{-CCH}_3)$ resonated at 219.3 ppm while the unprotonated ethyliyne carbon in the ruthenium analog resonated at 154.7 ppm. It is possible that the position of this peak could be drastically affected by a Knight shift due to the metal crystallite. Slichter [41] and Rhodes et al. [42] have studied platinum catalysts directly using ^{195}Pt NMR and showed that there is a Knight shift observed for the surface platinum atoms in clean surfaces. However, there was very little Knight shift

observed for the surface platinum atoms in hydrogen-covered catalysts, so it seems likely that the resonance of the ethylidyne carbon atom attached to the platinum surface should not be shifted far from the 300 ppm region. Hatzikos and Masel [27] have suggested that the presence of threefold hollow sites is necessary to form ethylidyne. It is possible that our highly disperse catalyst does not contain enough of these sites to allow us to observe ethylidyne, though Wang et al. [7] have suggested that ethylidyne is observed using NMR on catalysts with a dispersion almost as high as those used in this study. The catalysts used by Wang et al. [7], however, were supported on alumina and the ethylene coverages were very low. Alumina has proved to be active in the conversion of acetylene [38], so it is not clear whether the effects reported by Wang et al. [7] are affected by the use of alumina as the catalyst support. Gay [8] has shown that the support used can have an effect on the NMR spectrum observed when ethylene is adsorbed on the catalyst surface, though he was unable to observe ethylidyne on any of his catalysts. Unlike Gay [8], who used low coverages of ethylene, we observed a molecular ethylene peak.

Heating the samples to 413 K did not produce any observable wide peaks associated with strongly adsorbed species. The only change is the production of a small amount of weakly adsorbed ethane together with negligible amounts of

other weakly adsorbed species, most likely but-2-enes.

Ethane has been previously observed to be formed by self-hydrogenation of ethylene over the Pt(111) surface [23]. In the production of ethane there is a net addition of hydrogen to an ethylene molecule. This hydrogen is either present as an impurity in the gas adsorbed onto the sample or is produced by dehydrogenation of ethylene to produce surface species which we are not able to observe. The total amount of ethane produced is so small that the latter possibility is plausible.

Further heating the samples to 513 K produced a significant change in the surface species observed. For the first time we observe features attributed to species strongly adsorbed on the catalyst surface (as evidenced by the wide peaks) in addition to a number of weakly adsorbed species. The weakly adsorbed species observed are believed to be unreacted ethylene, ethane formed by self-hydrogenation of ethylene and both the cis- and trans-isomers of but-2-ene. Formation of the but-2-ene isomers has been observed by Pruski et al. [32] on the much more reactive Ru/SiO₂ system at room temperature. Ethylene and ethane are both clearly present in two states. In both cases, the upfield peak of the pair is narrower and corresponds to the state having the shorter T₁ relaxation time. Since we observe two peaks for ethylene adsorbed on the pure silica support, it seems likely

that the molecular C_2 species continue to be observed in both the gaseous and adsorbed state. The adsorbed state is probably predominately associated with the silica support. Heating the sample to 513 K appears to lead exclusively to the formation of weakly adsorbed species with even numbers of carbon atoms. This has also been observed for ethylene adsorbed on Ru/SiO₂ at room temperature [32]. There are a number of strongly adsorbed species present on the platinum catalyst after heating to 513 K. One of these is aromatic, as evidenced by the chemical shift. This is probably due to an aromatic carbonaceous overlayer or its precursor. This species remains largely protonated under these conditions. The wide upfield peak could be partially due to a CH₃ group in a species such as =CH-CH₃, which has been suggested as an intermediate in the hydrogenation of ethylene to ethane [4, 24], or to a -CH₂-CH₃ fragment.

Heating the sample to 673 K leads to further changes in the species observed. Definite evidence of carbon-carbon bond cleavage is seen for the first time, as shown by the formation of methane. Like the ethane and ethylene previously observed, methane appears to be observed in both gaseous and adsorbed forms. The more downfield of the pair of methane peaks, corresponding to the adsorbed state, has the longer T₁ relaxation time, as was the case for both ethane and ethylene on the sample that had been heated to

513 K. No evidence for the presence of ethylene is seen and on samples with initial ethylene coverages at the lower end of the range studied, ethane is also absent from the NMR spectrum obtained. Ethane hydrogenolysis is, of course, a very well known reaction and it is probable that ethane is an intermediate in one of the reaction pathways for the formation of methane from ethylene.

We also have evidence for both weakly and strongly adsorbed aromatic species present after heating the sample to 673 K. The formation of aromatic rings from C_2 hydrocarbons is not unprecedented. The formation of benzene from acetylene has previously been observed over the Pd(111) surface [43, 44] and has been shown to be structure-sensitive, occurring much more rapidly on the Pd(111) surface than on the Pd(100) or Pd(110) surfaces [44]. The strongly adsorbed aromatic species is almost certainly coke, which may be present on the surface of the platinum crystallites, the silica support, or both. The weakly adsorbed aromatic species is either a coke precursor or, possibly, coke weakly adsorbed on the silica support. Gallezot et al. [45] have shown that coke can occur both on the platinum surface itself and on the surrounding support, though they used an alumina support that is known to be catalytically active in its own right [38]. Gallezot et al. [45] found that the coke formed on their catalysts had some aromatic characteristics, but

were more amorphous than such model compounds as coronene and pentacene. We calculate that the overall stoichiometry of the strongly adsorbed coke is $C_{2.4}H$. Campbell et al. [46] have studied benzene adsorbed on the Pt(111) surface. Using TPD they found that the benzene decomposition occurred in three steps with maxima in the hydrogen desorption rates at 460 K, 540 K and between 600 K and 700 K. They found that the stoichiometry of the surface species after the 540 K desorption peak was C_2H , close to the value we measure. Following the method of Solum et al. [37], we are able to put a lower limit of 16 on the number of carbon atoms in the average coke cluster. This assumes a close-packed structure of aromatic rings and corresponds to four joined aromatic rings. The upper limit on the number of carbon atoms per coke cluster is then put at approximately 55 and corresponds to the case where the aromatic rings join to form lace-like structures. It seems likely that the coke particles would be closely packed, which puts the average number of carbon atoms in a cluster towards the lower end of this range.

CONCLUSION

Use of NMR spectroscopic techniques allows us a unique insight into the species that may be present on a catalyst surface under conditions more closely approximating typical reaction conditions than the ultra-high vacuum required for the spectroscopies more traditionally used in surface chemistry studies. The CP/MAS NMR experiment and direct excitation of ^{13}C nuclei give complementary information, together giving a more complete picture of species adsorbed on catalyst surfaces than either method used individually.

Ethylene adsorbed at high coverages on Pt/SiO₂ catalysts undergoes a number of changes as the system is thermally treated. At room temperature only ethylene is observed weakly adsorbed on the surface. Heating the samples to 413 K leads to the formation of small amounts of ethane. After heating to 513 K, cis- and trans-but-2-ene are also seen weakly adsorbed on the surface. In addition, strongly bound C_nH_m groups and highly protonated aromatic species are observed after heating the samples to 513 K.

Further heating the samples to 673 K leads to the breaking of carbon-carbon bonds, as evidenced by the formation of methane. In addition, weakly adsorbed aromatic species are observed. Heating the samples to 673 K also leads to the formation of strongly adsorbed coke having an overall stoichiometry of C_{2.4}H.

All the C₁ and C₂ hydrocarbons seen by direct excitation of ¹³C were present in two observable states, and the upfield peak from each species always had a shorter T₁ relaxation time. We believe that each of these species is observed both as a gas and in a weakly adsorbed form, predominantly associated with the silica support.

ACKNOWLEDGMENT

This work was supported by the U. S. Department of Energy, Office of Basic Energy Sciences under contract number W-7405-ENG-82. The authors would also like to acknowledge with thanks the assistance of Dr. V. Rutar for his assistance with the experiments on the Bruker MSL-300 spectrometer. In addition, we would like to thank Xi Wu for preparing the catalysts used in this work.

REFERENCES

1. Wang, P. K., Ansermet, J. P., Rudaz, S. L., Wang, Z., Shore, S., Slichter, C. P., and Sinfelt, J. H., Science **234**, 35 (1986).
2. Slichter, C. P., Ann. Rev. Phys. Chem. **37**, 25 (1986).
3. Wang, P. K., Ansermet, J. P., Slichter, C. P., and Sinfelt, J. H., Phys. Rev. Lett. **55**, 2731 (1985).
4. Sheng, T. C., and Gay, I. D., J. Catal. **77**, 53 (1982).
5. Sheng, T. C., and Gay, I. D., J. Catal. **71**, 119 (1981).
6. Ben Taarit, Y., Naccache, C. M., and Imelik, B., Chem. Phys. Lett. **47**, 479 (1977).
7. Wang, P. K., Slichter, C. P., and Sinfelt, J. H., J. Phys. Chem. **89**, 3606 (1985).
8. Gay, I. D., J. Catal. **108**, 15 (1987).
9. Alemany, L. B., Grant, D. M., Alger, T. D., and Pugmire, R. J., J. Am. Chem. Soc. **105**, 6697 (1983).

10. Shibanuma, T., and Matsui, T., Surf. Sci. **154**, L215 (1985).
11. Cruz, C. de la, and Sheppard, N., J. Chem. Soc., Chem. Commun., 1854 (1987).
12. Skinner, P., Howard, M. W., Oxton, I. A., Kettle, S. F. A., Powell, D. B., and Sheppard, N., J. Chem. Soc., Faraday Trans. II **77**, 1203 (1981).
13. Sheppard, N., J. Electron Spectr. and Rel. Phenom. **38**, 175 (1986).
14. Avery, N. R., and Sheppard, N., Proc. Roy. Soc. Lond. A **405**, 1 (1986).
15. Avery, N. R., and Sheppard, N., Proc. R. Soc. Lond. A **405**, 27 (1986).
16. Ibach, H., Hopster, H., and Sexton, B., Appl. of Surf. Sci. **1**, 1 (1977).
17. Ibach, H., and Lehwald, S., J. Vac. Sci. Technol. **15**, 407 (1978).

18. Baró, A. M., and Ibach, H., J. Chem. Phys. **74**, 4194 (1981).
19. Steininger, H., Ibach, H., and Lehwald, S., Surf. Sci. **117**, 685 (1982).
20. Kesmodel, L. L., Dubois, L. H., and Somorjai, G. A., J. Chem. Phys. **70**, 2180 (1979).
21. Salmeron, M., and Somorjai, G. A., J. Phys. Chem. **86**, 341 (1982).
22. Koestner, R. J., Van Hove, M. A., and Somorjai, G. A., J. Phys. Chem. **87**, 203 (1983).
23. Godbey, D., Zaera, F., Yeates, R., and Somorjai, G. A., Surf. Sci. **167**, 150 (1986).
24. Zaera, F., and Somorjai, G. A., J. Am. Chem. Soc. **106**, 2288 (1986).
25. Beebe, T. P., Jr., and Yates, J. T., Jr., J. Phys. Chem. **91**, 254 (1987).

26. Paál, Z., Fülöp, E., and Marton, D., React. Kinet. Catal. Lett. **38**, 131 (1989).
27. Hatzikos, G. H., and Masel, R. I., Surf. Sci. **185**, 479 (1987).
28. Windham, R. G., Koel, B. E., and Paffett, M. T., Langmuir **4**, 1113 (1988).
29. Davis, S. M., Zaera, F., and Somorjai, G. A., J. Catal. **77**, 439 (1982).
30. Wang, P. K., Ansermet, J. P., Slichter, C. P., and Sinfelt, J. H., Phys. Rev. Lett. **55**, 2731 (1985).
31. Wu, X., Gerstein, B. C., and King, T. S., J. Catal., submitted.
32. Pruski, M., Kelzenberg, J. C., Gerstein, B. C., and King, T. S., J. Am. Chem. Soc., accepted.
33. Pruski, M., and Gerstein, B. C., Chemistry Department, Iowa State University, in preparation.

34. Shoemaker, R. K., and Apple, T. M., J. Magn. Reson. **67**, 367 (1986).
35. Alla, M., and Lippmaa, E., Chem. Phys. Lett. **37**, 260 (1976).
36. Stejskal, E. D., and Schaefer, J., J. Magn. Reson. **18**, 560 (1975).
37. Solum, M. S., Pugmire, R. J., and Grant, D. M., Energy & Fuels **3**, 187 (1989).
38. Chin, Y. H., and Ellis, P. D., J. Am. Chem. Soc. **111**, 7653 (1989).
39. Aime, S., Milone, L., and Valle, M., Inorg. Chim. Acta **18**, 9 (1976).
40. Evans, J., and McNulty, G. S., J. Chem. Soc. Dalton Trans. **1**, 79 (1984).
41. Slichter, C. P., Surf. Sci. **106**, 382 (1981).
42. Rhodes, H. E., Wang, P. K., Stokes, H. T., Slichter, C. P., and Sinfelt, J. H., Phys. Rev. B **26**, 3559 (1982).

43. Sesselmann, W., Woratschek, B., Ertl, G., Küppers, J., and Haberland, H., Surf. Sci. **130**, 245 (1983).
44. Gentle, T. M., and Muetterties, E. L., J. Phys. Chem. **87**, 2469 (1983).
45. Gallezot, P., Leclercq, C., Barbier, J., and Marecot, P., J. Catal. **116**, 164 (1989).
46. Campbell, J. M., Selmanides, S., and Campbell, C. T., J. Phys. Chem. **93**, 815 (1989).

SUMMARY AND RECOMMENDATIONS

A number of conclusions may be drawn from the work discussed in this dissertation:

1. The ability to obtain an accurate measure of the proportion of the surface of a bimetallic crystallite taken up by the active metal is essential to the interpretation of reaction study data.
2. At temperatures below 510 K, the general effect of adding copper or silver to a silica-supported ruthenium catalyst is the same. The reason for this is that both silver and copper tend to preferentially populate the edge and corner sites of the crystallite, though copper is the more strongly segregating element and therefore the effect of adding copper is observed more rapidly.
3. At temperatures below 510 K, copper and silver modify the activity of the silica-supported ruthenium catalyst for the ethane hydrogenolysis reaction by removing the low-coordination sites, which are most active for the associative desorption and dissociative adsorption of hydrogen from the active surface.
4. At temperatures above 510 K, copper is able to act as a sink and source for hydrogen, therefore negating the effect of removing the ruthenium sites that are most active for adsorption/desorption of hydrogen. This leads to an apparent increase in specific activity for ethane hydrogenolysis of a

ruthenium catalyst as copper is first added at the highest temperatures studied.

5. Silver, for which hydrogen spillover has not been seen to occur, is not active for the adsorption/desorption of hydrogen at any of the temperatures studied in this work. The specific activity of the ruthenium catalyst for the hydrogenolysis of ethane therefore drops as silver is added at all temperatures studied.

6. Nuclear magnetic resonance has proven to be a valuable tool for studying high coverages of adsorbates on supported metal catalysts.

7. At room temperature, ethylene is seen to adsorb on silica-supported platinum catalysts with no observable reaction taking place.

8. Heating silica-supported platinum catalysts which are exposed to high coverages of ethylene at a temperature of 513 K leads to the formation of weakly adsorbed ethylene, ethane and cis- and trans-but-2-ene. In addition, strongly adsorbed C_nH_m fragments and highly protonated aromatic species are observed.

9. Further heating of these samples leads to the formation of weakly adsorbed methane and aromatic species together with strongly adsorbed coke. The overall stoichiometry of the coke may be determined, and was found to

be $C_{2.4}H$ for one sample studied, corresponding to aromatic structures containing between 16 and 55 carbon atoms.

Recommendations for Future Work

The recommendations for extension of this work fall into two general categories: work on the reactor system and NMR studies.

The work on the reactor studies could be usefully extended to other reactions. The first candidate would be propane hydrogenolysis. It would be interesting to compare the methane to ethane production ratio as copper is added to a ruthenium catalyst at the two temperature extremes used in this work. If, as has been suggested, the effectiveness of copper as a hydrogen source/sink changes between these temperature extremes it might be expected that the methane:ethane ratio in the product may be higher at higher temperatures. This reaction would also allow comparison of the relative rates of hydrogenolysis to isomerization over the system studied.

It might also be possible to extend the reaction studies to other catalyst systems, such as silica-supported platinum. This would require changing the method of heating the reactor, since it is not possible to introduce enough catalyst into the isothermal region of the tube furnace currently in use, and therefore the product concentrations are not high enough to measure accurately. Modifications to

the reactor system would also be required to investigate the ethylene hydrogenation reaction. This reaction is extremely exothermic and the current setup is unable to remove heat from the reactor fast enough to prevent thermal runaway. There are two modifications which may help alleviate this problem. Either a reactor could be built which incorporates a water (or other heat transfer medium) jacket or the reactor system could be modified to allow the use of a substantial helium diluent concentration in the feed stream. Helium should be used to minimize the problems caused by the diluent in the product analysis, since the carrier gas for the gas chromatograph system is helium.

The obvious extension of the NMR studies carried out and reported in this dissertation is the use of bimetallic catalysts instead of the monometallic silica-supported platinum catalyst used in this work. In fact, some preliminary work using ethylene adsorbed on Pt-Ag/SiO₂ catalysts was carried out before the complexity of the monometallic system became apparent. As can be seen in figures 1-3, it is possible to obtain spectra with this system. The catalysts used contained 4 wt % Pt and silver made up 20% of the total number of metal atoms in the sample.

Other useful extensions of the NMR work presented here would be to study the same system with catalysts of lower dispersion to show whether the species present on the surface

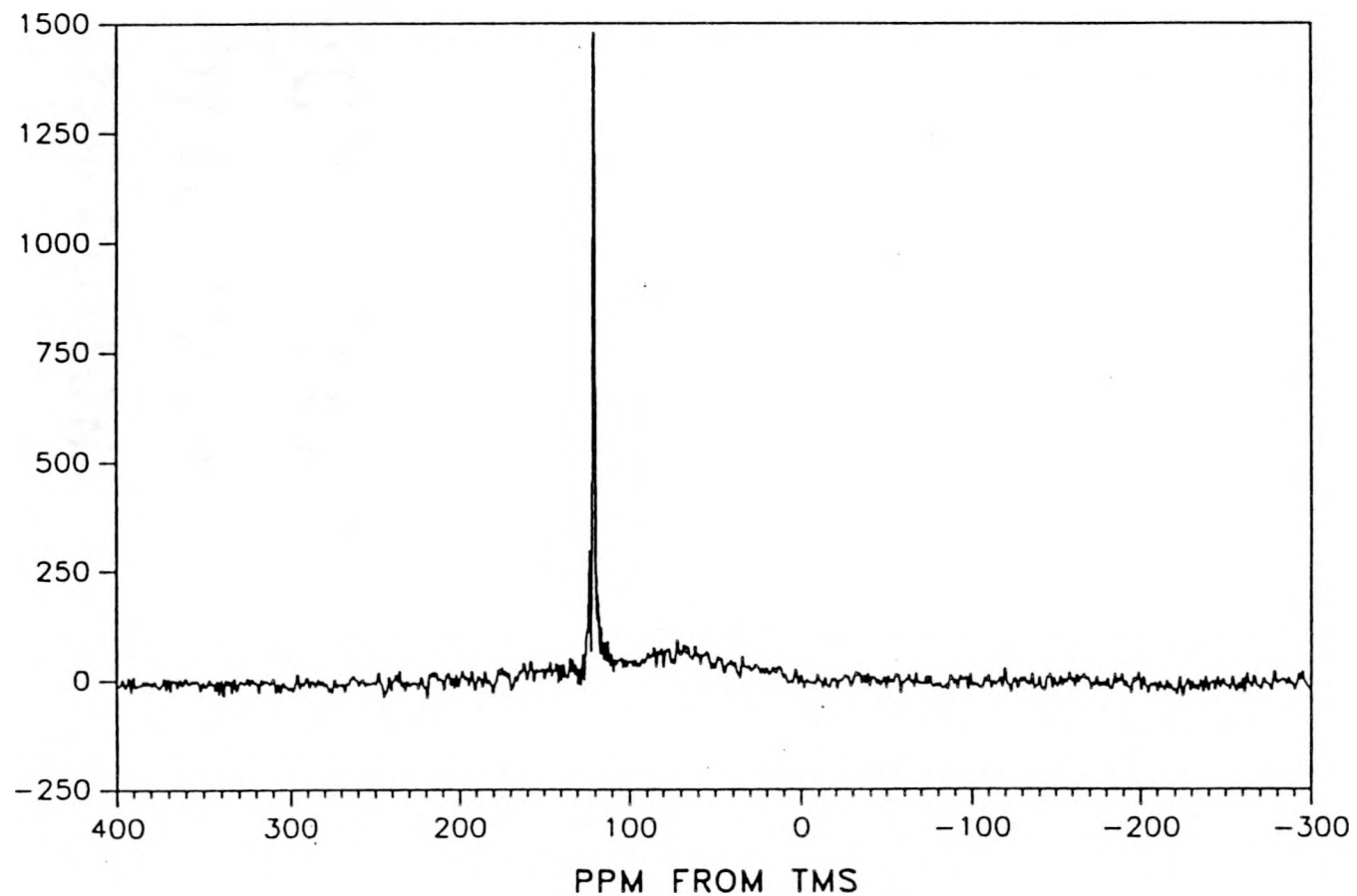


Figure 1. CP/MAS spectrum of ethylene adsorbed on Pt-Ag/silica, as prepared

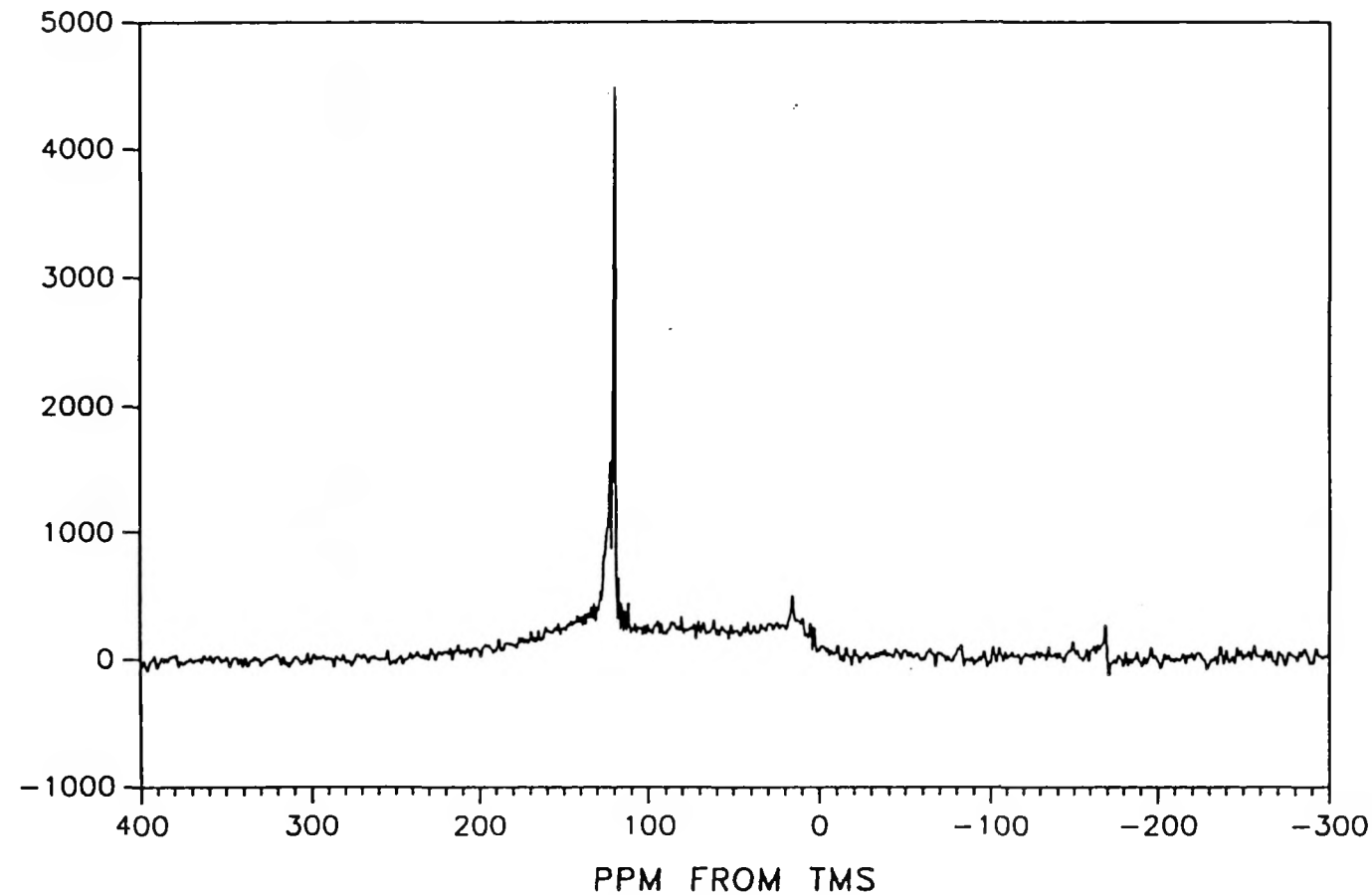


Figure 2. CP/MAS spectrum of ethylene on Pt-Ag/silica after heating to 413 K for 24 hours

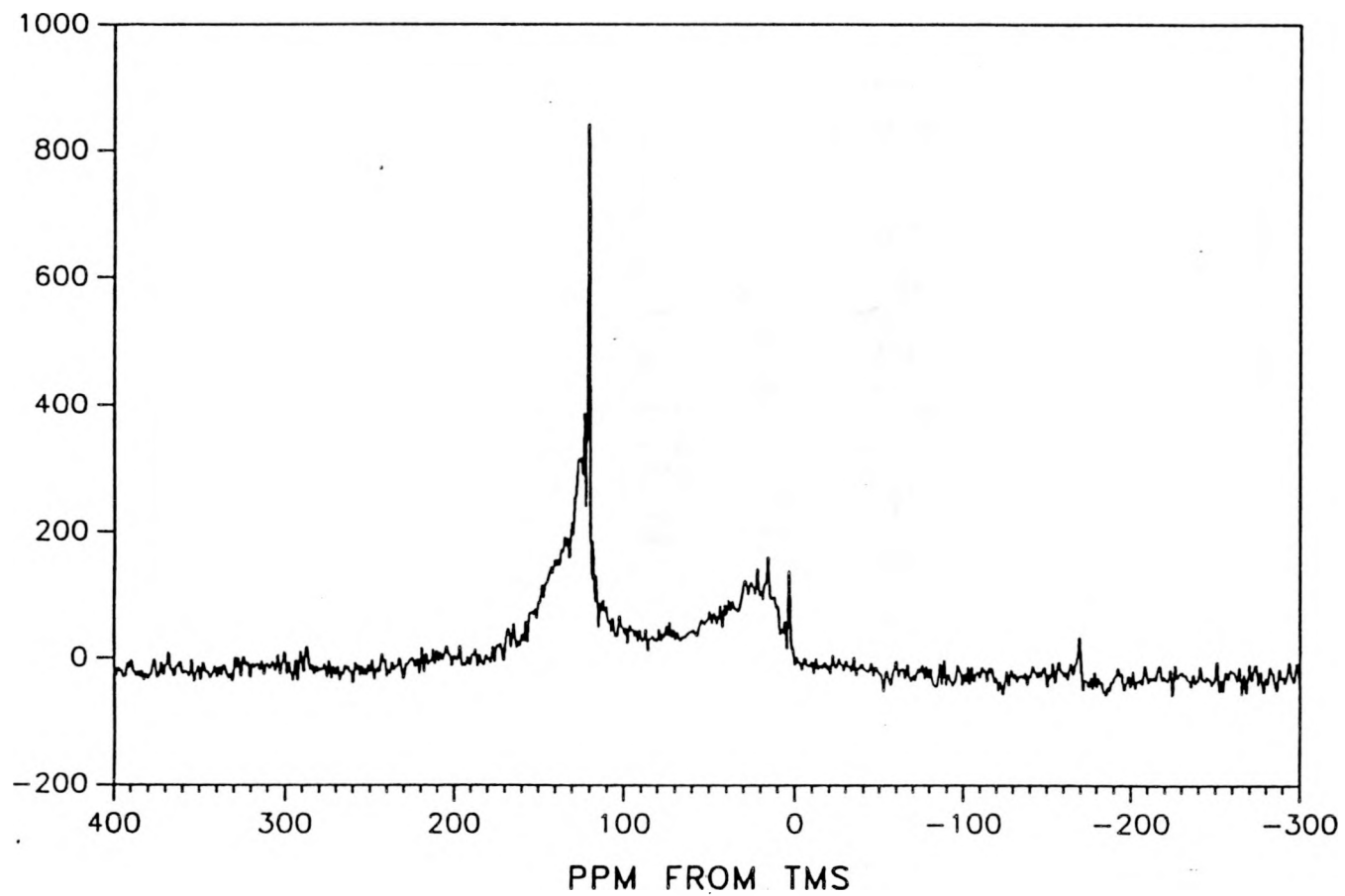


Figure 3. CP/MAS spectrum of ethylene on Pt-Ag/silica after heating to 513 K for 24 hours

changes when a significant proportion of the surface is made up of low index facets. It would also be interesting to use low coverages of ethylene on these catalysts in an attempt to find evidence for the ethyliyne species postulated to occur for low ethylene coverages on single crystal samples.

ADDITIONAL LITERATURE CITED

1. Hansen, M., "Constitution of Binary Alloys." 2nd Ed. McGraw-Hill, New York, 1958.
2. Sinfelt, J. H., "Bimetallic Catalysts." Wiley, New York, 1983.
3. Wu, X., Gerstein, B. C., and King, T. S., J. Catal. accepted.
4. Strohl, J. K., Ph.D. diss. Iowa State University, 1988.
5. Duncan, T. M., and Dybowski, C., Surf. Sci. Rep. **1**, 157 (1981).
6. Wang, P. K., Ansermet, J. P., Rudaz, S. L., Wang, Z., Shore, S., Slichter, C. P., and Sinfelt, J. H., Science **234**, 35 (1986).
7. Slichter, C. P., Ann. Rev. Phys. Chem. **37**, 25 (1986).

ACKNOWLEDGMENTS

I would like to express my gratitude and appreciation to Professor Terry King for his guidance and encouragement throughout the time I have spent at Iowa State. I would also like to thank Dr. Marek Pruski for his help with the NMR experiments, Xi Wu for his endless supply of catalysts and Professor Bernard Gerstein for his valuable insights.

Thanks are also due to the students, past and present, of Professors King and Gerstein, and to all those others whose camaraderie has made my time in Ames so enjoyable.

Finally, I thank my wife, Wendy, for her love, patience, understanding, and support, without which this would not have been possible.

This work was performed at Ames Laboratory under contract No. W-7405-ENG-82 with the U. S. Department of Energy. The United States Government has assigned the DOE report number IS-T 1405 to this dissertation.